COMPUTER - ASSISTED EXPERIMENTAL AND ANALYTICAL STUDY OF TIME / TEMPERATURE - DEPENDENT THERMAL PROPERTIES OF THE ALUMINUM ALLOY 2024 - T351

Dissertation for the Degree of Ph. D.
MICHIGAN STATE UNIVERSITY
KHOSROW FARNIA
1976

This is to certify that the

thesis entitled COMPUTER-ASSISTED EXPERIMENTAL AND ANALYTICAL STUDY OF TIME/TEMPERATURE-DEPENDENT THERMAL PROPERTIES OF THE ALUMINUM ALLOY 2024-T351 presented by

Khosrow Farnia

has been accepted towards fulfillment of the requirements for

Ph.D. degree in Mechanical Engineering

Date Feb 13, 1476

major professor

O-7639



. :

23

ABSTRACT

COMPUTER-ASSISTED EXPERIMENTAL AND ANALYTICAL STUDY OF TIME/TEMPERATURE-DEPENDENT THERMAL PROPERTIES OF THE ALUMINUM ALLOY 2024-T351

Ву

Khosrow Farnia

The aluminum alloy 2024-T351 (A1-2024-T351) belongs to a family of metals with a so-called precipitation-hardenable or heat-treatable characteristic. This alloy, when solution heat-treated and subjected to a temperature ranging from 300-500°F, undergoes changes in the microstructure which, in turn, influence the properties of the alloy.

In this investigation a transient thermal properties measurement facility was developed to study the thermal property changes of as received aluminum alloy 2024-T351 under the influence of isothermal precipitation hardening. The developed transient measurement facility utilized the IBM 1800 computer for both the acquisition of transient temperature measurements and the analysis of this data. The recent analytical method developed by J. V. Beck and S. Al-Araji ("Investigation of a New Simple Transient Method of Thermal Property Measurement," <u>Journal of Heat Transfer, Trans.</u>, <u>ASME</u> 96 (1974) Series C:59-64) was used to determine the values of thermal conductivity (k) and specific heat (c_p) utilizing the

transient temperature measurements resulting from the IBM 1800 computer. The transient thermal properties measurement technique was tested using Armco iron, as received A1-2024-T351 with no precipitation (fast measurement cycles), and the annealed A1-2024-T351 materials. For these three cases the k and c_p values are only temperature-dependent. The results of experiments are presented in both tabulated and equation form. The functional relations were found using the least-squares technique.

The tested transient thermal properties measurement facility was also used to obtain k and c_p values of as received A1-2024-T351 with precipitation under isothermal conditions. Values of k (in this case, time- and temperature-dependent) were mathematically modeled and the associated linear and nonlinear parameters were determined using the CDC 6500 computer. The mathematical model of k involves the volume fraction of precipitation. A differential equation is proposed which can be used to predict the instantaneous values of volume fraction of precipitation under arbitrary changes in temperature. In the solution of these equations the instantaneous values of k are calculated using the thermal conductivity-precipitation relationship.

It was found that the variation of c_p for as received A1-2024-T351 with ageing time at any fixed temperature was insignificant. However, the k values at any ageing temperature increase with ageing time to a maximum value. When precipitation is completed the values of k remain unchanged as ageing time increases. The increase in k values due to precipitation at isothermal ageing

temperature 350°F is 20.7%, while this increase for isothermal ageing temperature 425°F is only 11.6%. Relationships are given by which the increase in k and the maximum volume fraction of precipitation, at any ageing temperature, can be predicted.

A FORTRAN computer program was developed to solve numerically the partial differential equation of heat conduction and the proposed differential equation of precipitation. From values of precipitation, the time- and temperature-dependent values of thermal conductivity are calculated. The influence of precipitation on the temperature history, volume fraction of precipitate versus time, and the thermal conductivity history of the A1-2024-T351 material are presented graphically for a one-dimensional case with a step increase in surface temperature.

OF TIME/TEMPERATURE-DEPENDENT THERMAL PROPERTIES OF THE ALUMINUM ALLOY 2024-T351

Ву

Khosrow Farnia

A DISSERTATION

Submitted to
Michigan State University
in partial fulfillment of the requirements
for the degree of

DOCTOR OF PHILOSOPHY

Department of Mechanical Engineering

ACKNOWLEDGMENTS

A debt of gratitude is owed to the writer's major professor, Dr. James V. Beck, for his extensive and always perceptive comments during the period of research and for his detailed review of all chapters and valuable suggestions during the preparation of this dissertation.

The writer is also grateful to the other members of his committee, Professors Kenneth J. Arnold, Norman L. Hills, Mahlon C. Smith, and Denton D. McGrady, for their guidance and discussions.

The writer's thanks go out to very many cooperative and helpful personnel, in the Division of Engineering Research for providing the testing materials and eqipment, in the machine shop for being so patient and careful in machining the specimens and maintaining the equipment, and at the IBM 1800 computer center for making every effort to keep the computer running without failure during the ageing experiments.

Gratitude is also extended to the National Science Foundation and the Division of Engineering Research, for their financial support.

Finally, the writer is grateful to his wife, Cecelia, for her understanding and support during the graduate study and research. Her encouragement and sacrifice have been an invaluable contribution.

TABLE OF CONTENTS

																		Page
LIST	OF TA	BLES .	•		•	•		•	•	•		•		•	•	•		vi
LIST	OF FI	GURES	•	•	•	•	•	•	•	•	•	•	•		•	•	•	i
LIST	OF SY	MBOLS	•	•	•	•	•	•	•	•	•	•	•	•	•	•	•	хii
Chap	ter																	
1.	INTR	ODUCTIO	N		•	•	•		•						•	•	•	1
	1-1	0bject	ive	s a	nd	Imp	ort	anc	e o	f T	his	Re	sea	rch	•	٠	•	2
	1-2	Litera	tur	e_R	evi	ew	•	•						•	•	•	•	5 8
	1-3						•	-	•	•	.•	•	•	•	•	•	•	8
		1-3.1	Мо	di f	ied	An	gst	röm	Me	tho	d .	•	•	•	•	•	•	9
		1-3.2											•	•	•	•	•	11
		1-3.3	Th	e F	las	h M	eth	od	. •	•	•	•	• _	•	• .	•	•	13
		1-3.4											o D			ne		
													•			•	•	19
		1-3.5	Li	nea	r F	ini	te	Rod	an	d R	adi	al	Met	hod	S	•	•	21
•		DATUS A																
2.		RATUS A										RMI	NIN	GT	HER	MAL		
	PROP	ERTIES:	A	PPL	IED	10	AR	MCO	IR	ON	•	•	•	•	•	•	•	23
					_			_										
	2-1	Develo										•	.•	· -	. •	٠.	•	24
	2-2	Develo																0.0
		Proper											•		•	•	•	26
		2-2.1											•		•	•	•	27
		2-2.2											g	•	•	•	•	31
		2-2.3						ntr						•		•	•	31
		2-2.4											•			•	•	33
		2-2.5						ane		•	•	•	•	•	•	•	•	33
		2-2.6						omp					•			•	•	34
		2-2.7											•				•	34
	2-3																	
		Determ		th	e T	her	mal	Pr	ope	rti	es	of	Ref	ere	nce			
		Materi			•			•		•	•		•	•	•	•	•	35
		2-3.1						ria		•	•	•	•	•	•	•	•	35
		2-3.2	Th	erm	oco	up 1	e T	ype	an	d I	nst	a 1 1	ati	on	•	•	•	37
		2-3.3	E1	ect	ric	He	ate	r S	pec'	ifi	cat	i on	an	d H	eat			
			In	put	Me	asu	rem	ent						•				40

Chapt	er		Page
		2-3.4 System Calibration	. 42
		the IBM 1800 Computer	. 44
		Specific Heat	. 48
		2-3.7 Computer Program CALIBR	. 55
	2-4	Error Analysis	. 56
		2-4.1 Errors Due to Convection and Radiation	
		Heat Losses	. 57
		2-4.2 Determination of Overall Heat Transfer	
		Film Coefficient	. 59
		2-4.3 Regression Analysis of Heat Transfer	
		Film Coefficient	. 61
		2-4.4 Computer Program NLINA	. 66
		2-4.5 Errors Due to Energy Absorbed by the	
		Heater Assembly and Heat Sink Compound	
		(Silicone Grease)	. 66
		2-4.6 Errors Due to Unknown Location of the	
		Thermocouple Junctions	. 68
		2-4.7 Errors Due to Thermal Expansion	. 70
	2-5	Comparison and Discussion	. 73
3.	AI IIM	INUM 2024-T351 AND EXPERIMENTAL RESULTS	. 80
٠.		THOM EDET TOOT AND EXPERIENTAL REDUCTO	. 00
	3-1	The Sample Composition	. 80
	3-2	Metallurgy of Precipitation	. 81
	3-3	Sequence of Precipitation	. 84
	3-4	Different Techniques to Study Precipitation	•
	•	Hardening	. 87
	3-5	Experimental Procedure	. 88
	3-6	Description of the Experimental Data and Cor-	
		responding Thermal Conductivity-Time Curve	. 92
	3-7	Error Analysis	. 113
	3-8	Comparison and Discussion	. 117
			•
4.	MODE	LING	. 128
	4-1	Time and Temperature Dependence of Thermal Con-	
	• •	ductivity for Isothermal Ageing Condition	. 128
	4-2	Isothermal Experimental Data for Specific Heat	
		of As Received A1-2024-T351	. 132
	4-3	Comparison Between Dimensionless Thermal Conduc-	
	. •	tivity and Volume Fraction of Precipitation .	. 135
	4-4	Assumptions Regarding the Nature of Precipita-	
	• •	tion During Thermal Cycling	. 138
	4-5	Proposed Differential Equations of Precipitation	
		During Arbitrary Thermal Cycling	. 140

Chapter	r													Page
		4-5.1	Cycling	Therm	nal Pi	roc	ess (Step	Ri	se				
		4-5.2	Temperat Equation	of F	reci	pita	ation	Dur	ing	Do		•	•	141
			Cycling Temperat								in	•		144
			rison and f the Prop	Disci	ussio	1		•	•	•		•	•	146
,		Engine	eering Pro Thermal	blem	•	•			•	•	•	•	•	154 155
			Method o								•	•	•	156
5. S	SUMMA	ARY ANI	CONCLUSI	ONS .	•					•	•	•		168
5	5-1	Recomm	mendations	for	Furth	ner	Stud	у.	•		•	•	•	171
REFEREN	ICES				•									175

LIST OF TABLES

Table		Page
2-3.1	Values of \bar{k} and $\bar{\bar{c}}_p$ and their respective standard deviations as a function of temperature for Armco iron	54
2-4.1	Selected guard temperatures and corresponding heat transfer film coefficient	62
2-4.2	F-test criteria to determine the optimum value of order of polynomial n for a good fit	65
2-4.3	Correction data for a pair of Armco iron specimens	69
2-4.4	Correctional multipliers for a pair of Armco iron specimens, low heat input (about 272 watts)	71
2-4.5	Correctional multipliers for a pair of Armco iron specimens, high heat input (about 540 watts)	72
2-5.1	Thermal conductivity of Armco iron as given by various observers and present study	75
2-5.2	Specific heat of Armco iron as given by TPRC and present study	75
2-5.3	The percentage difference of corrected \hat{k} and \hat{c}_p of present data and TPRC as a function of temperature for Armco iron	76
2-5.4	Percentage error of \hat{k} and \hat{c} , as defined in Equations (2-5.7) and (2-5.8), as a function of temperature	78
3-5.1	Summary of tests arrangement for A1-2024-T351 specimens	90
3-6.1	Isothermal ageing test at 350°F, Test No. 1 for A1-2024-T351, values of K and C _p and their respective standard deviations	94

Table		Page
3-6.2	Isothermal ageing test at 350°F, Test No. 2 for A1-2024-T351, values of \bar{k} and \bar{c}_p and their respective standard deviations	95
3-6.3	Isothermal ageing test at 375°F, Test No. 1 for A1-2024-T351, values of \bar{k} and \bar{c}_p and their respective standard deviations p	98
3-6.4	Isothermal ageing test at 375°F, Test No. 2 for A1-2024-T351, values of \bar{k} and \bar{c}_p and their respective standard deviations p	99
3-6.5	Isothermal ageing test at $400^{\circ}F$, Test No. 1 for A1-2024-T351, values of \bar{k} and \bar{c}_p and their respective standard deviations	102
3-6.6	Isothermal ageing test at 400°F, Test No. 2 for A1-2024-T351, values of \bar{k} and \bar{c}_p and their respective standard deviations	103
3-6.7	Isothermal ageing test at 425°F, Test No. 1 for A1-2024-T351, values of \bar{k} and \bar{c}_p and their respective standard deviations p	106
3-6.8	Isothermal ageing test at 425°F, Test No. 2 for A1-2024-T351, values of \bar{k} and \bar{c}_p and their respective standard deviations p	107
3-6.9	Values of \bar{k} and \bar{c}_p and their respective standard deviations for as received A1-2024-T351 at low indicated temperatures	111
3-6.10	Values of \bar{k} and \bar{c}_p and their respective standard deviations for aged Al-2024-T351	112
3-6.11	Values of \bar{k} and \bar{c}_p and their respective standard deviations as a function of temperature for as received A1-2024-T351	114
3-6.12	Values of \bar{k} and \bar{c}_p and their respective standard deviations as a function of temperature for A1-2024-T351, annealed from 575°F	115
3-6.13	_ =	116
3-7.1	Correction data for a pair of A1-2024-T351	117

Table		Page
3-7.2	Correctional multipliers for a pair of Al-2024-T351 specimens	. 118
3-8.1	Comparison of present \hat{k}_a and ref. [24] and [21] for as received A1-2024-T351 and their respective percentage differences	. 120
3-8.2	Comparison of values of \hat{k}_{an} of present study and ref. [24] for annealed AI-2024-T351	. 121
3-8.3	Comparison of values of \hat{c}_p of present study and ref. [24] for A1-2024-T351	. 122
3-8.4	Typical values of percentage error, as defined in Equations (2-5.7) and (2-5.8), for \hat{k} and \hat{c}_p of A1-2024-T351	. 127

LIST OF FIGURES

Figure		Page
2-1.1	Infinite flat plate, insulated at the rear face	. 25
2-2.1a	Transient thermal properties measurement facility	. 28
2-2.1b	Side view of transient thermal properties measurement facility	. 29
2-2.1c	Temperature-controlled housing of the transient thermal properties measurement facility	. 30
2-2.2	Temperature-controlled housing (schematic)	. 32
2-2.3	Schematic diagram of DC power supply equipment.	. 36
2-3.1	Thermocouple installation on the flat surface of the specimen	. 39
2-3.2	Two types of electric heaters and two specimens schematically arranged for an experiment	. 41
2-3.3	A typical heated and insulated transient surface temp	. 47
2-3.4	Thermocouple arrangement and their respective locations in the flat surface of one specimen	. 49
2-3.5	A plot of step-wise calculated thermal conductivity	. 53
2-4.1	A configuration using idea of superposition to determine the effect of the heat losses at the rear face of the specimen	. 57
2-4.2	Configuration to determine the overall heat transfer coefficient	. 60
2-4.3	A plot of heat-transfer coefficient u as a function of guard temperature	. 67

Figure		Page
2-4.4	Configuration to show the location of the thermocouple junctions	70
3-2.1	Partial equilibrium diagram for aluminum side of aluminum-copper alloys, with temperature range for heat treating operations	82
3-6.1	Thermal conductivity as a function of time at 350°F for Aluminum 2024-T351	96
3-6.2	Specific heat as a function of time at 350°F for Aluminum 2024-T351	97
3-6.3	Thermal conductivity as a function of time at 375°F for Aluminum 2024-T351	100
3-6.4	Specific heat as a function of time at 375°F for Aluminum 2024-T351	101
3-6.5	Thermal conductivity as a function of time at 400°F for Aluminum 2024-T351	104
3-6.6	Specific heat as a function of time at 400°F for Aluminum 2024-T351	105
3-6.7	Thermal conductivity as a function of time at 425°F for Aluminum 2024-T351	108
3-6.8	Specific heat as a function of time at 425°F for Aluminum 2024-T351	109
3-8.1	Thermal conductivity of Al-2024-T351 as a function of temperature for annealed, aged, and as received conditions	125
4-1.1	Thermal conductivity of Al-2024-T351 as a function of ageing time	133
4-1.2	Time constant versus inverse absolute temp	134
4-5.1	Precipitation during up-cycling thermal process	143
4-5.2	Precipitation during down-cycling thermal process	143
4-5.3	Volume fraction of precipitate as a function of ageing time for as received Al-2024-T351	145

Figure		Page
4-6.1	A plot of thermal conductivity as a function of ageing time for Al-2024-T351 of present study and reference [1]	147
4-6.2	A plot of thermal conductivity as a function of ageing time for Al-2024-T351 of present study and reference [1]	148
4-6.3	A plot of electrical conductance as a function of ageing time for A1-2024-T351	151
4-7.1	Boundary conditions, initial condition, and nodal arrangement for Al-2024-T351 bar	157
4-7.2	Crank-Nicolson finite difference solution of conduction equation for A1-2024-T351 bar in cases of as received properties (no precipitation), as received with precipitation, and annealed conditions	161
4-7.3	Temperature history of the insulated surface of the Al-2024-T351 bar in cases of as received properties (no precipitation), as received with precipitation, and annealed conditions	162
4-7.4	Thermal conductivity history of the Al-2024-T351 bar in cases of as received properties (no precipitation) and the annealed condition	163
4-7.5	Thermal conductivity history of as received A1-2024-T351 bar with precipitation	164
4-7.6	Volume fraction of precipitate of as received	165

LIST OF SYMBOLS

Α Cross-sectional area of specimen. A, A₁, A₂ Linear parameters. A_t Total exposed area of the specimens B, B_1, B_2 Linear parameters. C Linear parameter. Nonlinear parameter. °C, C Degree Celsius. $C_{\mathbf{k}}$ Correction multiplier for thermal conductivity. Correction multiplier for specific heat. Average specific heat. Average of four \bar{c}_{p} values. Average of sixteen $\bar{c}_{_{D}}$ values. Specific heat of annealed specimen. Specific heat of as received specimen. Statistical F distribution. °F, F Degree Fahrenheit. Heat loss or heat gain. Н Instantaneous heat loss or heat gain. h °K Kelvin, the scale of absolute temperature. k Thermal conductivity. k Average of four k values.

Average of 16 k values.

Ē

Thermal conductivity value of as received specimen. ka k_{an} Thermal conductivity of annealed specimen. Thermal conductivity values at isothermal ageing condik_{ia} tions. Dimensionless thermal conductivity at isothermal ageing conditions. k_{ag} Thermal conductivity value of aged specimen. k_{agr} Thermal conductivity value of aged specimen measured at room temperature. k^j Thermal conductivity value on location i and at the time j. L Specimen thickness. Mean free path. l N Number of observation. Number of parameter. n P Power input. Cumulative heat added. Q Heat absorbed by heater assembly and silicone grease. $Q_{\mathbf{a}}$ Rate of heat input. q Resistance of electric heater. R R Void radius in the heat sink. R Universal gas constant. Radius. r RK_0 , RK_1 , Defined in Equation (4-7.8). RK₂, RK₃ Standard deviation. S T Temperature. Initial temperature. T,

```
T
             Temperature at the insulated surface.
TH
             Temperature at heated surface.
T_{\mathbf{f}}
             Final temperature.
T_{\mathbf{f}}
             Maximum front surface temperature.
T_{\rm m}
             Maximum back surface temperature.
Tm
             Limiting temperature.
T_{sa}
             Average specimen temperature.
Taq
             Ageing temperature.
TG
             Guard temperature.
Τj
             Temperature at location i and time j.
t
             Time.
             Heat transfer film coefficient.
٧
             Volume of the specimen.
٧
             Millivolt output of thermocouple.
             Average particle velocity.
٧
x, y, z
             Cartesian coordinate system.
X
             Sensitivity matrix, defined in Equation (2-5.4).
α
             Thermal diffusivity, units.
             Aluminum + copper in solution.
α
             Defined in Equation (4-7.6).
В
             Euler's constant = 0.5772.
γ
             Volume fraction of precipitate
η
             Maximum volume fraction of precipitate.
\eta_{\mathbf{m}}
ηj
             Volume fraction of precipitate at location i and time j.
             Maximum volume fraction of precipitate at location i and
             time j.
```

 $\begin{array}{lll} \theta & & \text{Heating time.} \\ \theta & & \text{Intermetallic compound (CuAl}_2) \\ \rho & & \text{Density.} \\ \tau & & \text{Time constant.} \\ \tau_{\pmb{i}}^{\pmb{j}} & & \text{Time constant at location i and time j.} \\ \underline{\psi} & & \text{Covariance matrix of the measurement errors.} \end{array}$

CHAPTER 1

INTRODUCTION

As received aluminum alloys, such as the 2024-T351 series, when subjected to temperatures ranging from 300-500°F undergo certain microstructural changes in which thermal, mechanical, and electrical properties are affected. Changes in the mocrostructure of as received aluminum 2024-T351, in the above temperature range, are called "precipitation hardening." The changes in mechanical and electrical properties of as received Al-2024-T351, due to precipitation hardening, have been reported by many investigators. With the exception of one study initiated at Michigan State University by Al-Araji [1], no attempts have been made to determine the effects of precipitation hardening on thermal properties of as received Al-2024-T351.

One objective of this investigation is to determine the thermal properties of Al-2024-T351 under the influence of the precipitation hardening which is an extension of the study performed by Al-Araji [1]. A further objective is to develop a more appropriate relationship for thermal conductivity, which is time- and temperature-dependent, and to relate this with the percent of precipitation for as received Al-2024-T351. More detailed objectives are given in the next section.

The measurement of thermal properties of as received A1-2024-T351 under isothermal ageing conditions was first reported by A1-Araji [1]. Temperature and time dependent values of thermal conductivity k(T,t) and specific heat $c_p(T,t)$ were given. An empirical mathematical model was also developed to predict the thermal conductivity under restricted conditions.

Values of temperature and time dependence of thermal conductivity of as received A1-2024-T351 obtained experimentally by A1-Araji [1] did not provide adequate information to correlate the thermal conductivity and percent of precipitation, and also, in some cases inconsistencies existed (see Chapter 4). Therefore, it necessitated the use of the same bar of A1-2024-T351 to verify the work that had already been accomplished and to obtain additional information needed to fulfill the objectives of this investigation.

1-1 Objectives and Importance of This Research

The following are the primary objectives of this research:

- 1. Modify previous equipment and develop additional units to accommodate the necessary transient thermal properties measurement facility for this investigation.
 - 2. Develop the associated measurement techniques.
- 3. Test the modified facility and new procedures by using a reference material such as Armco Magnetic Ingot Iron for DC Applications.
- 4. Compare the results obtained by the present method and those reported by other investigators.

- 5. Obtain values of thermal properties as a function of temperature for as received Al-2024-T351 before precipitation occurred (fast measurement cycles, so that it can be assumed that the amount of precipitation is negligible).
- 6. Obtain values of thermal properties as a function of temperature for annealed A1-2024-T351.
- 7. Perform isothermal ageing tests in the precipitation heat treating temperature range (300-500°F) to obtain values of temperature- and time-dependent thermal properties for as received A1-2024-T351 in the following manner:
 - a. obtain adequate and repeatable data in each selected isothermal ageing temperature;
 - b. hold the specimens in each selected isothermal ageing temperature for a sufficiently long ageing time so that it can be assumed that precipitation is completed at that temperature: and
 - c. choose the smallest possible time interval between the experiments, in the initial stage of precipitation and at high ageing temperatures, in order to obtain as many data points in relatively short measurement time as is possible.
- 8. Mathematically model the results of experiments and determine the relationship between k(T,t) and volume fraction of precipitation.

This research is important for several reasons:

1. The aluminum alloys of 2024-T351 series are commercially available and are used in various segments of the space industry and

in domestic heating equipment. To design the equipment to operate safely, a precise knowledge of the properties may be required.

- 2. In heat transfer applications, a knowledge of thermal properties are needed to solve the equation of conduction. The mathematical model of thermal properties (time and temperature dependent) resulting from this investigation may be used in equation of conduction to determine the temperature history of A1-2024-T351 accurately.
- 3. The change in thermal conductivity of A1-2024-T351 due to precipitation hardening is postulated to depend upon the amount of precipitation. Assuming this is true, the relationship involving thermal conductivity can also be used to determine the volume fraction of precipitation. The mathematical model of thermal conductivity and subsequently, the precipitation relationships, are important and useful not only in heat transfer applications but also in metallurgy and material science to study the microstructural changes of heat treatable alloys under the influence of ageing temperatures.
- 4. Accurate measurements of thermal properties using transient methods are attractive to scientists and related experts because of short measurement time, reduced cost of operations, and reduced heat losses. In addition, the transient methods can be used for materials whose thermal properties change rapidly with time. The transient procedure and the newly developed measurement techniques proved to be accurate (see Chapter 2) and rapid (approximately 35 seconds test duration for A1-2024-T351). The method can

be used for any heat treatable alloys, non-heat treatable solids, and biological materials to determine the thermal conductivity, specific heat, and thermal diffusivity simultaneously from a single test.

1-2 Literature Review

The kinetic theory of gases suggests the simple expression for the thermal conductivity

$$k = \frac{1}{3} \rho c_p v \ell \qquad (1-2.1)$$

where v is an average particle velocity, ℓ is mean free path, and ρc_D is heat capacity per unit volume.

In solids, usually more than one kind of excitation is present. Since the energy of various excitations (lattice wave, electronics excitations, and in some cases electromagnetic waves, spin waves, etc.) gives rise to the thermal conductivity, an equation analogous to (1-2.1) can be written by including the contributions of each kind of excitation to the thermal conductivity. A generalized form of expression for the thermal conductivity of solids is given by [2]

$$k = \frac{1}{3} \sum_{i} (\rho c_{p})_{i} v_{i} \lambda_{i}$$
 (1-2.2)

where the subscript i denotes the kind of excitation, and the summation is over all kinds.

Unfortunately, difficulty arises in estimating the components of equation (1-2.2). For some materials in particular,

there is no adequate theory available to predict the values of mean free path ℓ [2], and hence this method for determining the thermal conductivity of all solids cannot be used at the present time.

The determination of thermal conductivity with an experimental arrangement is accomplished by using a solution of the differential equation of conduction. The transient one-dimensional differential equation of conduction for homogeneous isotropic plates can be written as:

$$\frac{\partial}{\partial x} \left(k \frac{\partial T}{\partial x} \right) = \rho c_p \frac{\partial T}{\partial t}$$
 (1-2.3)

A steady state solution of Equation (1-2.3) with no radial heat losses and constant thermal conductivity leads to the well-known expression:

$$q = -k \frac{T(0) - T(L)}{\int_{0}^{L} \frac{dL}{A}} = kA \frac{\Delta T}{L}$$
 (1-2.4)

where q is the rate of energy input, A is the area normal to heat flow, and ΔT is the steady state temperature drop across the thickness L.

For heat flow in a circular cylinder of infinite length and with heat flow between radii r_1 and r_2 ($r_2 > r_1$) the equation analogous to (1-2.4) is

$$q = -k \frac{T(r_1) - T(r_2)}{r_1} = 2\pi k \frac{\Delta T}{\ln \left(\frac{r_2}{r_1}\right)}$$
 (1-2.5)

By measuring the energy input rate q and the steady state temperature drop ΔT , Equations (1-2.4) and (1-2.5) can be used to calculate the thermal conductivity. Based upon these equations, various suitable experimental devices have been developed to determine the thermal conductivity under steady state conditions.

The present investigation cannot use steady state methods because thermal properties of as received A1-2024-T351 are time and temperature dependent and most steady methods need a relatively large time for equilibrium. Since the present investigation requires a transient method to determine the thermal properties, a detailed description of steady state methods are not given, although the names of a few methods and corresponding references are mentioned.

One of the most accurate methods of steady state is the so-called Guarded Hot Plate Method. The National Bureau of Standards has used this method for the measurement of the thermal conductivity of low thermal conductivity materials [2, 3].

McElroy and Moore [4] investigated five different classes of radial heat flow methods to obtain the thermal conductivity of solid materials. It is reported that their configurations are most suitable for measurements on powders and loose fill insulations.

Watson and Robinson [5] modified Equation (1-2.4) to determine the thermal conductivity of solids and heat losses simultaneously from the results of two experiments.

1-3 Transient Methods

For each different set of boundary conditions, there is a unique solution to the transient equation of conduction (1-2.3) and hence, a possible new transient method to measure the thermal diffusivity, thermal conductivity, and/or both. Based on these solutions, various transient experimental equipment has been designed to determine the thermal properties. Each transient method, in general, differs from the others in the choice of the boundary conditions, heat source, and/or geometry.

In this section, the advantages of the transient methods over steady state methods are given briefly and in the remaining part of this chapter several transient methods are described.

The advantages of transient methods for measuring thermal-transport properties over the steady state methods are: First, the value of thermal diffusivity cannot be measured directly by steady state methods. However, by measuring thermal conductivity, specific heat, and rate of energy input, the value of thermal diffusivity can then be determined. In transient methods of measuring thermal diffusivity the rate of energy input is not needed. Second, the transient methods are faster than steady state, therefore the heat losses have a lesser influence when measurement times are short. Third, in most transient methods, accurate and

rapid-response instruments are essential. Fortunately, great advances in the field of instrumentation have been made in the past decade and are continuing. These advances have improved transient property measurements a great deal. Unfortunately, steady state methods cannot benefit to the same extent from these advances.

1-3.1 Modified Angström Method

The Angström method is the oldest periodic temperature method developed to determine thermal diffusivity of solids. The describing differential equation for this method is a modification of that given in (1-2.3). The one-dimensional equation of conduction with surface heat losses (radiation, conduction, and convection) and constant thermal conductivity may be written as:

$$\alpha \frac{\partial^2 (T - T_i)}{\partial x^2} = \frac{\partial (T - T_i)}{\partial t} + u (T - T_i)$$
 (1-3.1)

where T - T_i represents the transient temperature change in the sample, and u is a coefficient of surface heat losses (which takes into account heat losses by radiation, conduction, and convection). Equation (1-3.1) can be applied to various geometries with a periodic or sinusoidal heat source [6].

Sidles and Danielson [7] applied Equation (1-3.1) to a semi-infinite radiating rod with a heat source located at one end, whose temperature varies sinusoidally with time. The detailed mathematical derivations of the modified Angström method and measurement procedures are given in [6, 7]. A brief derivation of the

working equations is also described by [1]. A more complete description of the method, modifications, and application of Equation (1-3.1) to the other geometries can also be found in [6]. The mathematical derivations of this method are not repeated here. However, a brief description of the differences between the present method and modified Angström method is given below.

The following are the major differences between the present method of determining the thermal properties and the modified .
Angström method:

- 1. Although a similar transient partial differential equation like that of (1-2.3) is applied to a flat plate with one side heated and the opposite side insulated, the mathematical approach of the present method is quite different from the modified Angström method (see Chapter 2 for mathematical derivations of working equations of the present method).
- 2. The modified Angström method is quasi-steady state while the present method is transient.
- 3. In the modified Angström method a heat source whose temperature varies sinusoidally is needed. The present method does not have such a restriction.
- 4. The geometries are different (semi-infinite for the modified Angström method and finite for the present method).
- 5. The modified Angström method yields directly only the thermal diffusivity from a single test, while the present method is a multi-property method.

1-3.2 Line Source and Probe Methods

The solution of the transient differential equation of conduction (1-2.3) for an infinitely long, continuous, thin heat source, embedded in an infinite, homogeneous medium, initially at equilibrium is given [8] as:

$$T - T_i = -\frac{q}{4\pi k} \operatorname{Ei} \left(-\frac{r^2}{4\alpha t} \right)$$
 (1-3.5)

where T - T_i is the temperature rise in the medium at a distance r from the line heat source, q is a constant heat rate per unit length liberated from this source at the start of t=0, and α and k are thermal diffusivity and thermal conductivity of the medium, respectively. -Ei(-z) is the exponential integral which for small values of z may be approximated by the series expansion,

Ei
$$(-z) = \ln(z) - z + \frac{1}{4}z^2 + \cdots + \gamma$$
 (1-3.6)

where γ is Euler's constant = .5772156. For sufficiently large values of t, $z = \gamma^2/4\alpha t$ becomes small and then Equation (1-3.6) can be used in (1-3.5) to obtain

$$T - T_i \approx \frac{q}{4\pi k} \left[\ln t + \ln \left(\frac{4\alpha}{r^2} \right) - \gamma \right]$$
 (1-3.7)

For a time interval t_2 - t_1 , the temperature rise ΔT at a point in the medium is

$$\Delta T = \frac{q}{4\pi k} \ln \left(\frac{t_2}{t_1} \right)$$
 (1-3.8)

A plot of ΔT versus $\ln (t_2/t_1)$ is a straight line with a slope of $q/4\pi k$. From the measured temperatures and corresponding times, the slope of the plotted line can be determined. Using the known values of q the value of k can be calculated.

Taylor and Underwood [9] modified Equation (1-3.8) to be

$$\Delta T = \frac{q}{4\pi k} \ln \left(\frac{t_2 - t_c}{t_1 - t_c} \right)$$
 (1-3.9)

where $t_{\rm C}$ is a time constant factor which is used to correct the data obtained. The value of $t_{\rm C}$ has to be found experimentally for each particular material to take into account the uncertainties introduced by the effects of contact resistance and the presence of temperature sensor.

The determination of thermal conductivity by the probe method is an extension of the line source method. Wechsler and Kritz [10] used Equation (1-3.9) and evaluated the performance of 18 laboratory probes for soil and insulation material at various low temperatures.

The line source and probe methods are reported to be suitable for low thermal conductivity materials and plastic foam, powders, rock, etc. The disadvantages of these methods are the uncertainties introduced by the effects of contact resistance and material dependence of the value of $t_{\rm c}$ in Equation (1-3.9). See [2], pp. 376-388. Another disadvantage is that these methods are quasi-steady state and accurate values of thermal property cannot be obtained if the properties of the material are time dependent.

The major differences between the present method and the line source and probe methods are the following:

- 1. Same as 1 in Section 1-3.1.
- 2. Same as 2 in Section 1-3.1.
- 3. For the line source and probe methods a constant heat source is needed. The present method does not have such a restriction.
- 4. The geometries are different.
- 5. The line source and probe methods are single property methods. With these methods only the values of thermal conductivity can be determined. The present method is a multi-property method.

1-3.3 The Flash Method

The flash method [11] is a transient procedure for which the heat source is flash lamp or some other almost instantaneous heat source. The method can be used to determine thermal diffusivity, heat capacity, and thermal conductivity. Small thermally insulated specimens of uniform thickness are mounted in a ceramic holder. The front surface of the specimen is blackened with camphor black to increase the absorptivity of the surface. The energy input to the sample comes from a commercial flash tube. The specimen assembly is installed a short distance from the envelope of the flash lamp. Chromel-alumel thermocouple leads are pressed against the back surface and the signal from the thermocouple is recorded using an oscilloscope.

The derivation of the equations utilized in this method are found in [1, 3, 11]. It is appropriate to mention the working equations to clarify the differences between the flash method and the present method.

Parker and coworkers [11] assumed that the pulse radiant energy is absorbed instantaneously and uniformly in a small depth at the front surface of the thermally insulated solid of thickness L. For this case and for opaque materials the temperature history at the insulated surface is given [3, 11] as:

$$\frac{T(L,t) - T_i}{T_m - T_i} = 1 + 2 \sum_{n=1}^{\infty} (-1)^n e^{-n^2 \omega}$$
 (1-3.11)

where

$$\omega = \pi^2 \alpha t / L^2,$$

 α = thermal diffusivity,

T_i = initial temperature,

T(L,t) = temperature at the rear surface, and

 $T_{\rm m}$ = the maximum temperature at the rear surface.

Parker et al. [11] plotted $[T(L/t)-T_i]/(T_m-T_i)$ versus ω (Figure 1 in [11]) and suggested two conditions from which thermal diffusivity could be calculated:

1. When $[T(L,t)-T_i]/(T_m-T_i) = .5$, ω is equal to 1.38, and therefore,

$$\alpha = 1.38 L^2/\pi^2 t_{1/2}$$
 (1-3.12)

where $t_{1/2}$ is the time needed for the back surface to reach half the maximum temperature rise.

2. It is also suggested that an extrapolation of the "straight line" portion of the curve given by Equation (1-3.11) may be employed to determine the thermal diffusivity α . It is rather difficult to determine what portion of the curve can be considered

to be the ideal straight line; it is also reported that a small error in the slope determination of this method can lead to a considerable error in the value of thermal diffusivity. Nevertheless, it is reported that the ω = .48 corresponds to a time in which the extrapolated straight line portion of the curve intercepts the ω axis and hence:

$$\alpha = .48 L^2/\pi^2 t_x$$
 (1-3.13)

where t_{χ} is the time axis intercept of the temperature versus time curve.

Beck et al. [12] analytically investigated the optimum heat-pulse experiment for determining thermal properties. The investigation indicates the choice of the one-half time method, that is the first method using Equation (1-3.12), is superior to any other arbitrary time (such as the 1/4 time), providing that there are no heat losses in the system. On the other hand, if it is not convenient to record the back face temperature for a sufficient time to determine T_m or the system cannot be well insulated, then the second method [Equation (1-3.13)] is more appropriate [3, 11].

If there are no heat losses and if the amount of heat absorbed by the front surface is measured, the product of the density and the specific heat of the material can be calculated from:

$$\rho c_{p} = \frac{Q}{AL(T_{m} - T_{i})}$$
 (1-3.14)

where Q is the total energy input and A is the cross-sectional area of the specimen. The thermal conductivity can be found by the relationship:

$$k = \alpha \rho c_{p} \tag{1-3.15}$$

The maximum front surface temperature rise for a flash tube radiation source is given [11] by:

$$T_f - T_i = 38 L (T_m - T_i)/\alpha^{1/2}$$
 (1-3.16)

where the constant 38 depends on the characteristic of the flash lamp, L is in centimeters, α is in centimeters squared per second, and T_m , T_f , and T_i are in °C.

The advantages of the flash method are the following:

- 1. It needs a simple energy source for a very short time interval. The flash tubes, and recently the laser, are two such energy sources which are readily available.
- 2. The use of a small-sized specimen can be considered to be an advantage of the flash method due to compact testing equipment. However, too small specimens may cause other difficulties in regard to thermocouple size, availability of surface area for thermocouple placement, and difficulties in thermocouple installation and handling, unless well-designed equipment is provided.

The disadvantages of the flash method are:

1. Both methods, that is Equations (1-3.12) and (1-3.13), of determining thermal diffusivity depend on the shape of the curve resulting from the working Equation (1-3.11). Small heat losses

and slightly inaccurate temperature measurements may result in considerable error in α .

- 2. Despite the relatively high temperature rise near the heated surface, the flash method neglects the variation of thermal diffusivity with temperature.
- 3. The effect of the relatively high temperature rise near the heated surface appears to be critical for heat treatable alloys in which time and temperature are both important. It is demonstrated for heat treatable alloys, such as received A1-2024-T351, that higher temperatures result in shorter ageing times (see Figures 3-6.1 through 3-6.8 in Chapter 3). In fact, no time is needed for alloys to reach a state of complete precipitation when ageing temperatures exceed their annealing temperatures. The maximum front surface temperature can be calculated using Equation (1.3.16) given by Parker et al. [11]. The value of the maximum front surface temperature for as received A1-2024-T351 specimen, when ageing temperature is 425°F, indicates that the portion of the specimen near the heated surface has reached the annealing temperature during the first ageing test. Therefore, no additional information for this portion of the specimen can be obtained from additional tests.

Differences between the present and the flash methods are the following:

1. As mentioned in Section 1-3.1, these methods differ in their mathematical derivations for obtaining the working equations.

- 2. In the present method, values of thermal properties are directly determined using the measured transient temperatures. The transient temperatures obtained by the flash method are used to determine $t_{1/2}$ for Equation (1-3.12) or t_x for Equation (1-3.13) by curve fitting or by visual inspection, etc. A small error in determining the values of $t_{1/2}$ or t_x may be compounded to lead to a considerable error in the values of thermal properties.
- 3. The heat losses by the present method are believed to be less than by the flash method and can be treated with less difficulty (see Chapter 2). The heater for the present method is sandwiched between two identical mating specimens. The heat source for the flash method is the radiant type and since there is no direct contact between the heat source and the specimen, the heat losses of the flash method may be much more than the present method.
- 4. The results of ageing tests for as received A1-2024-T351 at high temperatures (above 400°F), using the flash method, may be inaccurate for two reasons. First, the temperature rise near the heated surface in the flash method, unlike the present one, is relatively large. Second, the precipitation rate at high temperatures is greater (see Chapter 4). For these two reasons, a significant nonhomogeneity in the specimens occurs during ageing tests, and therefore can give inaccurate results.

1-3.4 Nonlinear Estimation Method to Determine the Thermal Properties

The nonlinear estimation method is a procedure to estimate thermal properties by making calculated temperatures agree in a least-squares sense with corresponding measured temperatures. In this transient procedure, generally a finite-difference method and a digital computer are used to reduce the solution of the equation of conduction (1-2.3) to a set of algebraic equations which are solved simultaneously. In addition to the prescription of the thermal histories of the boundaries of the sample, a transient measured temperature at a location of the sample is also needed. The measured and corresponding calculated temperatures of the prescribed location are made to agree in a least-squares sense by minimizing a sum of squares.

The computer program PROPERTY developed by Beck [13] incorporates the nonlinear estimation method. Program PROPERTY uses the Crank-Nicolson finite-difference approximation with two sets of boundary conditions to determine the thermal diffusivity or thermal conductivity and specific heat. To calculate the thermal diffusivity only, time variable heated surface temperatures and initial conditions are needed. An insulation condition could also be used for the other boundary condition to solve the partial differential equation of conduction. In addition, a measured transient temperature is needed at some location other than where the surface temperature is prescribed. A convenient location for

this additional thermocouple, in this investigation, is on the insulated surface [12, 14] opposite the heated surface.

To determine the thermal conductivity and specific heat simultaneously, the surface heat flux history must be known instead of the surface temperature. A transient temperature history measured at any location in the specimen is needed for the sum of squares function. Optimum locations for measuring transient temperatures are at the heated and/or insulated surfaces [15].

The experimental data collected by the present method can be introduced as an input to program PROPERTY to determine the thermal diffusivity or thermal conductivity and specific heat. In fact, a few sets of experimental data generated in the present research have been analyzed using program PROPERTY.

PROPERTY is a multi-purpose program with several built-in options. It can be used in composite geometry to determine the thermal properties of a single material. PROPERTY can also be used to determine the temperature variable properties which are given sequentially. This program provides much useful information including the sum of squares of residuals (i.e., a degree of agreement between the calculated and measured temperatures). The program, due to its versatility, requires a relatively large computer capacity; unfortunately, it cannot be run on the IBM 1800 computer which is readily accessible to the Department of Engineering Research.

The working equations for this investigation (derived in Chapter 2) are such that a simple FORTRAN program can make the

necessary calculations efficiently and effectively. The computer program COND (also see Chapter 2) was developed to process the experimental data obtained for this investigation using the IBM 1800 computer. Property values obtained by program COND are nearly the same as those obtained by program PROPERTY for the purpose of this investigation.

1-3.5 Linear Finite Rod and Radial Methods

The mathematical principles for linear finite rod and radial methods are similar to the nonlinear estimation method (see Section 1-3.4).

Klein et al. [16] applied the linear finite rod method to determine the thermal diffusivity of Armco iron. The transient temperature measurements were performed at three different locations along the length of the finite rod with a coaxial radiation guard of the same material. A heater was attached to the sample at one end to provide the energy input. In each test, the measurement of transient temperatures at the first and third locations of the rod were used as empirical boundary conditions. Assuming a constant thermal diffusivity for each test (small temperature rise) and estimating an initial value of α , the transient differential equation of conduction (1-2.3) was solved by a finite-difference method. Using the estimated α , empirical boundary conditions, and initial temperature, a set of values of temperatures as a function of time were calculated for the second locations. The calculated and corresponding measured temperatures then were

compared and minimized in a least-square sense to obtain the thermal diffusivity [16].

Carter et al. [17] used a three cylindrically symmetric stack of disks with an axial heater. This method because of its geometrical configuration is called the "radial method."

Three thermocouples were embedded in the midplane at three radii to record the temperature as a function of time. A calculation procedure similar to the linear finite rod method then follows and thermal diffusivity of the sample can be determined.

CHAPTER 2

APPARATUS AND TRANSIENT METHOD OF DETERMINING THERMAL PROPERTIES: APPLIED TO ARMCO IRON

This chapter is divided into several sections, each dealing with an important part of the transient method for determining the thermal properties of solids. The first section concerns the analysis developed by Beck [18]. Since detailed derivations of the method are given in [1, 18, 19], only the working equations and the related assumptions are described in the first section of this chapter.

The second section of this chapter deals with the adaptation of the previous experimental apparatus to a thermofoil electric heater as a heat source, and development of several new components to accommodate the necessary transient measuring equipment for determining the thermal properties for this investigation.

In the third section a new procedure for transient temperature measurements is described. The thermal conductivity and specific heat of the reference material, Armco Magnetic Ingot Iron, as a function of temperature are determined. To perform the transient temperature measurements and carry out the necessary calculations, numerous computer programs are developed.

In the fourth section a detailed error analysis is given and the possible errors are investigated. In this study the

working equations are modified to take into account the estimated combined radiation, conduction, and convection heat losses. The values of thermal conductivity and specific heat are compared with literature values. Recommended values of thermal conductivity and specific heat of Armco iron as a function of temperature are given in the last section.

2-1 Development of Working Equations

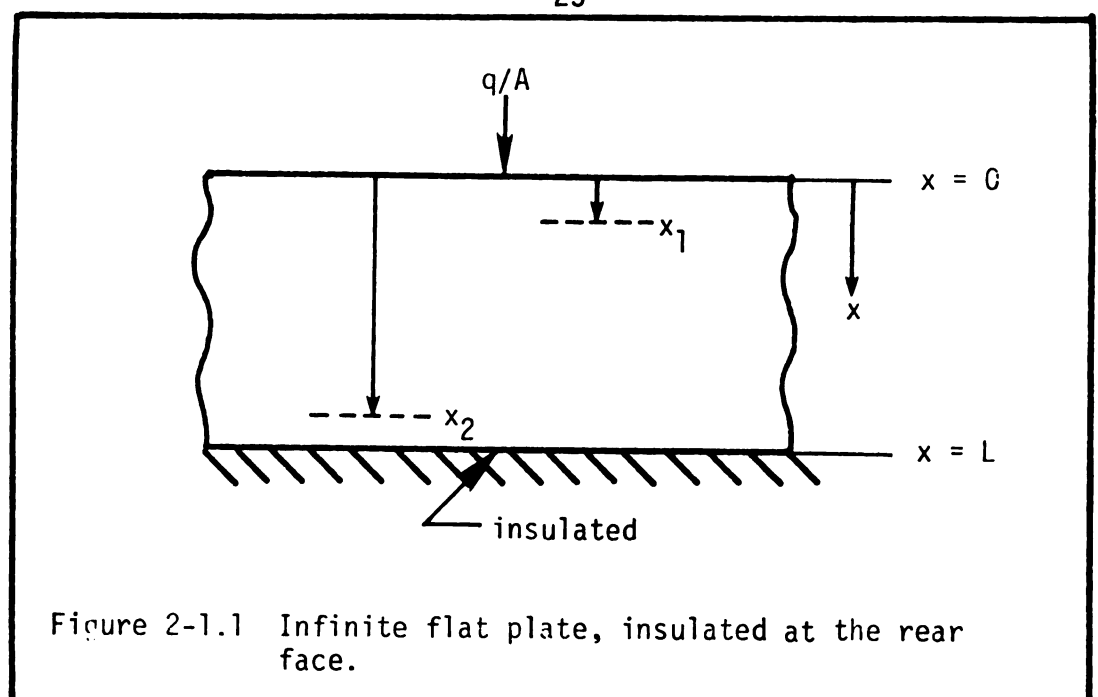
The general partial differential equation of heat conduction with no internal heat generation can be written as:

$$\frac{\partial}{\partial x} \left(k \frac{\partial T}{\partial x} \right) + \frac{\partial}{\partial y} \left(k \frac{\partial T}{\partial y} \right) + \frac{\partial}{\partial z} \left(k \frac{\partial T}{\partial z} \right) = \rho c_p \frac{\partial T}{\partial t}$$
 (2-1.1)

where k, ρ , c_p , T, and t are thermal conductivity, density, specific heat, temperature, and time, respectively.

Beck [18] introduced a transient method for the determination of thermal conductivity and specific heat which can be applied to various geometries [1, 19]. The detailed derivations can be found in [19]. The thermal conductivity (k) of a flat plate with thickness L heated on one side and insulated on the opposite side (Figure 2-1.1) can be calculated using:

$$k = \frac{\frac{Q}{A} \frac{L}{2} \left[\left(\frac{x_2}{L} - 1 \right)^2 - \left(\frac{x_1}{L} - 1 \right)^2 \right]}{\int_0^{\infty} [T(x_2, t) - T(x_1, t)] dt}$$
(2-1.2)



In developing Equation (2-1.2), the following assumptions are made:

- Thermal conductivity (k) remains constant for the short heating time and small temperature rise across the specimen;
- 2. the cumulative heat added (Q) during heating period is finite;
- 3. the density of specimen (ρ) is constant;
- 4. there are no heat losses; and
- 5. the solid is homogenous.

The upper limit of integration in Equation (2-1.2) corresponds to a time elapsed in which the specimen attains its equilibrium temperature.

The cumulative heat flux (Q/A) added to the plate is given [19] as:

$$\frac{Q}{A} = L \int_{T_i}^{T_f} \rho c_p dT$$
 (2-1.3)

where T_i and T_f are the initial and final uniform temperatures of the specimen, respectively. If the temperature rise due to a short heating time is small, then the temperature dependency of (ρ) in Equation (2-1.3) can be ignored. Let us define

 $\bar{c}_p = \int_{T_i}^{T_f} c_p \, dT/(T_f - T_i)$, with this assumption and definition, it follows that $\rho \int_{T_i}^{T_f} c_p \, dT = Q/AL$ or

$$\bar{c}_{p} = \frac{Q/A}{\rho L \left(T_{f} - T_{i}\right)} \tag{2-1.4}$$

The assumptions 2, 3, 4, and 5 made in Equation (2-1.2) also prevail in Equation (2-1.4).

Utilizing the required measurements, Equations (2-1.2) and (2-1.4) are used to calculate the thermal conductivity and specific heat, respectively.

During the experiments the transient temperatures are measured in order to evaluate $\int\limits_0^\infty \left[T(x_2,t)-T(x_1,t)\right]dt$. Also, the heat input (Q), initial temperature (T_i) , and final temperature (T_f) are measured. By also substituting the numerical values of x_1 , x_2 , L, ρ , and A into the working Equations (2-1.2) and (2-1.4), thermal conductivity (k) and average specific heat (\bar{c}_p) are determined.

2-2 Development and Description of Transient Thermal Properties Measurement Facility

Part of the facility used in this investigation is a modification of that described in [1]. Other parts were developed to make up the required facility for transient thermal properties measurement. The combined equipment consists of (1) a hydraulic system, (2) temperature-controlled housing, (3) temperature controllers, (4) computer signal conditioner, (5) thermocouple panel, (6) the IBM 1800 computer, and (7) a DC power supply.

For this investigation, the previously available equipment (numbers 1 through 4) were modified and the remaining (number 5 through 7) were developed, adapted, and added to the previous equipment. The combined equipment (except the IBM 1800 computer) is shown in Figure 2-2.1. A brief description of this equipment and its function for this investigation is given in this section.

2-2.1 Hydraulic System

The hydraulic system consists of (1) a hydraulic pump, (2) a non-shock cylinder-piston assembly, (3) a hand gate valve, and (4) a load frame.

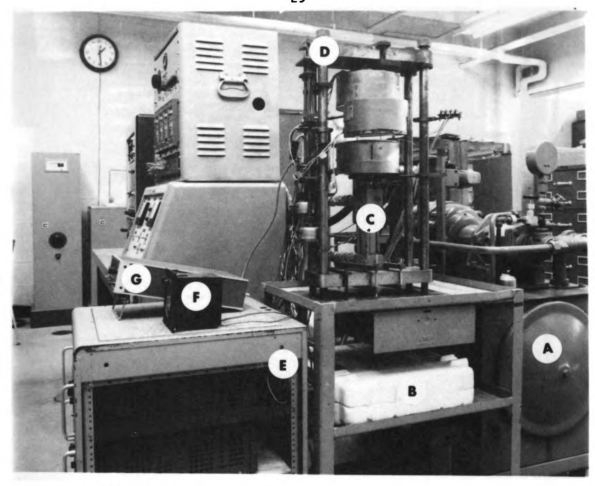
The hydraulic pump is a 20 gpm (150-1500) psi, of the pressure-compensated type, and can produce adequate force to move the piston without shocks at both ends of the stroke. The load frame assembly itself consists of two steel flat plates with four adjustable connecting steel rods.

The speed of the piston can be regulated by the hand gate valve. The non-shock cylinder-piston assembly is installed on the lower steel plate of the load frame which is attached to a steel stand.



- A--Computer signal conditioner. The computer cables are connected from back face.
- B--Amplifier digital display (DVM).
- C--Ten DC DANA amplifiers.
- D--Temperature controllers.
- E--Thermocouples panel.
- F--Control panel.
- G--Three dualled NJE DC power supplies.

Figure 2-2.la Transient thermal properties measurement facility.



A--Hydraulic pump.

B--Insulation box containing the thermocouples terminal board.

C--Cylinder-piston assembly.

D--Load frame.

E--Timer switch and relay contact.

F--Electric timer.

G--AC/DC digital multi-meter.

Figure 2-2.1b Side view of transient thermal properties measurement facility. The hydraulic system and the associated piping are also shown.



- A--Upper stationary temperature-controlled specimen housing. Upper specimen not shown.
- B--Lower movable temperature-controlled specimen housing.
- C--The lower encased specimen.
- $\ensuremath{\mathsf{D--Auxiliary}}$ specimen's heater. Not used in this investigation.

Figure 2-2.1c Temperature-controlled housing of the transient thermal properties measurement facility.

2-2.2 Temperature-Controlled Housing

The temperature-controlled housing is composed of two identical mating cylinders. The upper cylinder is fastened to the upper steel plate of the load frame while the lower one is connected to the piston of the hydraulic pump. The schematic diagram of the housing is shown in Figure 2-2.2.

Each cylinder consists of an outer shell and a guard heater. The space between the guard and outer shell is filled with high temperature Fiberglas insulation. The outer shell is made of sheet metal, while the guard is a copper cup with 7/16 inch thick walls. The height of the guard is 2.25 inches and its diameter is 4.875 inches. On the outer circumference of the guard is a helical groove containing an electrical heating coil. One end of the guard is fastened to a transite disk attached to a circular steel plate. The specimen is supported inside the guard by three 0.138 inch diameter, hollow screws. One end of each screw is fastened to the specimen while the other end is into the transite backing. Partially hollow, supporting screws were used to minimize the heat loss from the specimen.

The temperature of the guard is maintained by a temperature controller (see next section).

2-2.3 Temperature Controller

The temperature of each guard heater was controlled by an Electromax Mark III Leeds and Northrup temperature controller.

This temperature controller maintained the copper guard temperature

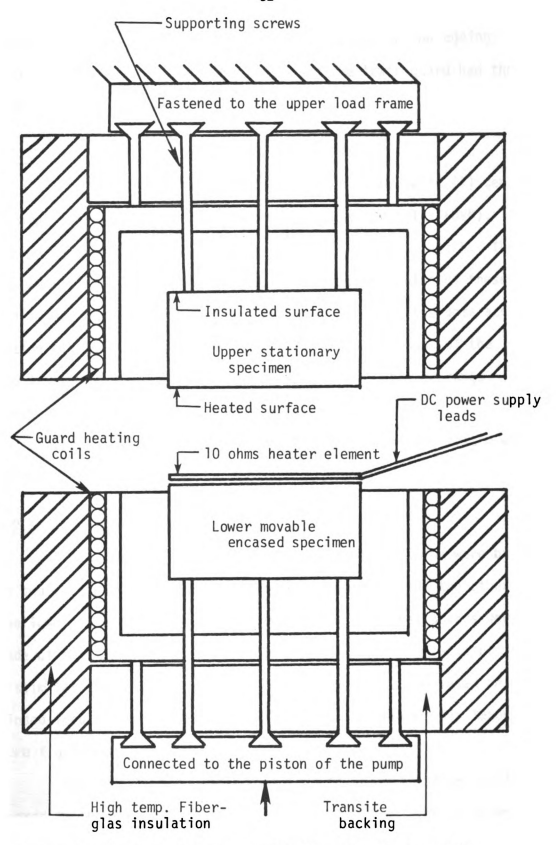


Figure 2-2.2 Temperature-controlled housing (schematic).

within 1.5°F about the set point temperature during the ageing tests. In all experiments, the upper and the lower guard had the same set point temperature.

2-2.4 Computer Signal Conditioner

The computer signal conditioner is equipped with (1) ten DC amplifiers, (2) a built-in amplifier digital display (DVM), (3) an intercom system, and (4) a computer interrupt switch. The ten amplifiers are DANA model 3400. The output of nine of these amplifiers can be transmitted by computer cables to the data acquisition station (IBM 1800 computer). The maximum output of the amplifiers is \pm 10 volts with a nominal 20 percent over range capability. The amplifier gain was selected to be 750.

Before each series of tests, the amplifiers and system were calibrated with a constant electrical DC signal.

2-2.5 Thermocouple Panel

Thermocouple leads for the heaters and specimens were brought to two terminal boards, one for the upper assembly and the other for the lower assembly. The metal strips of the terminal boards were made of similar thermocouple metals to minimize the effects of dissimilar metal junctions. The terminal boards were placed in a closed insulation box to reduce the effects of ambient air temperature fluctuations.

Copper extension leads were used to connect the terminal boards to the taper-pin terminal blocks which were located adjacent to the control panel.

2-2.6 The IBM 1800 Computer

The IBM 1800 equipment consists of an analog and a digital computer (internally connected to form a unit), a 1442 card read/punch, a 1443 line printer, an 1816 typewriter/keyboard, and a 563 call comp. The analog and digital computers can operate independently or can be used as a unit in experimental applications.

For this investigation, the analog computer received the amplified thermocouple signals resulting from the heated and insulated surfaces of the specimens. Then the corresponding digitized signals were introduced to the digital computer for storing in a process disk or for any desired mathematical operations with appropriate conversion coefficients (i.e., millivolt-temperature conversion; see also Section 2-3.4). At the end of each experiment, the digital computer of the IBM 1800 is used to calculate the thermal conductivity and specific heat using the punched, transient, digitized thermocouple's result (see Section 2-3.6). The 563 Calcomp is used to plot and tabulate the results of experiments obtained for this investigation.

2-2.7 DC Power Supply Equipment

The energy input to the specimens was obtained from three identical regulated DC power supplies (NJE Corporation, Model QR 160-3, 50-160 DC volts).

Since a single power supply could not provide sufficient current for the low resistance thermofoil electric heater (see Section 2-3.3), three identical units were dualled in a parallel

fashion according to the manufacturer's specifications [20]. By having a three dualled power supply, the input energy to the specimens can be varied from 270 to 600 watts.

The power output was controlled and timed by a triple-pole-double-throw relay contact, a timer switch, a toggle switch, and a timer (see Figure 2-2.3). Components involved in the controlling aspects of power output are the two poles of the relay contact, toggle switch, and timer switch. Two poles of the relay contact are placed in series to carry the power input to the thermofoil electric heater. The reason for using two combined poles for power was to prevent high current arcing across the poles. The duration of an experiment was nominally made 15 seconds using the timer switch. The experiment was initiated by manually pressing the toggle switch.

Components involved in the timing aspects of power output are the third pole of the relay contact and a timer capable of measuring the heating time within 0.001 minute. When the toggle switch is pressed, the timer is simultaneously activated by the third pole. When the timer switch disconnects the power input to the heater, it also disconnects the power to the electric timer.

2-3 Method of Transient Temperature Measurements to Determine the Thermal Properties of Reference Material

2-3.1 Reference Material

In order to test a new technique, it is customary to compare values obtained using the new method with the known values of a reference material. For several reasons, the reference material in

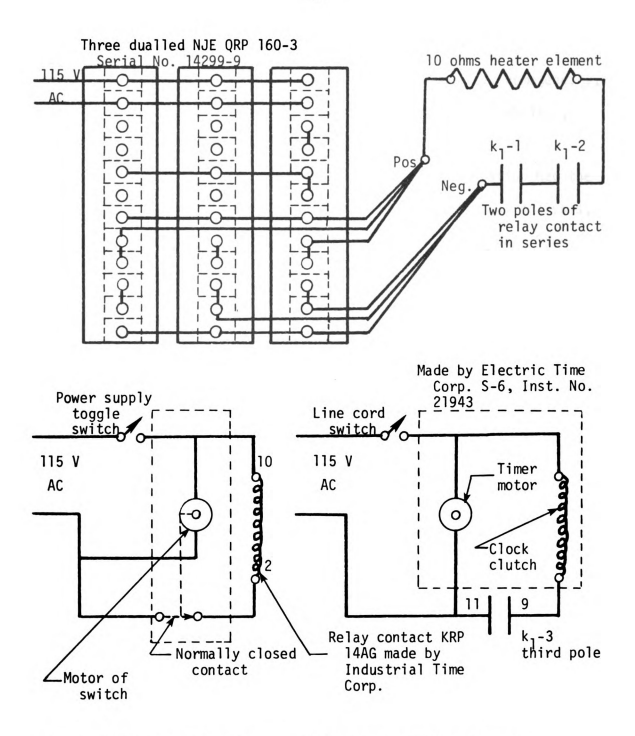


Figure 2-2.3 Schematic diagram of DC power supply equipment.

this investigation was selected to be Armco Magnetic Ingot Iron for DC Applications. These reasons include its high purity, homogeneity, stability over the testing temperature range, ready availability, and well-known property values [2, 21, 22, 23, 24].

The reference material provided by Steel Corporation had the density of 7.86 gr/cm^3 (490.70 lb m/ft³) and had a typical analysis, in weight % of C = .015%, Mg = .028%, Ph = .005%, S = 0.25%, Si = .003%, and the balance (99.924%) Fe.

2-3.2 Thermocouple Type and Installation

The thermocouple type "J" (iron and constantan) with 30 gage (0.010 inch) wire diameter was selected. Each thermocouple lead was electrically insulated with Fiberglas and the assembly was protected from moisture penetration by another layer of Fiberglas impregnated with wax. The diameter of the thermocouple assembly ranged from 0.048 to 0.050 inch.

The size selection was a compromise between minimum temperature perturbation in the specimen and the installation plus handling durability of the wires.

The millivolt output of each thermocouple was amplified, transmitted to the IBM 1800 computer, and then this calibrated transient data was converted directly to temperature.

For type "J" thermocouples the temperature-voltage relaionship can be accurately approximated by the relation $T = A + BV + CV^2$ for the temperature range of 80-500°F.

Every experiment required two specimens. Each specimen used four thermocouples on each flat surface. Thermocouples were installed on the surface 3/4 inch from the outer edge. Each thermocouple assembly was brought in through a 0.055 inch slanted hole which was drilled from the outer edge of the specimen, 1/4 inch below the flat surface and 90° apart (see Figure 2-3.1). Note that the thermocouple assembly diameter is approximately 0.050 inch and the diameter of each slanted hole is made to be no larger than 0.055 inch to minimize the error caused by drilling holes into the body of the specimen.

Four elliptical cavities were created on each flat surface by the slanted holes. Along the minor axis and away from the cavities, two slots, 0.25 inch in length, 0.010 inch in depth, and 0.010 inch in width were machined. The thermocouple assembly was brought in through the slanted hole and approximately 0.40 inch of thermocouple insulation was stripped back. The hot junction was made by placing the circular thermocouple leads into the rectangular machined grooves and peening 0.125 inch of the thermocouple elements (Figure 2-3.1). Hot junctions of this type are called separated junctions because the surface becomes an electrical conductor between the elements of each thermocouple.

It is shown [25] that the output of thermocouple in a separated junction is a weighted mean of the two individual junction temperatures plus some error. The error in a separated junction may be positive or negative, depending upon the junction temperature and the corresponding Seebeck coefficient of the thermocouple elements.

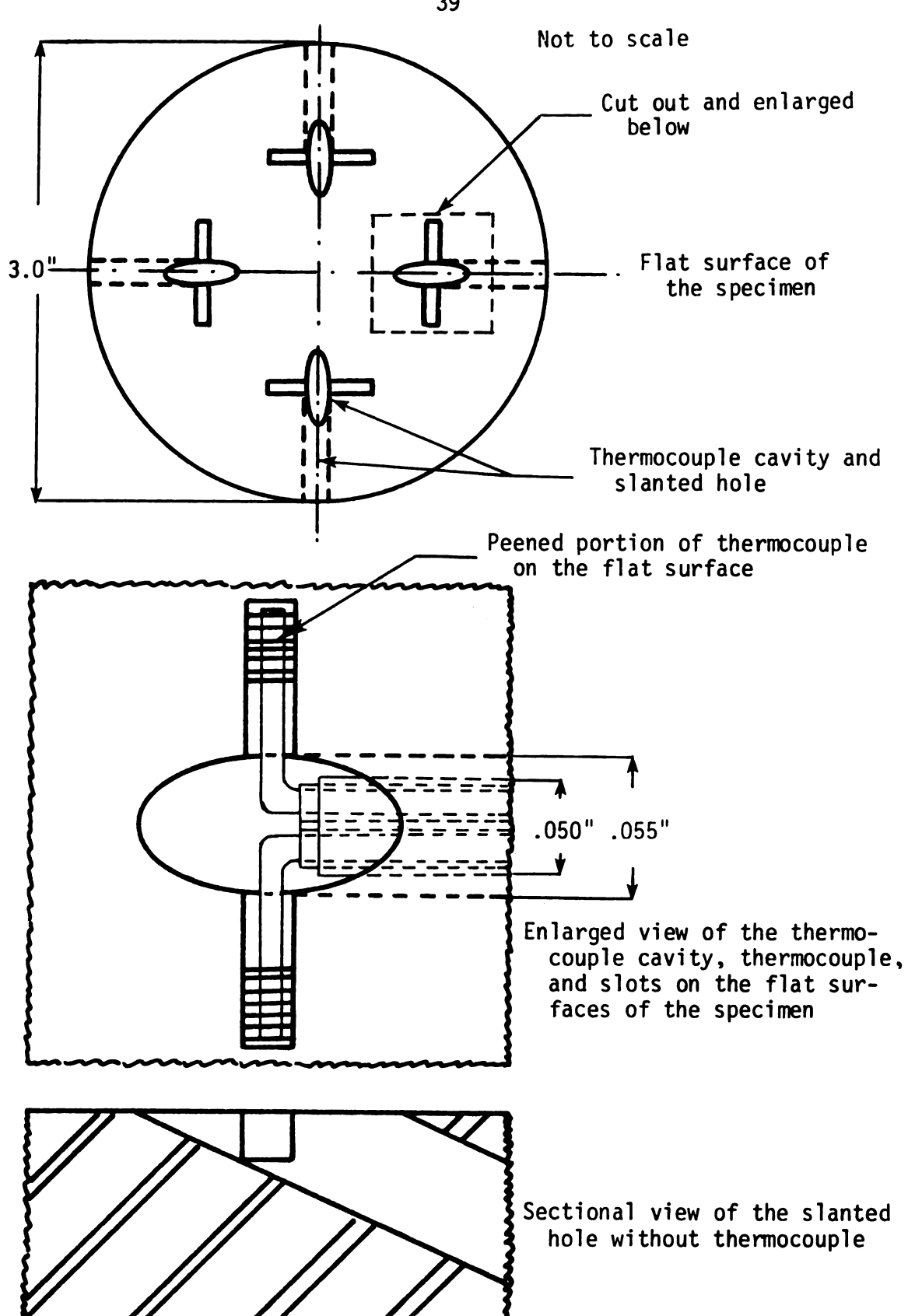


Figure 2-3.1 Thermocouple installation on the flat surface of the specimen.

The error in a separated junction is zero if the two individual junction temperatures are the same. Since the test materials have relatively high conductivities and since the leads are installed close together, the errors due to this effect are very small.

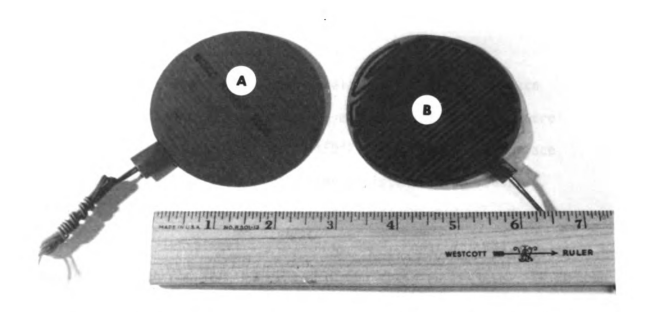
2-3.3 Electric Heater Specification and Heat Input Measurement

The thermofoil heater element is a flexible surface heater custom-made by Minco Products, Inc. Each heater is a thin, flexible, etched-element providing approximately uniform heat flux over a 3-inch diameter region. The nominal heater resistance is about 10 ohms.

Two types of heater elements were used in this investigation. One had Kapton film insulating material (with a maximum allowable temperature of 450°F), having a thickness of 0.008 inch. The other type of heater had silicone rubber insulation, with a thickness of approximately 0.016 inch, and could be used up to a temperature of 500°F (see Figure 2-3.2).

In order to increase the temperature response of the thermocouples on the heated surfaces, a 0.015 inch thick layer of the heat sink compound (silicone grease) was uniformly applied to both heated surfaces by using a special comb.

The power input to the specimens was calculated by $P = V^2/R$, where V is the DC voltage drop across the heater element and R is its electrical resistance. The DC voltage drop was measured by an AC/DC digital multi-meter, Keithley Model 171. A comparison of this multi-meter with a standard digital multi-meter, available in



- A--Thermofoil electric surface heater with silicone rubber insulation.
- B--Thermofoil electric surface heater with Kapton film insulating material.
- $\mbox{C--Two identical mating specimens with thermofoil surface heater between them. } \label{eq:condition}$



Figure 2-3.2 Two types of electric heaters and two specimens schematically arranged for an experiment.

the Department of Electrical Engineering at Michigan State University, gave nearly identical readings in the voltage range of the present investigation.

The resistance-temperature relationship of the surface heater was obtained in the following manner. The specimens were heated in steps by a heater up to 450°F. The specimens' surface temperatures and corresponding heater resistance were measured. At the end of each step, the resistance was measured by a Wheatstone-Bridge made by Industrial Instruments, Inc., Model No. RN1, Serial No. 6712, which was checked with a 10 ohm standard resistor. With this device the resistance can be measured within 0.001 ohm (0.01%).

The thermocouple output corresponding to the average surface temperature was measured by the multi-meter with a temperature reading to within $0.03^{\circ}F$.

Using the method of least-squares a temperature-resistance relationship was found. For a given thermofoil heater, a typical relationship found was R = 9.26920 + .00054 T where T is in °F. As can be seen, the resistance is a weak function of temperature.

2-3.4 System Calibration

It is absolutely necessary to calibrate the equipment that amplifies and transmits the thermocouple's signal from the laboratory to the computer. This process makes the necessary adjustments for the amplifiers and proper corrections for cables and other parts of the system.

Several methods of calibration were tried to obtain a calibration relation between the voltage output of a thermocouple, V, and corresponding temperature, T. A second order polynomial, $T = A + BV + CV^2$, was found to be adequate.

From knowledge of the testing temperature range, the type of thermocouples, and the reference junction temperature, the maximum amplifier gain can be specified. The ambient temperature, about 80°F, was selected to be the reference junction temperature. During tests the ambient temperature was also recorded and necessary corrections were made for ambient temperatures other than 80°F. Note that, in the calculations of k and \bar{c}_p , a reference temperature correction is not needed because both calculations depend only on temperature differences.

The gain of the amplifiers was adjusted in the following manner. The millivolt corresponding to the midpoint of the testing temperature was introduced to each amplifier by a parallel input connection. The output of each amplifier was observed on the digital display of the computer signal conditioner (see Section 2-2.4). The predetermined gain then was adjusted by a gain adjustment screw. Shorting out the amplifier input, a zero reading should appear on the DVM. This reading was adjusted to read zero using the zero adjustment screw. This procedure was repeated for each amplifier until no change in the zero and output readings was observed on the DVM display.

After the amplifiers were adjusted, the testing temperature span was divided into the two groups of 80 to 300°F and 300 to 500°F.

The millivolts corresponding to each subgroup temperature were found in [25] and a calibration relation was found for each group using five different temperatures.

The DC source used to obtain the millivolt corresponding to a temperature was Leeds and Northrup Potentiometer, Cat. No. 8687. The voltage corresponding to each subgroup temperature was measured by the multi-meter, and then introduced to the nine amplifiers. The output of these nine amplifiers was transmitted to the IBM 1800 computer. Computer program TAITA was used to obtain punched data cards. Computer program CALIBR uses the data resulting from the TAITA and applies the least-squares technique to determine the calibration relation.

Descriptions of programs TAITA and CALIBR are given in Sections 2-3.5 and 2-3.6, respectively.

2-3.5 Transient Temperature Measurements Using the IBM 1800 Computer

The transient temperature measurements were made using the computer program TAITA which is a multi-purpose program stored in a process disk. This program receives the output of nine thermocouples simultaneously. Then the calibrated millivolt output is directly converted to temperature using the calibration relation, $T = A + BV + CV^2$, where A, B, and C are different for each thermocouple. The temperature output of each thermocouple can be optionally punched into computer cards or printed on computer paper, and/or punched and printed for the three consecutive periods of

pretest, test, and after test. The experimental data obtained in the pretest and after test periods are not stored in the disk. In this investigation, these two periods are basically for inspections. A visual inspection can be made regarding the nonequilibrium specimens' temperature, accuracy of the calibration relation, and the time required for specimens to reach equilibrium. These periods are also useful to check the uniformity of initial and final temperatures of the specimens, proper thermocouple installations, etc.

In the test period 250 x 9 data points, with a prescribed time interval between the data points, were stored in the process disk. This period was started by the laboratory located interrupt switch and was terminated automatically by the computer after storing the 250 x 9 data points with the prescribed time interval between them. At the end of the test duration, any portion of the stored data can be punched into computer cards or all can be destroyed, if it is desired. The desired portion of the test period data (which was punched on computer cards) was used to calculate the thermal conductivity and specific heat using the computer program COND and the IBM 1800 computer. A brief description of the computer program COND is given in Section 2-3.6.

In this investigation, Armco iron specimens, 3 inches in diameter and 1 inch in thickness (see Figure 2-3.4 on page 49) were used. Tests were run with constant heat inputs between 272 and 600 watts. The heating time was fixed at 15 seconds nominally. The value of the Fourier modulus, $\theta \alpha/L^2$, associated with this heating time is 0.475 (θ is heating time, α is thermal diffusivity, and

L is the specimen thickness). For the case of constant heat flux on the heated surface and insulated at the rear face of the specimen, an optimum test duration of $(\Delta t\alpha)/L^2=0.65$ was reported in [26] (Δt is time for test duration). To find the optimum dimensionless heating time of the present investigation (which involves a constant heat flux period followed by a period of zero heat flux), an analysis similar to those in [26] is needed. The result of the analysis yields a Fourier modulus of about 0.50 for the heating time.

Several experiments with different heating times, test durations, and time intervals between the data points were performed in an effort to determine experimentally satisfactory values for the above elements in this investigation. A 15 second heating time, about 40 seconds test duration, and a 300 milliseconds time interval between the data points were found to produce satisfactory test results. The temperature history of the heated and insulated surfaces using a heating time of 15 seconds and a time interval between data points of 300 milliseconds is shown in Figure 2-3.3. Before the start of the heating period, both surfaces were at uniform initial temperatures and after about 40 seconds (see Figure 2-3.3) they again attain final uniform temperatures. Slight differences between the insulated and heated surface temperatures at initial and final stages of testing can be credited to slight inaccuracies in the calibration of the system. These slight inaccuracies are corrected when the data are used to calculate the thermal conductivity and specific heat (see next section).

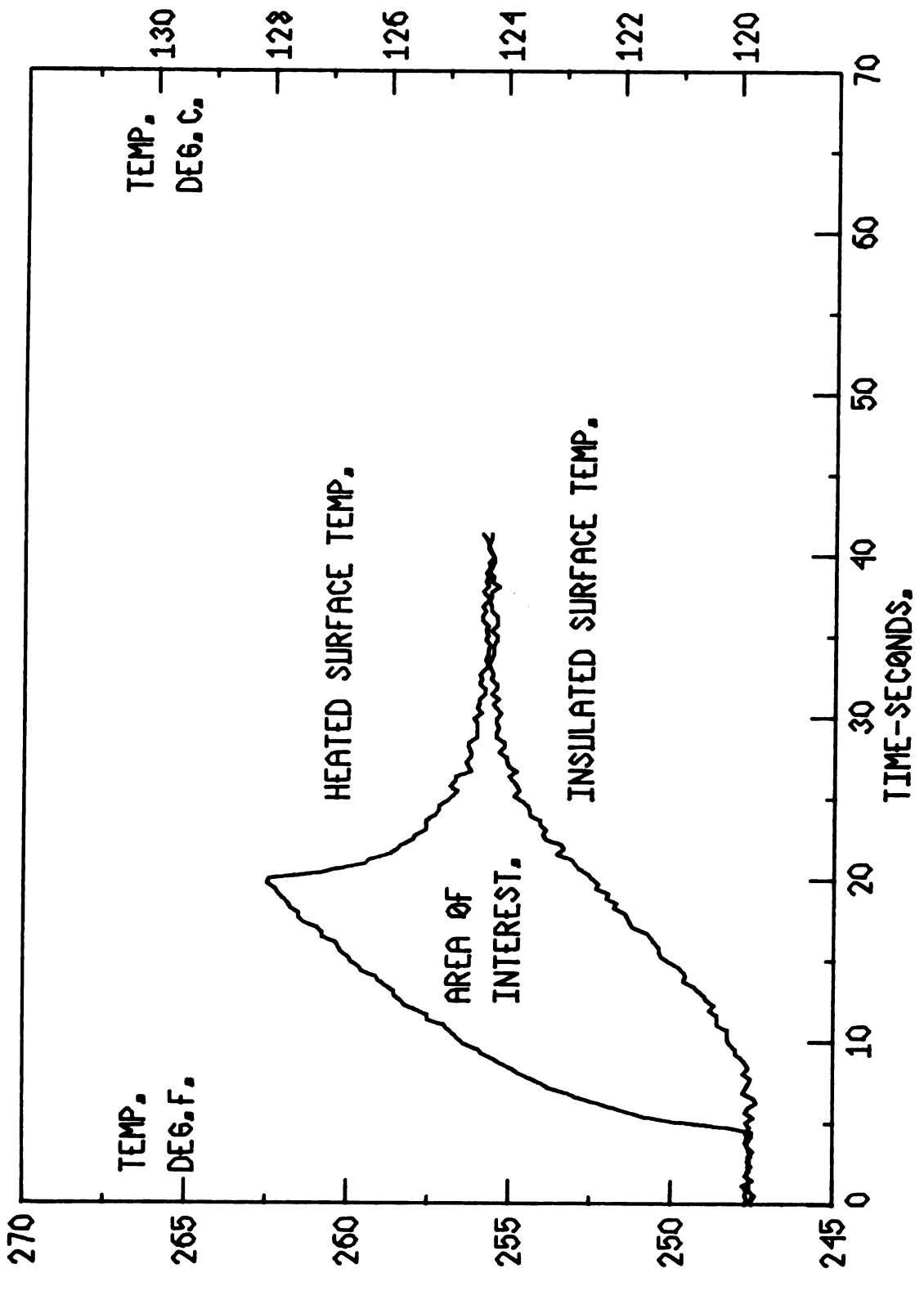


FIGURE 2-3.3 A TYPICAL HEATED AND INSULATED TRANSIENT SURFACE TEMP.

2-3.6 Calculation of Thermal Conductivity and Specific Heat

To calculate a value of thermal conductivity, transient temperature histories (resulting from two thermocouples installed at two different locations in the direction of the heat flow) are needed. Several tests with thermocouples attached to various locations of the flat surfaces of the specimen were run in an effort to determine the location which can produce satisfactory test results. The final choice of the location and the thermocouple arrangement (shown in Figure 2-3.4) was found to give repeatable results which are comparable to those of the other investigators [21, 22, 23, 24]. With two specimens in each experiment and with thermocouple arrangement as shown in Figure 2-3.4, it is possible to obtain eight independent values of thermal conductivity and specific heat from eight symmetric locations of the two specimens. There are only eight amplifiers (the last amplifier was used to record the guard temperature) available to transmit thermocouples' signals. Two thermocouples on each flat surface, 180° apart, were electrically averaged (i.e., to obtain information from 16 thermocouples using only eight amplifiers) before being amplified. With this arrangement, values of thermal conductivity and specific heat, given in the final analysis, are the average of four independent values obtained from two specimens in each experiment using 16 thermocouples.

In addition to the transient temperature measurements, the uniform initial and final temperatures of the specimens were also measured using the same thermocouples. The initial uniform

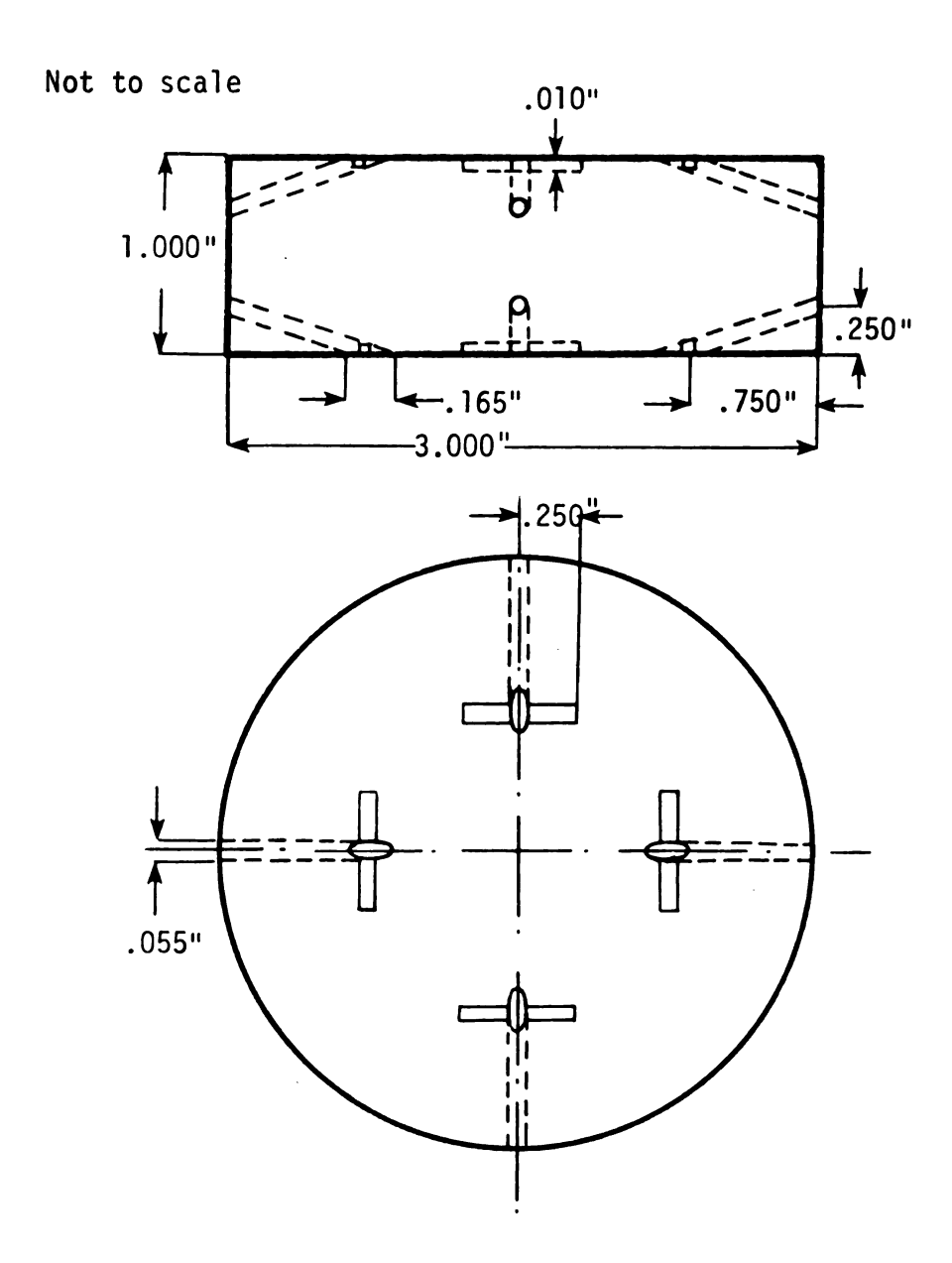


Figure 2-3.4 Thermocouple arrangement and their respective locations in the flat surface of one specimen.

the electric heater. All experiments were initiated by pressing the computer interrupt switch and 3-4 seconds later pressing the power input switch of the electric heater. The final uniform temperature was obtained by allowing sufficient time for the specimens to come to equilibrium and then taking measurements for an additional 3-4 seconds.

COND is a FORTRAN computer program that was developed to calculate the thermal conductivity k and specific heat \bar{c}_p . The input data to this program are the number of data points for the initial, transient, and final temperature measurements; the time interval between the data points; heating time; DC voltage drop across the heater; and parameters to calculate the heater resistance (Section 2-3.3). For a given specimen the sequence of calculations for k and \bar{c}_n are as follows:

- 1. calculate the average initial and final temperature, and from these obtain the average specimen temperature (T_{Sa}) ;
- 2. calculate average heater resistance, using T_{Sa} and the resistance parameters;
- obtain a set of normalization coefficients to correct the transient temperature measurements (see below) using initial and final uniform temperatures;
- 4. normalize the transient temperatures and calculate the values of k and \bar{c}_D for the four locations;
- 5. calculate the average \bar{k} and \bar{c}_p values for the experiment (a typical step-wise calculated \bar{k} is shown in Figure 2-3.5 on page 53); and
- 6. determine the variances and standard deviations for \overline{k} and $\overline{c}_{_{D}}.$

The procedure to determine the normalization coefficients is given next. The following symbols are defined as:

- 1. T is normalized and T is the uncorrected temperature for a thermocouple;
- 2. the subscripts I and H designate the insulated and heated surfaces, respectively;
- the subscripts i and f designate the initial and final temperatures, respectively; and

4.
$$\overline{T}_i = (T_{Ii} + T_{Hi})/2$$
 and $\overline{T}_f = (T_{If} + T_{Hf})/2$.

It is expected that T_{Ii} and T_{Hi} are equal and that T_{If} and T_{Hf} are equal. Since each thermocouple signal is amplified and transmitted separately, it is very difficult to measure the same temperatures for all locations despite the accuracy of the calibration. At equilibrium the specimens are at certain uniform temperatures and hence all thermocouples installed on the specimens should register very nearly the same average temperature. If they do not, the average of each thermocouple reading is made the same using the relationships:

$$\dot{T}_{I} = A_{1} + B_{1}T_{I}$$
 (2-3.1)

$$\overset{\star}{T}_{H} = A_{2} + B_{2}T_{H}$$
(2-3.2)

where A_1 , B_1 , A_2 , and B_2 are normalization coefficients. The four normalization coefficients for a given pair of thermocouples are obtained from the simultaneous solution of:

$$\overline{T}_{i} = A_{1} + B_{1}T_{1i}$$

$$\overline{T}_{f} = A_{1} + B_{1}T_{1f}$$

$$\overline{T}_{f} = A_{2} + B_{2}T_{Hi}$$

$$\overline{T}_{f} = A_{2} + B_{2}T_{Hf}$$

The transient temperatures resulting from each pair of thermocouples will be normalized according to Equations (2-3.1) and (2-3.2).

Experiments were run for two pairs of Armco iron specimens: one pair at low heat input (about 272 watts), the other at high heat input (about 540 watts). A typical step-wise calculation of \bar{k} is shown in Figure 2-3.5. The \bar{k} starts from a large value, its values decrease as time increases and after approximately 35 seconds, when specimens establish equilibrium temperature, the \bar{k} values remain practically unchanged as calculations continue. The results of the experiments are shown in Table 2-3.1.

The unbiased estimated standard deviations for \bar{k} and $\bar{\bar{c}}_p$ were calculated using:

$$S_k = \begin{bmatrix} \frac{1}{3} & \frac{4}{5} & (k_i - \bar{k})^2 \end{bmatrix}^{1/2}$$
 (2-3.3)

$$S_{c_p} = \begin{bmatrix} \frac{1}{3} & \frac{4}{5} \\ \frac{1}{3} & \frac{5}{5} \end{bmatrix} (\bar{c}_{pi} - \bar{c}_p)^2$$
 (2-3.4)

where k_i and \bar{c}_{pi} are the values of thermal conductivity and specific heat, respectively, from two sets of thermocouples installed on two opposite portions of each specimen. \bar{k} and \bar{c}_p are the average of four values of thermal conductivity and specific heat, respectively, resulting from eight symmetric portions of two specimens. The values of standard deviations are also given in Table 2-3.1. The data shown in this table indicate that the values of \bar{k} and \bar{c}_p are unaffected by using two different power inputs. Since for lower heat input the temperature rise of the specimens is lower which is important for

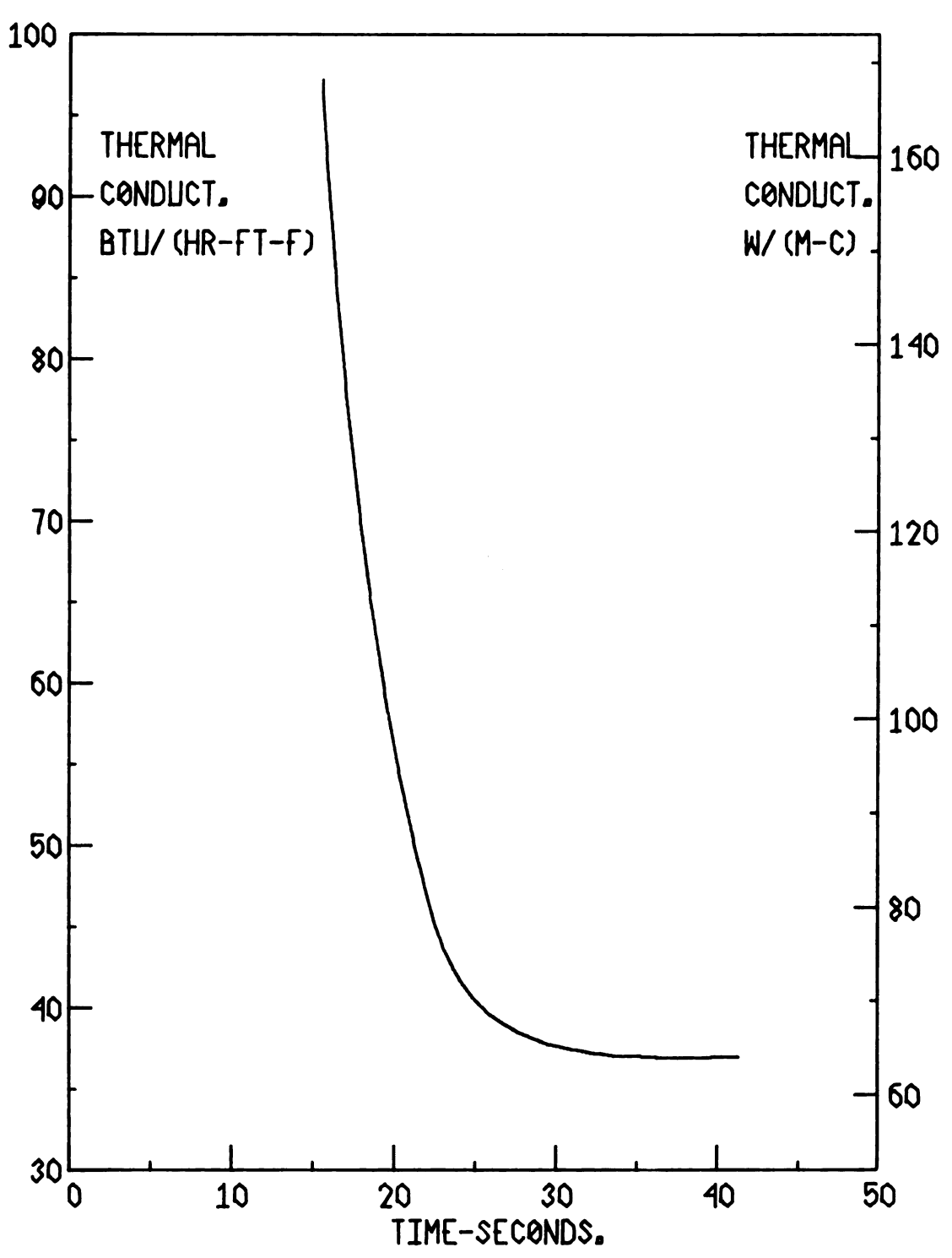


FIGURE 2-3.5 A PLOT OF STEP-WISE CALCULATED THERMAL CONDUCTIVITY (EACH STEP 300 MILLISECONDS)

TABLE 2-3.1 VALUES OF \bar{K} AND $\bar{\bar{C}}_{p}$ AND THEIR RESPECTIVE STANDARD DEVIATIONS AS A FUNCTION OF TEMPERATURE FOR ARMCO IRON.

			UNCOR	RECTED		CORRE	
RUN	SAMPLE	ĸ	s _K	ξ̄ _P	scp	ĸ	Ē₽
NO.	TEMP.	В	Τυ	В.	ГП	ЦТВ	ВТИ
	DEG.F.	HR-	FT-F	LBN	1-F	HR-FT-F	LBM-F
LOW HEAT INPUT			T (ABOUT	272 NAT1	\$)		
1 2	86.0	42.80	1.22	.114 7	.00147	42.10	.1129
2	90.0	42.35	0.30	.1181	.00167	41.81	.1159
3	149.0	39.55	1.59	.1183	.00179	38,62	-1173
4	154.5	39.54	1.10	-1180	.00087	38.96	.1157
5 6 7	205.7	37.36	1.55	.1210	.00115	37.05	.1190
6	247.0	36.37	1.00	.1207	.00153	35,21	.1206
7	251.5	37.27	1.85	. 1206	.00254	36.53	.1190
8	305.0	36, 46	3.13	-1240	.00432	36.28	.1205
9	352.5	33.91	1.11	-1286	.00331	33, 48	.1259
10	361.5	35.82	3.12	.1297	.00332	36,77	.1219
	HIGH HEAT INPUT (ABOUT 540 WATTS)						
1	97.0	42.56	2.18	.1156	.00149	42.04	.1133
3	100.0	41.56	0.66	.1176	.00128	41.16	.1151
	165.0	39.81	2.70	.1130	.00224	39.42	.1153
4	208.0	38.55	3.24	.1192	.00390	38,00	.1170
5	227.0	36.50	0.34	.1218	.00151	36.68	.1172
6	261.0	36.59	1.92	. 1210	.00332	36.25	.1181
7	270.0	35.79	0.51	.1238	.00234	35,82	.1196
	313.5	35.90	2.55	.1255	. 00485	35.74	.1219
9	362.5	34.53	0.82	.1293	.00274	34, 42	.1253
10	367.5	35.24	2.20	.1289	.00329	35, 40	.1240

temperature-dependent thermal properties materials, it was decided to use the low heat input to obtain \bar{k} and $\bar{\bar{c}}_p$ for A1-2024-T351 specimens (see Chapter III).

2-3.7 Computer Program CALIBR

In a previous section (2-3.5), the function of program TAITA and related procedures were briefly described. It was also mentioned that to operate the program nine sets of calibration relations were needed (one for each thermocouple). The equation for the millivolt-temperature conversion is $T = A + BV + CV^2$ where T is temperature and V is the millivolt output of the thermocouples. Now if we follow the same procedure, except A and C are set equal to zero and $B = 1/(gain \ of \ amplifier)$, then the data punched into computer data cards is the millivolt output of thermocouples plus some external interference (if there is any). Using this procedure with each of five temperature levels mentioned in Section 2-3.4, a new set of data can be obtained.

Computer program CALIBR is a FORTRAN program and was developed to receive five different temperatures and corresponding millivolts for nine thermocouples. For each temperature level and for each thermocouple 50 data points, with a time interval between data points of 300 milliseconds, were punched into computer cards. The program determines the average millivolts for each temperature level and for nine thermocouples, and then uses the least-squares technique to estimate the nine sets of coefficients of A, B, and C for the temperature-millivolt conversion equation of $T = A + BV + CV^2$.

2-4 Error Analysis

In any experimental method one should investigate possible causes of error and correct for them, if possible. Errors in the present experiment include:

- errors due to convection and radiation heat losses;
- 2. errors due to energy absorbed by the heater assembly and heat sink compound (silicone grease);
- 3. errors due to the unknown locations of the thermocouple junctions; and
- 4. errors due to thermal expansion.

Other errors due to presence of the thermocouples and the associated holes and thermocouple leads may also be involved. However, at the present time the mathematical and/or experimental methods of determinations are not fully available.

Klamkin [27] analyzed a case with a steady state heat flow in a semi-infinite body with vertical hole and analytically obtained the solution:

$$\frac{T_{0R} - T_{0\infty}}{(q/A) R/k} = 2/\pi$$
 (2.4.1)

where R is the radius of vertical hole and T_{0R} , $T_{0\infty}$ are the disturbed and undisturbed temperatures on the heated surface, respectively. A rough comparison of Equation (2-4.1) and working Equation (2-1.2) indicates that for a vertical and unfilled hole a correction less than 1 percent is needed. Thermal effects of a vertical void in a heat sink was also investigated by Beck and Hurwicz [28] and a relation similar to (2-4.1) was obtained. The

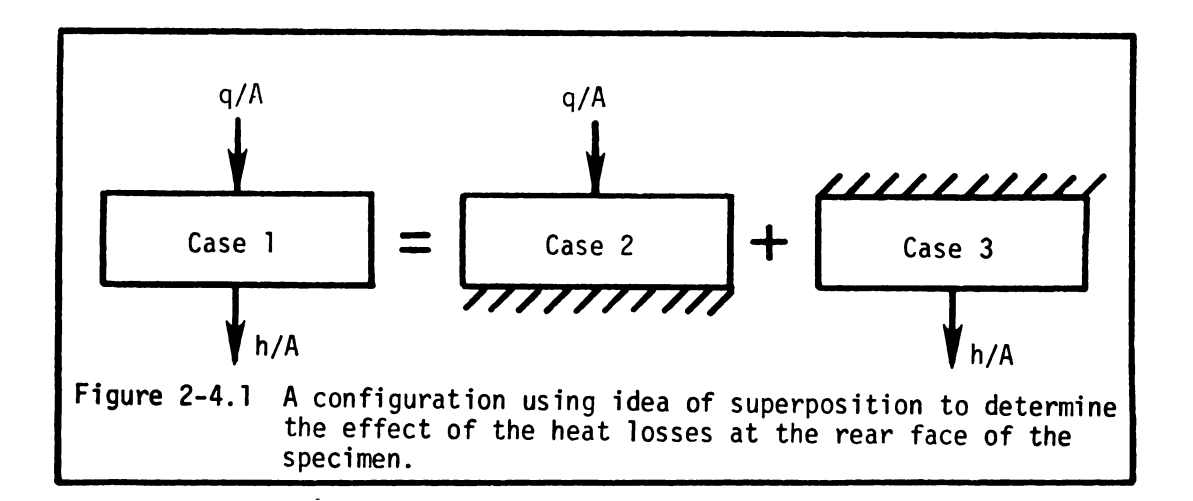
results of these analyses cannot be directly applied to the present case because of geometrical differences.

An attempt to analyze the disturbances created by the thermocouple itself was initiated experimentally. Four slanted holes with diameters of 0.055 inches, 0.125 inches, 0.1875 inches, and 0.250 inches were drilled in a symmetrical arrangement on the heated surface of a specimen. Experiments were run and comparisons were made between transient temperatures, measured on the periphery of the 0.055 inch slanted hole and the others. Consistent results were not obtained. It is believed that the disturbances created by the thermocouple itself in this investigation are small.

2-4.1 Errors Due to Convection and Radiation Heat Losses

Ť._.

The working equations for one-dimensional heat flow of Figure 2-4.1, Case 1, can be derived similarly to that of Equations (2-1.2) and (2-1.4). The derivation and terminology are identical in these equations, with the exception of the term h/A which



is the instantaneous flux of heat, gained or lost, depending upon the specimen and guard temperatures. Using the idea of superposition (see Figure 2-4.1) and assuming that the net effect in Case 1 is the sum of those of Case 2 and Case 3, or

$$\int_{0}^{\infty} \Delta T_{1} dt = \int_{0}^{\infty} \Delta T_{2} dt + \int_{0}^{\infty} \Delta T_{3} dt$$
 (2-4.2)

From Equation (2-1.2) we can obtain an expression for the $\int_0^\infty \Delta T_2 dt$. By a similar approach as in Case 2, one can obtain:

$$\int_{0}^{\infty} \Delta T_{3} dt = \frac{-\frac{H}{A} \frac{L}{2} \left(\frac{x_{1}^{2}}{L^{2}} - \frac{x_{2}^{2}}{L^{2}} \right)}{k}$$

where H/A = $\int_0^{t_1} h/A \, dt = -\int_0^{t_1} k \left[\frac{\partial T(L,t)}{\partial x} \right] \, dt$ and $\Delta t = t_1 - 0$ is the test duration. Upon substituting the $\int_0^\infty \Delta T_2 \, dt$ and $\int_0^\infty \Delta T_3 \, dt$ expressions into Equation (2-4.2) and solving for k, the result follows as:

$$k = \frac{\frac{L}{2} \left[\frac{Q}{A} \left[\left(\frac{x_1}{L} - 1 \right)^2 - \left(\frac{x_2}{L} - 1 \right)^2 \right] + \frac{H}{A} \left[\left(\frac{x_2}{L} \right)^2 - \left(\frac{x_1}{L} \right)^2 \right]}{\int_0^\infty \left[T(x_1, t) - T(x_2, t) \right] dt}$$
(2-4.3)

By using the First Law of Thermodynamics for Case 1 of Figure 2-4.1, the average value of specific heat can be determined as:

$$\bar{c}_{p} = \frac{(Q-H)/A}{\rho L(T_{f} - T_{i})}$$
 (2-4.4)

where H in equations (2-4.3) and (2-4.4) is the heat loss (or gain) due to total exposed surface area. For the calculation of thermal conductivity we assume that total heat loss occurs at the rear face of the specimens. An objective is to evaluate the value of H and then determine the corresponding correction.

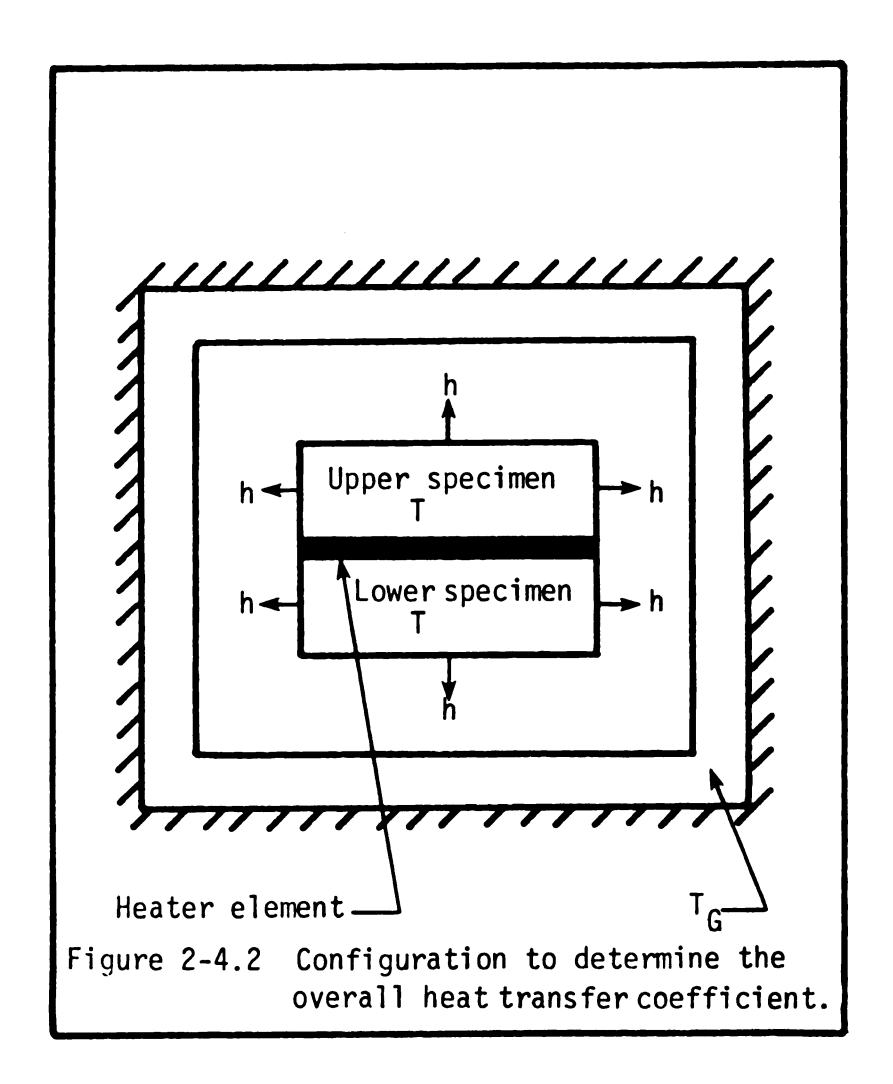
2-4.2 Determination of Overall Heat Transfer Film Coefficient

One method of calculating H is to determine the natural convection and radiation heat transfer in an air space [29]. The schematic geometry can be seen in Figure 2-4.2. The heat transfer calculations should be performed for the rear surfaces and the circumferences of the specimens. The calculations are time consuming and in some cases uncertain because the emissivities are not accurately known.

Another method of evaluating H is to determine experimentally the overall heat transfer film coefficient and then calculate the heat loss using this coefficient. Referring to Figure 2-4.2, the rate of heat loss from specimens to guards, for time larger than zero, is approximately given by:

$$h = - \rho c_p V \frac{dT}{dt} = uA_t (T - T_G)$$
 (2-4.5)

where ρ , c_p , V, and A_t are the specific weight, specific heat, total volume, and total exposed area of the specimens. Let us make the following assumptions:



- the temperature T of the specimen is uniform at any time t;
- 2. the overall film coefficient (u) is constant with time; and
- 3. the surrounding temperature $(T_{\mbox{\scriptsize G}})$ is uniform with time and position.

For these conditions the solution to Equation (2-4.5) is

$$\frac{T - T_G}{T_i - T_G} = \exp \left[-\frac{uA_t}{\rho c_p V} t \right]$$
 (2-4.6)

where T_i is the initial specimen's temperature.

 T_G , T_i , A_t , ρ , c_p and V are known. The objective is to determine the overall film coefficient (u) using measurements of T as a function of t.

To obtain measurements of T versus t, the guards and specimens were heated to a predetermined temperature T_G . Then the specimens alone were heated 15 seconds. After an elapsed time of approximately 45 seconds, temperatures versus time were recorded. Note that a one-cycle heating (15 seconds) of the specimen creates the same temperature differential between the specimens and the guards as during the tests. After one cycle of heating, the specimens gradually cool and approach the temperature of the guards.

Experiments of this type were repeated for the selected guard temperatures in the testing temperature range and the film coefficient u was determined.

The values of film coefficient for high and low heat inputs, as a function of guard temperature and specimens' temperature rise $(T_i - T_f)$ are given in Table 2-4.1.

<u>2-4.3 Regression Analysis of Heat</u> Transfer Film Coefficient

For the lower temperatures and smaller temperature differences between the specimens and guards, it can be assumed that u varies primarily with guards' temperature. For two heat inputs the values of u as a function of guards' temperature is shown in Table 2-4.1.

TABLE 2-4.1. Selected guard temperatures and corresponding heat transfer film coefficient.

	Temp. of Guards	T _i - T _f	u
Run No.	°F	°F	Btu
	,	,	(hr-ft ² -°F)
Low heat inp	ut (272 watts)		
1	81.8	7.46	1.63
2	156.9	7.38	3.34
3	204.6	8.48	3.58
4.	255.1	8.17	3.67
5	303.6	8.67	5.21
6	352.5	6.51	6.41
7	405.2	7.12	8.63
High heat in	put (540 watts)		
1	83.0	15.17	1.66
2	155.8	13.06	2.62
3	205.1	15.62	2.87
4	255.6	15.28	3.50
5	307.5	16.28	4.29
6	353.1	13.88	4.95

A least-squares technique can be performed to obtain the functional relationship between u and guards' temperature. For a given heat input this relationship can be written as a polynomial of degree n

$$u = \sum_{n=0}^{n} A_n T_G^n$$
 (2-4.7)

where A_n are parameters and will be determined with a set of experimental data.

The unbiased sample variance of u is defined as:

$$S^{2} = \frac{1}{N-n-1} \sum_{i=1}^{N} (u_{i} - \hat{u}_{i})^{2}$$
 (2-4.8)

where N is the number of observations, u_i is data given in Table 2-4.1, and \hat{u}_i is the corresponding estimated value from Equation (2-4.7).

In performing the least-squares method with a statistical justification, it is assumed that errors are independent (independent observation), and have a zero mean, constant variance, and normal or Gaussian distributions.

The question is how high an order of the polynomial must be used to obtain a reasonably good fit. There are some possible arbitrary criteria [30] and a statistical method for an optimum value of n. An arbitrary criterion states that a value of n is optimum if the sample unbiased standard deviation, S, obtained from Equation (2-4.8) is minimum, or the next higher order polynomial causes a 10 percent or less reduction in the value of S.

The statistical method of obtaining an optimum value of n is more complicated. This method will be applied to the data of Table 2-4.1 and an optimum number of parameters with their numerical values will be determined.

The method is based on statistical F distribution [31]. The form of a statistic $F_{\mathbf{x}}$ is defined as:

$$F_{x} = \frac{S^{2}(n-1) - S^{2}(n)}{S^{2}(n)/(N-n-1)}$$
 (2-4.9)

This ratio is said to have one degree of freedom for the numerator and N-n-1 degree(s) of freedom for the denominator; the ratio is a measure of how much the additional term in the polynomial can improve the fit. For a 5 percent probability and various values of N-n-1, the corresponding values of F are found in [31] and are shown in Table 2-4.2. The criterion is that the additional term is not needed if

$$F_{x} < F \tag{2-4.10}$$

Comparing F and observed values of $F_{\rm X}$ given in Table 2-4.2 and with given F-test criteria in Equation (2-4.10), it can be concluded that, for both heat inputs, only two parameters are needed for a good fit.

The two linear equations to calculate the overall film coefficient are, for low heat input,

$$u = -0.2963 + 0.0196 T_G$$
, (2-4.11)

and for high heat input,

$$u = 0.6235 + 0.0118 T_{G}$$
 (2-4.12)

where T_G is in °F and can be used between 80 and 425 °F and u is in $Btu/(hr-ft^2-°F)$.

TABLE 2-4.2 F-test criteria to determine the optimum value of order of polynomial n for a good fit.

n = Degree of Polynomial	No. of Parameters	D.F. = Degree of Freedom N-n-l	S(n)*	S(n-1)-S(n) (a)	S(n)/D.F. (b)	F _x = a/b	**
N = 7 = Experin	= Experimental data pc	points, low heat input	input				
0	_	9	32.192				
_	2	S	2.712	29.48	.542	54.39	6.61
2	ო	4	1.189	1.523	.297	5.13	7.71
က	4	က	.374	.815	.124	6.57	10.1
4	S	2	.172	.202	980.	2.35	18.5
N = 6 = Experi	= Experimental data po	points, high heat input	input				
0	_	2	7.078				
_	2	4	101.	6.977	.025	279.08	7.71
2	က	က	.058	.043	.019	2.26	10.1
က	4	2	.036	.022	.018	1.22	18.5
4	വ	_	.004	.032	.004	8.00	161.0

*Defined in Equation (2-4.8).

**P. R. Bevington, Data Reduction and Error Analysis for the Physical Sciences (New York: McGraw-Hill Book Co., 1969), p. 318.

A plot of u versus temperature for low and high heat inputs is shown in Figure 2-4.3.

Knowing the overall film coefficient, the heat loss in one single test can be determined by

$$H = A_t u (T_{Sa} - T_G) \Delta t$$
 (2-4.13)

where $T_{Sa} = (T_i + T_f)/2$, A_t is the total exposed surface area of specimens, and the quantity Δt is the test duration of 41.4 seconds.

2-4.4 Computer Program NLINA

The NLINA is a FORTRAN computer program developed to estimate linear and nonlinear parameters.

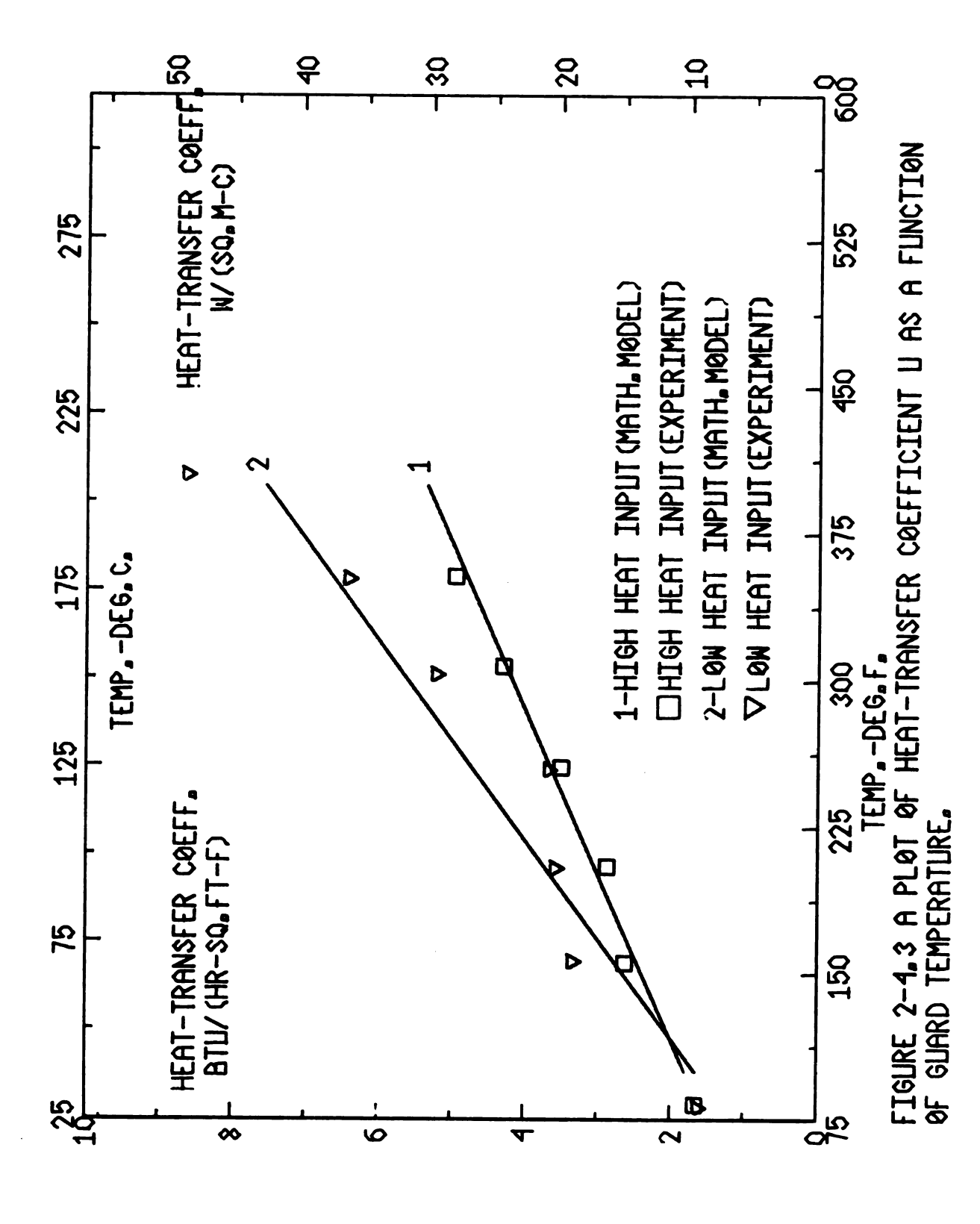
The program uses the Gaussiterative procedure with the Box-Kanemasu [32] modification. Convergence frequently occurs in less than 5 iterations for well-designed experiments with good initial parameter estimates.

NLINA computer program was used to estimate the heat transfer film coefficient u in Equation (2-4.6). The estimated values of u as a function of guards' temperature are shown in Table 2-4.1.

Applications of NLINA for the more complex nonlinear parameters are given throughout Chapters 3 and 4.

2-4.5 Errors Due to Energy Absorbed by the Heater Assembly and Heat Sink Compound (Silicone Grease)

The electric heater used in the measurement of the properties of Armco iron was the Kapton type (see Section 2-3.3) with a heater element thickness of 0.008 inch. The two heated surfaces



contained a layer of approximately 0.015 inch of silicone grease. The silicone grease was spread by a special comb to provide uniform distribution throughout the heated surfaces. Much of the silicone grease squeezes out whenever the two heated surfaces, with the electric heater in between, are pressed together. We assume that one-half of the silicone grease squeezes out. Then the thickness L_{Sh} of the silicone grease and heater element is 0.015" + 0.008" = 0.023". Then the amount of heat absorbed by the silicone grease and the heater element can be calculated by:

$$Q_a = \rho c_p L_{Sh} A (T_f - T_i)$$
 (2-4.14)

where Q_a is the amount of heat absorbed by the silicone grease and the heater element. The ρc_p product for most solids (excluding porous materials) is between 40 to 55 Btu/(ft³-F). Since this product is not known for silicone grease or Kapton and further, since L_{Sh} is uncertain, the value of $\rho c_p = 52.0$ Btu/(ft³-F) was arbitrarily chosen. Using Equation (2-4.14) the values of Q_a are calculated for low and high heat inputs and are listed in Table 2-4.3.

<u>2-4.6 Errors Due to Unknown Location of the Thermocouple Junctions</u>

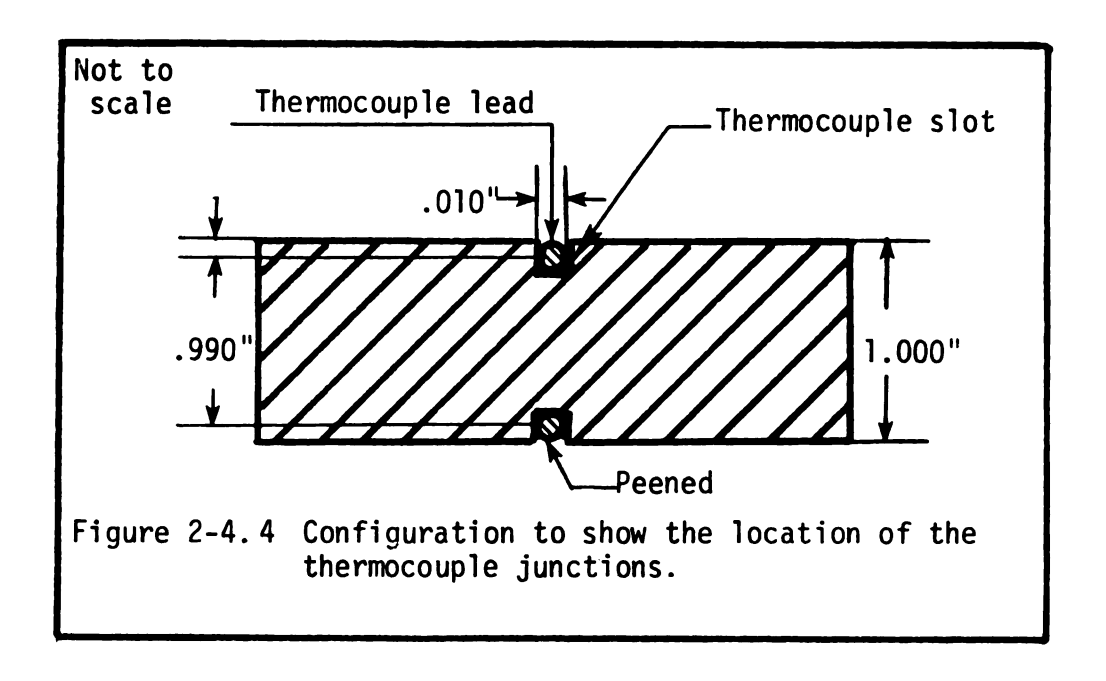
The thermal conductivity was determined using Equation (2-1.2). For the Armco iron specimens the locations of the thermocouples, x_1 and x_2 , were set equal to zero and one, respectively. There is some uncertainty in these values. When thermocouples are

TABLE 2-4.3 CORRECTION DATA FOR A PAIR OF ARMCO IRON SPECIMENS.

GLIARD	SAMPLE	HEAT	HEAT	Q _A	* H	DL/L ₀
TEMP.	TEMP.	INPUT	INPUT	(2-4,14)	(2-4.13)	V
DEG.F.	DEG.F.	WATTS	ВТИ	ВТИ	ита	
		LUCAT TH	DUT (ADAU	T 070 H01	[TO)	
	LON	HEHI IN	PUT (ABOU	T 272 WAT	(3)	
80.	86.0	276.31	3.9292	.042	.020	.00036
80.	90.0	276.35	3.9290	.040	.033	.00039
150.	149.0	275.41	3.9164	.040	-,007	.00077
150.	154.5	286.61	4.0757	.043	.031	.00081
200.	205.8	274.18	3.8000	.030	.055	.00114
250.	247.0	273.97	3.8959	.040	036	.00140
250.	251.0	275.73	3.9210	.040	.012	.00143
300.	305.0	272.90	3.8807	.030	.073	.00178
350.	352.5	272.53	3.8754	.037	.043	.00209
350.	361.5	272.18	3.8705	.037	.199	.00215
	HI	HEAT I	NPUT (ABO	UT 540 NA	atts)	
80.	97.0	535,38	7.6130	.070	.070	.00043
80.	100.0	545.03	7.7500	.070	.082	.00045
150.	165.0	530.11	7.5380	.078	.004	.00087
200.	208.0	527.31	7.4980	. 077	.063	.00115
200.	227.0	538.35	7.6550	.077	.212	.00127
250.	261.0	525, 40	7.4710	.076	.103	.00150
250.	270.0	550.07	7.8220	.078	.188	.00155
300.	313.5	538.30	7.6540	.075	.148	.00184
350.	362.5	522,21	7. 4260	.071	.156	.00215
350.	367.5	533.86	7.5910	.073	.210	.00219

* NEGATIVE HEAT LOSS MEANS HEAT GAIN TO THE SPECIMENS.

attached to the specimen, the center of the thermocouples are about 0.005 from the surface of interest (see Figure 2-4.4).



If the center of the thermocouples best measures the local temperature, the x_1 and x_2 values in Equation (2-1.2) ought to be 0.005 inch and 0.995 inch, respectively. The respective correction multipliers are shown in Tables 2-4.4 and 2-4.5. Note that no comparable correction is needed for specific heat as can be seen from Equation (2-1.4).

2-4.7 Errors Due to Thermal Expansion

There is no thermal expansion correction needed for the specific heat because ρAL in Equation (2-4.4) is a constant.

The term L/A in Equation (2-4.3) for k should be corrected for thermal expansion. The coefficient of thermal expansion

TABLE 2-4.4 CORRECTIONAL MULTIPLIERS FOR A PAIR OF ARMCO IRON SPECIMENS.LOW HEAT INPUT (ABOUT 272 WATTS).

GUARD SAMPLE CKA CKTC CKE CKH C1 TEMP. TEMP. DEG.F 80. 86.0 .9898 .9000 .9093 1.005 0.93 80. 90.0 .9896 .9900 .9992 1.008 0.93 150. 149.0 .9896 .9900 .9985 0.998 0.93 150. 154.5 .9895 .9900 .9984 1.008 0.93 200. 205.8 .9899 .9900 .9977 1.014 0.98	.15) 84 87 77 86
DE6.F. DE6.F.	84 87 77 86
80. 86.0 .9898 .9900 .9993 1.005 0.93 80. 90.0 .9896 .9900 .9992 1.008 0.93 150. 149.0 .9896 .9900 .9985 0.998 0.93 150. 154.5 .9895 .9900 .9984 1.008 0.93	87 77 86
80. 90.0 .9896 .9900 .9992 1.008 0.98 150. 149.0 .9896 .9900 .9985 0.998 0.98 150. 154.5 .9895 .9900 .9984 1.008 0.98	87 77 86
150.	77 86
150. 154.5 .9895 .9900 .9984 1.008 0.98	36
200. 205.8 .9899 .9900 .9977 1.014 0.96	22
	g Z
250. 247.0 .9898 .9900 .9972 0.990 0.99	58
250. 251.0 .9898 .9900 .9971 1.003 0.98	90
300. 305.0 .9901 .9900 .9964 1.019 0.96	9 5
350. 352.5 9905 9900 9958 1.011 0.93	87
350. 361.5 .9905 .9900 .9957 1.051 1.05	27
GUARD SAMPLE CCPA CCPTC CCPE CCPH CC	P
TEMP. TEMP. (2-4)	
DEG. F. DEG. F	
80. 86.0 .9896 1. 1. 0.995 .98	
80. 90.0 .9898 1. 1. 0.992 .983	
150. 149.0 .9897 1. 1. 1.002 .993	
150. 154.5 .9896 1. 1. 0.992 .98:	
200. 205.8 .9900 1. 1. 0.987 .975	
250. 247.0 .0808 1. 1. 1.000 .000	_
250. 251.0 .9898 1. 1. 0.997 .989	-
300. 305.0 .0000 1. 1. 0.081 .073	
350. 352.5 .0000 1. 1. 0.080 .076	
350. 361.5 .9904 1. 1. 0.949 .936	97

TABLE 2-4.5 CORRECTIONAL MULTIPLIERS FOR A PAIR OF ARMCO IRON SPECIMENS. HIGH HEAT INPUT (ABOUT 540 WATTS).

GLIARD TEMP.	\$AMPLE TEMP.	c _{KA}	^C KTC	¢KE	c ^{KH}	^C K (2-4, 15)
DEG.F.	DEG.F.					
80.	97.0	.9894	.9900	.9991	1.009	0.988
80.	100.0	.9896	.9900	.9991	1.010	0.089
150.	165.0	- 9896	.9900	.0082	1.012	0.000
200.	208.0	.9897	.9900	.9977	1.008	0.086
200.	227.0	-0800	.9900	.9974	1.027	1.005
250.	261.0	~ 6866	.9900	.9970	1.013	0.991
250.	270.0	.9901	.9900	.0060	1.024	1.001
300.	313.5	.9902	.9900	.9963	1.010	0.996
350.	362.5	.9905	.9900	.9957	1.021	0.007
350.	367.5	.9905	.9900	.9056	1.028	1.005
GLIARD	SAMPLE	C _{CPA}	CCPTC	C _{CPE}	CCPH	CCP
TEMP.	TEMP.					(2-4, 16)
DEG.F.	DEG.F.					
80.	97.0	. 9896	1.	1.	0.991	. 9803
80.	100.0	.0808	1.	1.	0.080	.0701
150.	165.0	.0807	1.	1.	0.088	.9772
200.	208.0	.0808	1.	1.	0.002	.0814
200.	227.0	.0000	1.	1.	0.072	.9625
250.	261.0	.0800	1.	1.	0.086	.0762
250.	270.0	.9901	1.	1.	0.076	.9663
300.	313.5	.9902	1.	1.	0.981	.0711
350.	362.5	.9904	1.	1.	0.070	.9697
350.	367.5	.9904	1.	1.	0.971	.9619

 $[\Delta L/L_0 = (L-L_0)/L_0$ where L_0 is the length at room temperature and L is the corresponding length at higher temperature] is given in Table 2-4.3 and corresponding correction multipliers are shown in Table 2-4.4 and 2-4.5.

The following notation is used in Tables 2-4.4 and 2-4.5. Subscript k stands for average thermal conductivity and subscript cp stands for average specific heat. A correction multiplier of unity means that no correction is needed.

- 1. C_{ka} = correction multiplier for \bar{k} due to the energy absorbed by the heater assembly (Section 2-4.5).
- 2. C_{ktc} = correction multiplier for \bar{k} due to the thermocouple placement (Section 2-4.6).
- 3. C_{ke} = correction multiplier for \bar{k} due to thermal expansion (Section 2-4.7).
- 4. C_{kh} = correction multiplier for \bar{k} due to heat loss or gain (Section 2-4.1).

 $\rm C_{cpa}, \, \rm C_{cptc}, \, \rm C_{cpe}, \, \, and \, \, \rm C_{cph}$ are similar correction multipliers for $\bar{\bar{c}}_{\rm p}.$

The total effective corrections for \bar{k} and $\bar{\bar{c}}_p$ are:

$$C_{k} = C_{ka} \times C_{ktc} \times C_{ke} \times C_{kh}$$
 (2-4.15)

$$C_{cp} = C_{cpa} \times C_{cptc} \times C_{cpe} \times C_{cph}$$
 (2-4.16)

2-5 Comparison and Discussion

The least-squares technique was applied to the thermal conductivity and specific heat values given in Table 2-3.1. The F-test criteria (Section 2-4.3) was used to determine the optimum order of polynomial. It was found that the linear relationships for \bar{k} and \bar{c}_p versus temperature are a reasonably good fit. The equation for thermal conductivity is similar to the one given in [21] and [23]. The values obtained for three temperature levels are tabulated in Table 2-5.1, which also shows results of TPRC [24], reference 22, and reference 23. Table 2-5.2 shows the specific heat values of the present data and the results given by TPRC.

The Armco iron material selected for this investigation is similar to that of [22]. Its thermal conductivity at 100°C, determined by the present method and apparatus, is only 1.90 percent lower than in [22].

The material composition of the recommended curve given by TPRC is not specified and it is questionable whether or not a correction is made in regard to the thermal expansion. The percentage differences of corrected \bar{k} and \bar{c}_p obtained by the present method and those given by TPRC are listed in Table 2-5.3. As temperature increases, the percentage differences for corrected thermal conductivity is increasing and for corrected specific heat is decreasing. The values of \bar{k} obtained by the present method, in the limited temperature range (30-180°C), is in agreement with the values given by TPRC within 2 percent while \bar{c}_p of the present method is 5.03 percent higher than TPRC at 30°C and only 1.79 percent higher at 150°C.

The Armco iron material used in [23] is similar to the material of the present investigation with the exception that the

TABLE 2-5.1	Thermal conductivity of Armco iron as given by vari	ious
	observers and present study.	

т		Thermal	Conductivity,	k, in watts/(m-	C)
°C	Chang and Blair [22]*	TPRC [24]**	Powell et al. [23] [†]	Present Study Uncorrected ^{††}	Present Study Corrected ^{††}
30		72.0	72.13	72.35	71.12
100	67.0	66.9	67.54	66.42	65.76
150		63.20	64.26	62.18	61.93

^{*}H. Chang and M. G. Blair, "A Longitudinal Symmetrical Heat Flow Apparatus for the Determination of the Thermal Conductivity of Metals: on Armco Iron." Thermal Conductivity--Proceedings of Eighth Conference, 1969, pp. 689-698.

TABLE 2-5.2 Specific heat of Armco iron as given by TPRC and present study.

т		Specific Heat, $\bar{\bar{c}}_p$, in J	/(Kg,C)
°C	TPRC*	Present Study Uncorrected **	Present Study Corrected**
30	.451	.4821	.4737
100	.472	.5061	.4955
150	.502	.5233	.5110

^{*}Y. S. Touloukian, ed., <u>Thermophysical Properties of High</u> <u>Temperature Solid Materials</u>, Vol. 1, 1966, pp. 583-585 for Armco Iron, and Vol. 2, 1966, pp. 735-737 for aluminum alloys.

^{**}Y. S. Touloukian, ed., <u>Thermophysical Properties of High</u> <u>Temperature Solid Materials</u>, Vol. 1, 1966, pp. 583-585 for Armco iron, and Vol. 2, 1966, pp. 735-737 for aluminum alloys.

D. C. Larson, R. W. Powell, and D. P. DeWitt, "The Thermal Conductivity and Electrical Resistivity of a Round-Robin Armco Iron Sample, Initial Measurements from 50 to 300°C." Thermal Conductivity--Proceedings of Eighth Conference, 1969, pp. 675-587.

^{††}Table 2-3.1.

^{**}Table 2-3.1.

TABLE 2-5.3 The percentage difference of corrected \hat{k} and \hat{c}_p of present data and TPRC as a function of temperature for ARMCO iron.

T °C	% Difference for k	% Difference for \hat{c}_p
30	1.23	5.03
100	1.73	4.97
150	2.05	1.79

material used in [23] contains an addition of .083 percent copper (see [22]). The uncorrected value of thermal conductivity of the present method at 30° C is only .30 percent higher than the value given by [23], while at 150° C the value of \bar{k} obtained by the present method is 3.34 percent lower than that of [23].

The least-squares results for \bar{k} and \bar{c}_p using the corrected values of Armco iron given in Table 2-3.1 are:

$$\hat{k} = 73.42 - .0766 T$$
 (2-5.1)

$$\hat{c}_{p} = .4644 + .000311 T$$
 (2-5.2)

which may be used between 30 and 180°C. Units for \hat{k} are watts/(m-C) and for \hat{c}_p are J/(Kg-C).

The unbiased estimated sample variance of \overline{k} or $\overline{\overline{c}}_p$ is given as:

$$s^{2} = \frac{1}{N-2} \sum_{i=1}^{N} (Y_{i} - \hat{Y}_{i})^{2}$$
 (2-5.3)

where N = number of data points = 20; Y_i = measured \bar{k} or \bar{c}_p , corrected values of Table 2-3.1; \hat{Y}_i = calculated \hat{k} or \hat{c}_p by Equations (2-5.1) or (2-5.2), respectively; and S is the estimated standard deviation of \bar{k} or \bar{c}_p .

The covariance matrix of $\hat{\underline{Y}}$ is given [33]:

$$Cov (\hat{\underline{Y}}) = \underline{X} (\underline{X}^T \underline{\psi}^{-1} \underline{X})^{-1} \underline{X}^T$$
 (2-5.4)

where the components of \underline{X} matrix can be determined by the temperature values given in Table 2-3.1, superscript T stands for matrix transpose, and superscript -1 stands for matrix inverse. With independent and constant variance errors, replacing $\underline{\psi}$ by $s^2\underline{I}$ where s^2 is a sample variance of \overline{k} or \overline{c}_p estimated by Equation (2-5.3) and \underline{I} is the identity matrix, the diagonal terms of Equation (2-5.4) give the variance of \hat{Y} for any given temperature level. The estimated standard error of \hat{Y} for any temperature level is found by taking the square root of the diagonal terms of Equation (2-5.4). For two-parameter cases, such as Equations (2-5.1) and (2-5.2), Equation (2-5.4) for an arbitrary temperature T is expanded and necessary calculations are carried out. The results are:

est. s.e.
$$(\hat{k}) = (.908 - 1.35 \times 10^{-2} \text{ T} + 6.19 \times 10^{-5} \text{ T}^2)^{1/2}$$

$$(2-5.5)$$

est. s.e.
$$(\hat{c}_p) = (1.39 \times 10^{-5} - 2.06 \times 10^{-7} \text{ T} + 0 \times 10^{-9} \text{ T}^2)^{1/2}$$
(2-5.6)

The estimated percentage error for \hat{k} and \hat{c}_p as a function of temperature [33] is given as:

for
$$\hat{k}$$
: $\frac{\text{est. s.e. } (\hat{k}) \times 100}{\hat{k}}$ (2-5.7)

for
$$\hat{c}_p$$
: $\frac{\text{est. s.e. } (\hat{c}_p) \times 100}{\hat{c}_p}$ (2-5.8)

For the three temperatures of 30, 100, and 150°C, the percentage error of corrected thermal conductivity and specific heat, as defined in Equations (2-5.7) and (2-5.8) are given in Table 2-5.4.

TABLE 2-5.4 Percentage error of \hat{k} and \hat{c}_p , as defined in Equations (2-5.7) and (2-5.8), as a function of temperature.

T °C	Percentage Error of k	Percentage Error of c _p
30	1.05	.62
100	.64	.33
150	.84	.40

The values of thermal conductivity and specific heat can be calculated by the linear Equations (2-5.1) and (2-5.2), respectively. The corresponding error can be determined by Equations (2-5.7) and (2-5.8).

It is believed that the values of thermal conductivity and specific heat calculated by these equations are accurate, within the corresponding percentage errors defined in Equations (2-5.7) and (2-5.8), and the percentage differences obtained with the results of other investigators are within tolerance of measurement errors.

CHAPTER 3

ALUMINUM 2024-T351 AND EXPERIMENTAL RESULTS

This chapter deals with the application of the method developed in Chapter 2. Various experiments were performed on the A1-2024-T351 specimens. Thermal property values for the isothermal ageing, as received, and annealed conditions have been determined.

The least-squares method is used to obtain the thermal conductivity and specific heat versus temperature relationship for the data associated with as received and annealed conditions. A mathematical model for the thermal conductivity versus time is proposed and the associated parameters are found using the computer program NLINA.

An error analysis similar to that described in Chapter 2 is made. The thermal conductivity and specific heat values of Al-2024-T351 are compared with the available literature values. The recommended values of thermal properties as a function of temperature, for the as received and annealed conditions, can be found in Section 3-8.

3-1 The Sample Composition

The aluminum alloy (A1-2024-T351) selected for the experiment was provided by Kaiser Aluminum Company. This alloy is solution heat treated and naturally aged to a substantially stable

condition. The typical analysis in weight % is: 3.8-4.9% copper, 0.50% maximum silicon, 0.50% maximum iron, 0.30-0.90% manganese, 1.2-1.8% magnesium, 0.10% maximum chromium, 0.25% maximum zinc, 0.20% maximum zirconium plus titanium, 0.15% maximum titanium, 0.05% maximum others each, 0.15% maximum other total, and the balance of the remaining is aluminum.

The density of the alloy at $68^{\circ}F$ is given as 173 lbm/ft^3 (2.77 gr/cm³) and its mechanical properties at various conditions can be found in [1, 24, 34].

3-2 Metallurgy of Precipitation

The principal alloying element in the aluminum 2024-T351 is copper. This alloy is precipitation-hardenable or "heat treatable" because the presence of copper, under certain conditions, makes the alloy susceptible to the heat treating operations in which the microstructure and consequently the properties are altered in the solid state. The theoretical aspects of precipitation hardening, due to the thermal heat treatment, for all heat treatable alloys are not, as yet, fully developed. However, it is known that precipitation hardening changes the mechanical and electrical as well as the thermal properties of A1-2024-T351 and as a consequence, these properties are time and temperature dependent.

Figure 3-2.1 represents a partial equilibrium phase diagram for the aluminum side of aluminum-copper alloys. Since the experimental measurement procedures of the present investigation are based on the information obtained from this phase diagram, a brief

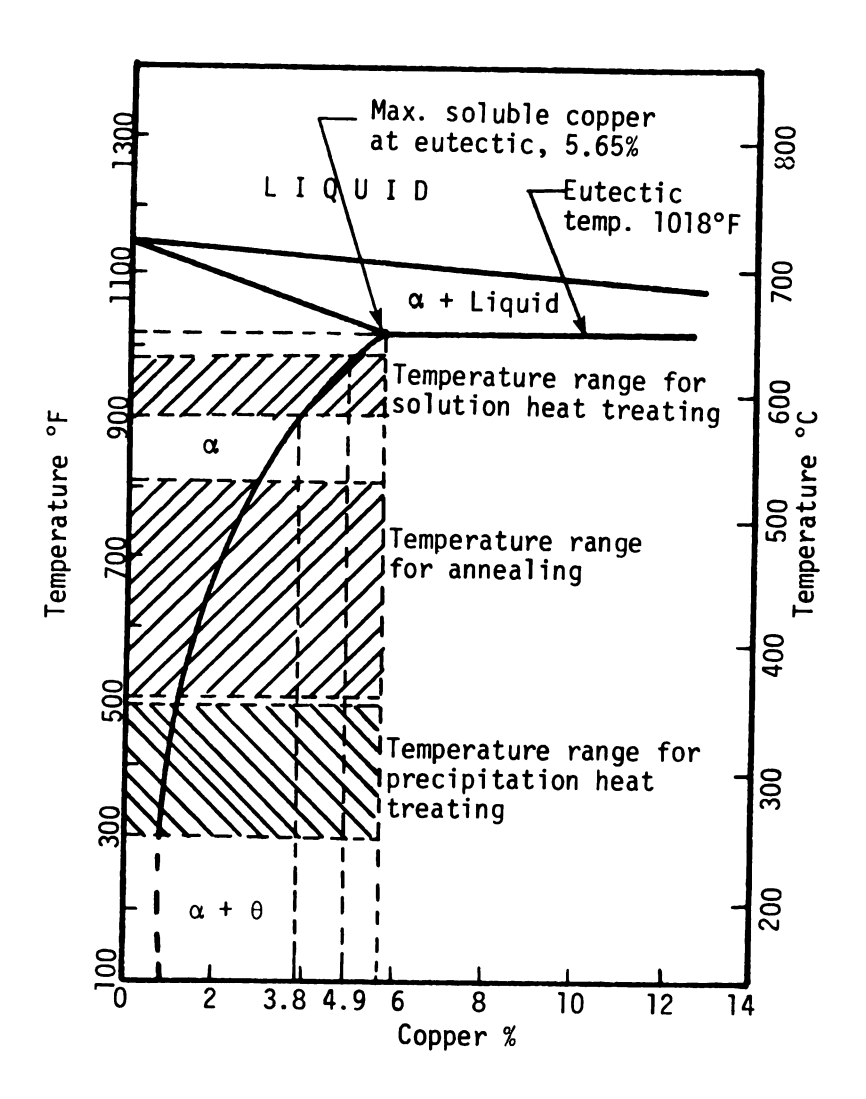


Figure 3-2.1 Partial equilibrium diagram for aluminum side of aluminum-copper alloys, with temperature range for heat treating operations.

description of the phase diagram is given in the remaining part of this section.

The eutectic point is a point in which two metals are completely soluble in the liquid state and completely insoluble in each other in the solid state. The corresponding temperature and percent of copper composition at this point for A1-2024-T351, as shown in the diagram, are 1018°F and 5.65%, respectively.

The region of the solid solution of aluminum (Al or α region) is a single phase homogenous region which differs from the liquid solution region only in its physical condition. According to the typical analysis given in Section 3-1, the percent of the copper composition varies from 3.8 to 4.9. The corresponding solution heat treating temperature (see Figure 3-2.1) varies from 900 to 980°F, respectively [34].

The solid solution of aluminum plus the intermetallic compound region is a two phase region. This sometimes is called the $\alpha+\theta$ region where α refers to aluminum plus copper in solution and θ refers to the intermetallic compound (CuAl $_2$). The microstructure and the stability of the alloys in this region depend on the condition of the intermetallic compound (θ). With sufficiently slow cooling from the solid solution heat treating temperature (see Figure 3-2.1), CuAl $_2$ precipitates from the α solid solution in the intermediate temperature range. The intermetallic compound CuAl $_2$, surrounding the solid solution aluminum, appears as segregate particles and is stable in its microstructure. This equilibrium state can be obtained by a prolonged annealing process, just below the solution

heat treating temperature [35]. On the other hand, when water quenching from the α solid solution region, the homogeneous solid solution is retained near room temperature. In this state the solid solution is supersaturated and the alloys are unstable. At any temperature level, the unstable supersaturated alloys undergo a microstructural change to attain stability. The property changes due to changes in microstructure at low temperature are called "natural ageing." Other names, such as "pre-precipitation" or "cold hardening," are also associated with low temperature precipitation hardening [36]. Low temperature precipitation hardening is identified as the first stage of decomposition of the supersaturatured solid solution. The pre-precipitation process ultimately approaches a stable condition and may require a few hours, a few days, or a few years, depending upon the nature of the alloys. Reheating the alloys to the precipitation heat treating temperature range (300-500°F), the CuAl₂ (θ) is precipitated which is the second stage of precipitation and is sometimes called "warm hardening" or "artificial ageing." It is believed that artificial ageing corresponds to a true precipitation in which the particles (θ) can be made visible by the electron microscope or by X-ray diffraction techniques.

3-3 Sequence of Precipitation

There has been a half century of work and research by many investigators to present a model which can describe the stages of age-hardening. The pioneers in this area were Guinier [37] and Preston [38]. They presented the idea of a zone, a small region in

the matrix enriched with solute atoms. The differences between zones and precipitates are that zones do not have well-defined boundaries and lattice structure; however, they are perfectly coherent with the lattice structure of the matrix. The approximate diameters of the zones, after rapid quenching from solid solution temperature and measuring at room temperature, are about 30-50 Angströms. The zones of this nature, called GP[1] (Guinier-Preston Zones 1), consist of copper-rich regions of disk-like shape, formed on {100} planes of the aluminum matrix ({100} designates a face of cubic lattice structure).

The sequence of precipitation for the Al-Cu alloys is given as:

Quenched supersaturated
$$\longrightarrow$$
 GP[1] \longrightarrow $\frac{\text{GP[2]}}{\text{or }\theta''}$ \longrightarrow θ' \longrightarrow θ .

The description of the zone formation at various stages of precipitation has been modified many times since its introduction.

Despite development of sophisticated electronic equipment which can provide detailed information regarding the atomic structure of the zones, discrepancies exist about the sequence of the age-hardening process and the nature of the microstructure of the precipitates.

It is believed that the first stage of precipitation, immediately after quenching, corresponds to pre-precipitation or cold hardening, which does not concern the present investigation. It is also found that at about 100°C or higher the GP[1] zones are replaced by coherent zones of GP[2] and

subsequently, due to higher temperatures or longer time, to coherent θ' . The difference in microstructure between θ' and θ is the state of coherency. When particles grow, their coherency strain decreases and at the over-aged condition (whether with high temperature or low temperature and longer time), the noncoherent θ will be segregated. The coexistence of θ precipitates with the aluminum matrix in a stable two-phase structure is the indication of completion of true precipitation hardening.

The four stages of the decomposition (sequence of precipitation) of the quenched solid solution depend strongly on the temperature level of the precipitation process. In the process of precipitation diffusion occurs. The high rate of diffusion immediately after quenching is credited to the existence of excess vacancies in the supersaturated solid solution [34]. The vacancies play an important role in the zones formation and affect the mechanical, electrical, and thermal properties of the alloys. The high rate of diffusion due to vacancies during the zones formation occurs along the grain boundaries, subgrain boundaries, and dislocations, causing distortion in the lattice structure of the matrix. This type of mechanism, at any given temperature level, will continue until all stable particles θ are segregated.

It is a complicated process to determine the effects of each minor constituent [39] on the mechanical, electrical, and thermal properties of the alloys. However, by property measurement, the net effects on the microstructure can be studied.

The above is an introduction to the sequence of precipitation of Al-Cu alloys. For more complete reviews of precipitation hardening and zones formation, see [34, 40, 41, 42, 43, and 44].

3-4 Different Techniques to Study Precipitation Hardening

Specialized equipment and several techniques have been used to obtain valuable information about various aspects of precipitation hardening. The oldest method used to measure the degree of decomposition of supersaturated solid solution is the hardness measurement. Using this method, certain patterns of age-hardening can be traced easily and quickly. However, the hardness-time curve is a poor indication of the sequential changes in the microstructure of heat treatable alloys [43].

The measurements of electrical resistance of quenched Al-Cu alloys have been used to study the precipitation processes. It is a rapid and simple method to obtain quantitative information. Recently, this method has been used primarily in pre-precipitation because it normally takes less than five seconds to make the first measurement after a rapid quenching [43].

Many investigators have used the X-ray diffraction technique to study the individual precipitates during the various stages of precipitation. The electron diffraction is another technique by which the individual precipitates of atomic dimensions can also be directly observed [45].

Many other property measurements have also been used to find correlation between changes in microstructure and property

changes of the alloys. Some of these properties are magnetic, elastic, etc.

Research has supported the theory that the hardness-time measurement can be used to study the microstructural changes during the precipitation processes (see [40], p. 17). Reports indicate that Young's modulus of quenched Al-Cu alloys, measured dynamically, can be related to the kinetics of the precipitation processes [43, 46]. Based on these findings, it is reasonable to assume that the thermal conductivity-time curves obtained in this investigation (see Chapter 4) can also be used to study the microstructural changes and consequently the precipitation hardening of as received Al-2024-T351.

3-5 Experimental Procedure

The aluminim 2024-T351 specimens were made from a 3.5 inch bar. The aluminum bar with the composition given in Section 3-1 was purchased in January 1971. This bar was used in the experimental investigation carried out by Al-Araji [1] and the remaining part of the bar was stored in the laboratory until beginning this experimental work in October 1974. The equipment, measurement techniques, and the method of determining of thermal conductivity and specific heat were similar to that of the reference metal, Armco iron (Chapter 2), with the exception of specimen thickness and the electric heater element. The specimen thickness was increased to 1.5 inch to obtain approximately the same Fourier modulus $(\alpha\theta/L^2)$ as the Armco iron specimen (see Section 2-3.5), thereby obtaining

approximately the same temperature drop across the specimens during the transient experiments. A heater element with silicone rubber electrical insulation material was used. The approximate thickness of the heater element was about 0.016 inch.

Each experiment was performed after installing two specimens in their respective housing and applying a thin layer (0.015 inch) of silicone grease to their heated surfaces, then attaching the heater element on the bottom heated surface of the specimen, and finally, raising the bottom specimen assembly to come into intimate contact with the upper specimen.

In this investigation, it was desirable to run the following tests on samples of A1-2024-T351:

- 1. Isothermal ageing tests on as received A1-2024-T351 to obtain values of thermal properties as a function of temperature and time.
- 2. Temperature dependent tests on as received A1-2024-T351 to obtain thermal properties as a function of temperature only (i.e., tests at relatively low temperatures or at high temperatures in short time periods, so that it can be assumed no precipitation has occurred).
 - 3. Temperature dependent tests on annealed A1-2024-T351.

A summary of tests arrangement for A1-2024-T351 specimens is shown in Table 3-5.1. In the isothermal ageing tests, 16 fresh as received aluminum specimens were used. For each isothermal temperature, two tests with four fresh specimens were run to ascertain the reproducibility of ageing curves (thermal conductivity-time

TABLE 3-5.1 Summary of tests arrangement for A1-2024-T351 specimens.

Ageing Temp. °F	Test No.	No. of Exp.	No. of Fresh Spec.	Spec. Temp.	Remarks
350 -	2	26 26 27 27 22 22	2 2	80-95 350 80-95 80-95 350 80-95	Room temp. exp. before isothermal ageing test no. 1. Isothermal testing at 350°F for test no. 1. Room temp. exp. after isothermal ageing test no. 1. Room temp. exp. before isothermal ageing test no. 2. Isothermal testing at 350°F for test no. 2. Room temp. exp. after isothermal ageing test no. 2.
375 -	5 1	22 22 22 29 29	0 0	80-95 375 80-95 80-95 375 80-95	temp. exp. before isothermal ageing test no. ermal testing at 375°F for test no. l. temp. exp. after isothermal test no. l. temp. exp. before isothermal ageing test no. ermal testing at 375°F for test no. 2. temp. exp. after isothermal test no. 2.
400	1 2	21 22 30 30	2 2	80-95 400 80-95 80-95 400 80-95	temp. exp. before isothermal ageing termal testing at 400°F for test no. I temp. exp. after isothermal test no. temp. exp. before isothermal ageing termal testing at 400°F for test no. temp. exp. after isothermal test no.
425 –	1 2	2 16 2 29 29	2 2	80-95 425 80-95 80-95 425 80-95	Room temp. exp. before isothermal ageing test no. 1. Isothermal testing at 425°F for test no. 1. Room temp. exp. after isothermal test no. 1. Room temp. exp. before isothermal ageing test no. 2. Isothermal testing at 425°F for test no. 2. Room temp. exp. after isothermal test no. 2.
		30	2 2 2	80-300 80-400 80-400	rementno precipitatio rom 575°F. rom 925°F.

curves). Before running each ageing test, at least two experiments, at about room temperature, were run to insure the proper thermocouple installation and to evaluate the reproducibility of test results. After this preliminary testing (adjustments being made if necessary), the guards were set to one of the desired nominal isothermal ageing temperatures. The time required for quards to be heated from room temperature to the desired set point temperature was approximately 25 minutes. In this period, the specimens generally remained below 150°F. When the temperature of the guards arrived at the set point temperature, the two specimens were heated by the electric heater between them. The time required for specimens to be heated from 300°F to 350°F was about 3 minutes. Immediately after the specimens reached the desired temperature, the first experiment was run. The second experiment was started after the specimens and their surroundings had attained the equilibrium temperature. This procedure was repeated and the following were recorded for each isothermal ageing temperature: (a) cumulative ageing time and (b) the corresponding values of thermal conductivity and specific heat (see next section). Note that when specimens and their surroundings attained equilibrium temperature, the quard heaters can maintain the specimens and their surroundings within approximately 1.5°F of the set nominal isothermal temperature for an indefinite time period. With this arrangement, the time interval between the two consecutive ageing experiments can be made as long as desired.

After a series of ageing experiments at a nominal isothermal temperature and the elapse of sufficient time, the values of thermal

conductivity then would normally fluctuate about a mean value. Reaching this state, it was assumed that the precipitation was completed at that isothermal temperature and the ageing test then was terminated by disconnecting the electric power to the guard heaters. After termination of the isothermal ageing tests, the specimens were cooled slowly to room temperature. Two more experiments were run at room temperature (see Table 3-5.1). The data from these experiments were also used in modeling (see Chapter 4).

The procedure to obtain values of \bar{k} and \bar{c}_p , as a function of temperature, for the as received and annealed Al-2024-T351 specimens, are given in the next section.

3-6 Description of the Experimental Data and Corresponding Thermal ConductivityTime Curve

For every isothermal ageing temperature two tests, namely, tests "1" and "2," were run using as received A1-2024-T351 specimens. In each ageing test, two as received specimens were used and, at most, 30 ageing experiments were performed (see Table 3-5.1). It is important to note that, for the isothermal ageing temperature 350°F, a total of 52 experiments were run and 208 (52 x 4 = 208) values of thermal conductivity and specific heat were calculated for eight symmetric locations on four as received A1-2024-T351 specimens. A similar calculation can be made to determine the number of experiments and consequently the number of thermal conductivity and specific heat values obtained for ageing temperatures

375, 400, and 425°F. The quantitative information obtained from these experiments was used to determine a resonably well-fitted mathematical model for thermal conductivity, as a function of ageing time, for each ageing temperature. This mathematical model is:

$$k_{ia}(T,t) = k_{ia}(0) + [k_{ia}(t_{max}) - k_{ia}(0)][1 - e^{-(t/\tau)^n}]$$
(3-6.1)

where $k_{ia}(0)$ and $k_{ia}(t_{max})$ are values of k at the initial and final ageing time, and τ is time constant. The time exponent n is assumed to be equal to 1. The actual value of n was determined for each isothermal ageing temperature and an average value nearly unity was obtained (see Chapter 4). The parameters $k_{ia}(0)$, $k_{ia}(t_{max})$, and τ were determined using the computer program NLINA (see Section 2-4.4). The dimensionless thermal conductivity $k^+ = [k_{ia}(T,t) - k_{ia}(0)]/[k_{ia}(t_{max}) - k_{ia}(0)]$, obtained from mathematical model (3-6.1), is in general in accordance with the relationship given for precipitation [40, 41].

The ageing experimental data for four isothermal ageing temperatures is given in Tables 3-6.1 through 3-6.8. The tables contain the run number (number of ageing experiment), ageing time, and corresponding values of \bar{k} and \bar{c}_p and their respective values of standard devations [see Equations (2-3.3) and (2-3.4)].

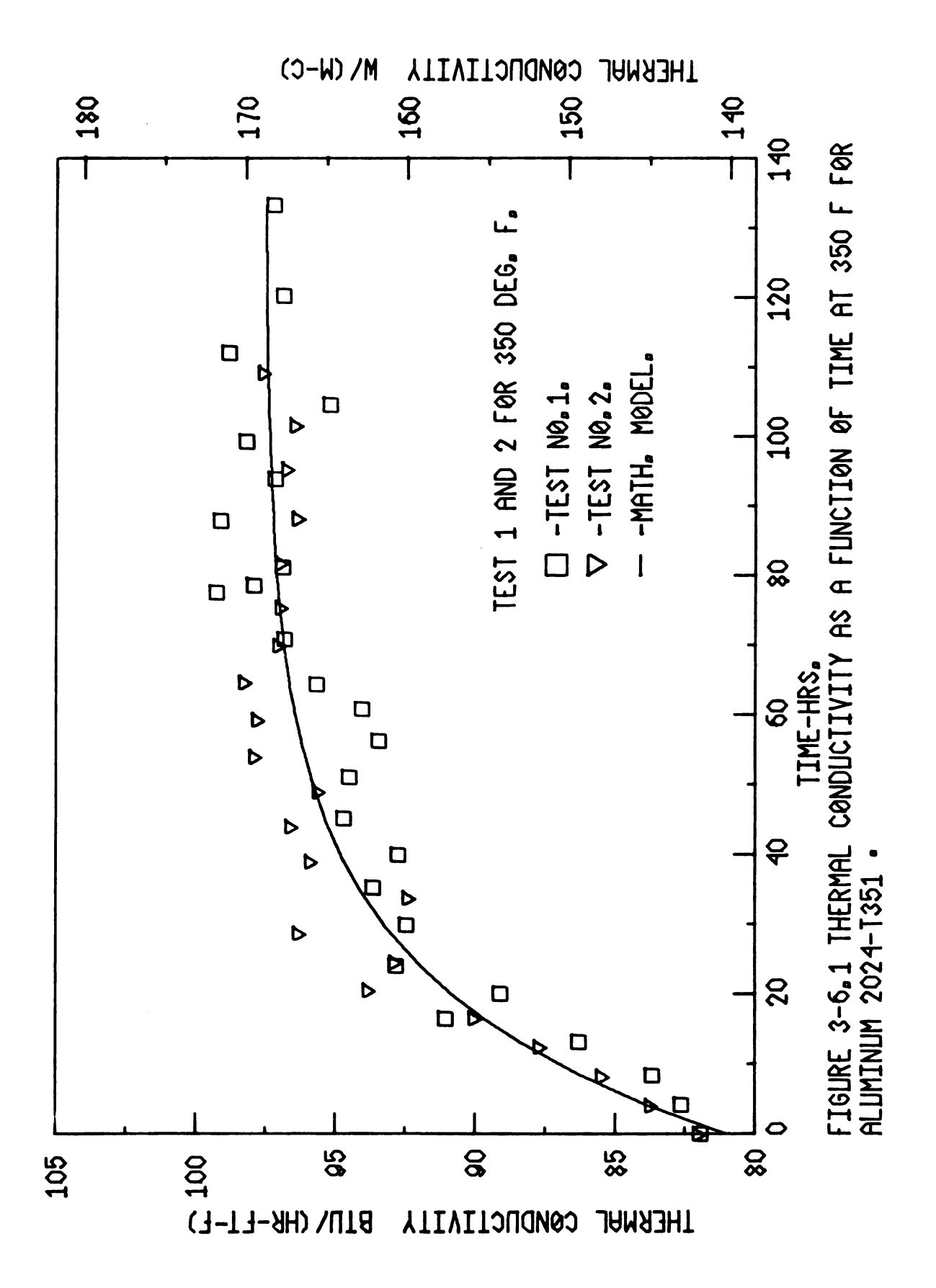
The data points from two ageing tests for every isothermal ageing temperature are also plotted with time and are shown in Figures 3-6.1 through 3-6.8. The solid curve shown on every

TABLE 3-6.1 ISOTHERMAL AGEING TEST AT 350 DEG. F. TEST NO. 1 FOR AL-2024-T351. VALUES OF \bar{K} AND $\bar{\bar{C}}_P$ AND THEIR RESPECTIVE STANDARD DEVIATIONS.

RUN	TIME	Κ̈	s _K	ξ̄ _P	SCP
NO.		ВТ	ת	ВТ	
	HRS.	HR-F	T-F	LBM	I - F
1	.00	81.92	6. 46	2436	.00617
2	4, 23	82.63	3.45	2356	.00613
1 2 3	8.41	83,68	5.32	. 2360	.00619
4	13.16	86.31	7.56	.2372	.00730
	16, 46	91.05	6.97	.2344	.00747
6	20.08	89,10	4,58	. 2339	.00266
5 6 7 8	24.08	92.83	8.63	. 2352	.00633
8	29.91	92.45	3.03	. 2346	.00656
0	35, 25	93.64	5,62	. 2347	.00598
10	39.96	92.76	4.32	2353	.00684
11	45.16	94.69	5.01	. 2331	.00550
12	51.08	94.51	7.65	2345	.00439
13	56,30	93.45	4.96	. 2342	.00721
14	60.88	94.06	4, 81	. 2355	.00598
15	64,30	95.68	5.34	. 2353	.00548
16	70.90	96.82	5.07	. 2346	.00510
17	77.63	99.27	7.64	.2386	.00917
18	78,63	97.92	4.97	.2348	.00845
10	83.21	96.88	6. 72	. 2330	.00751
20	87.88	99.13	7.14	. 2333	.00711
21	93.88	97.17	6,03	. 2327	.00771
22	99.30	98.19	6.23	. 2353	.00836
23	104.55	95. 21	5.29	. 2325	.00626
24	112.13	98.82	4.23	. 2368	.00586
25	120.33	96.88	8.37	. 2368	. 00693
26	133.25	97.23	5, 42	.2334	.00653

TABLE 3-6.2 ISOTHERMAL AGEING TEST AT 350 DEG. F. TEST NO. 2 FOR AL-2024-T351. VALUES OF \bar{K} AND \bar{C}_P AND THEIR RESPECTIVE STANDARD DEVIATIONS.

RUN	TIME	Ē	s _K	Ēρ	SCP
NO.		ВТ		B1	
					
	HRS.	HR-F	1-1	LBM	1-1
1	.00	82.06	3,38	.2396	.00471
1 2	4.06	83.79	0.39	. 2362	.00298
3 4	8.30	85.5 3	1.62	.2342	.00202
4	12.53	87.75	4,69	.2367	.00303
5	16,53	90.08	3.19	. 2333	.00179
6	20.58	93.86	2.20	. 2329	.00078
7	24.58	92.91	0.89	. 2359	.00257
8	28.71	96.36	3.03	.2337	.00346
9	33.78	94. 43	2.57	. 2343	.00281
10	38.98	95. 9 5	1.89	.2349	.00398
11	43.98	96.64	2.82	. 2350	.00099
12	48.98	95.67	6, 05	.2357	.00588
13	54,03	97.94	2.78	. 2352	.00141
14	59.31	97.85	2.86	.2332	.00273
15	64,65	98.31	3.75	. 2353	.00190
16	69.98	97.08	3.53	. 2346	.00301
17	75.38	97.01	6.95	. 2356	.00410
18	81.83	97.02	5.55	. 2351	.00345
19	88.15	96.40	1.86	.2340	.00079
20	95,28	96. 80	3.89	.2351	.00261
21	101.61	96, 47	1.41	.2320	.00195
22	109.23	97.65	3,65	. 2351	.00438
<u> </u>					



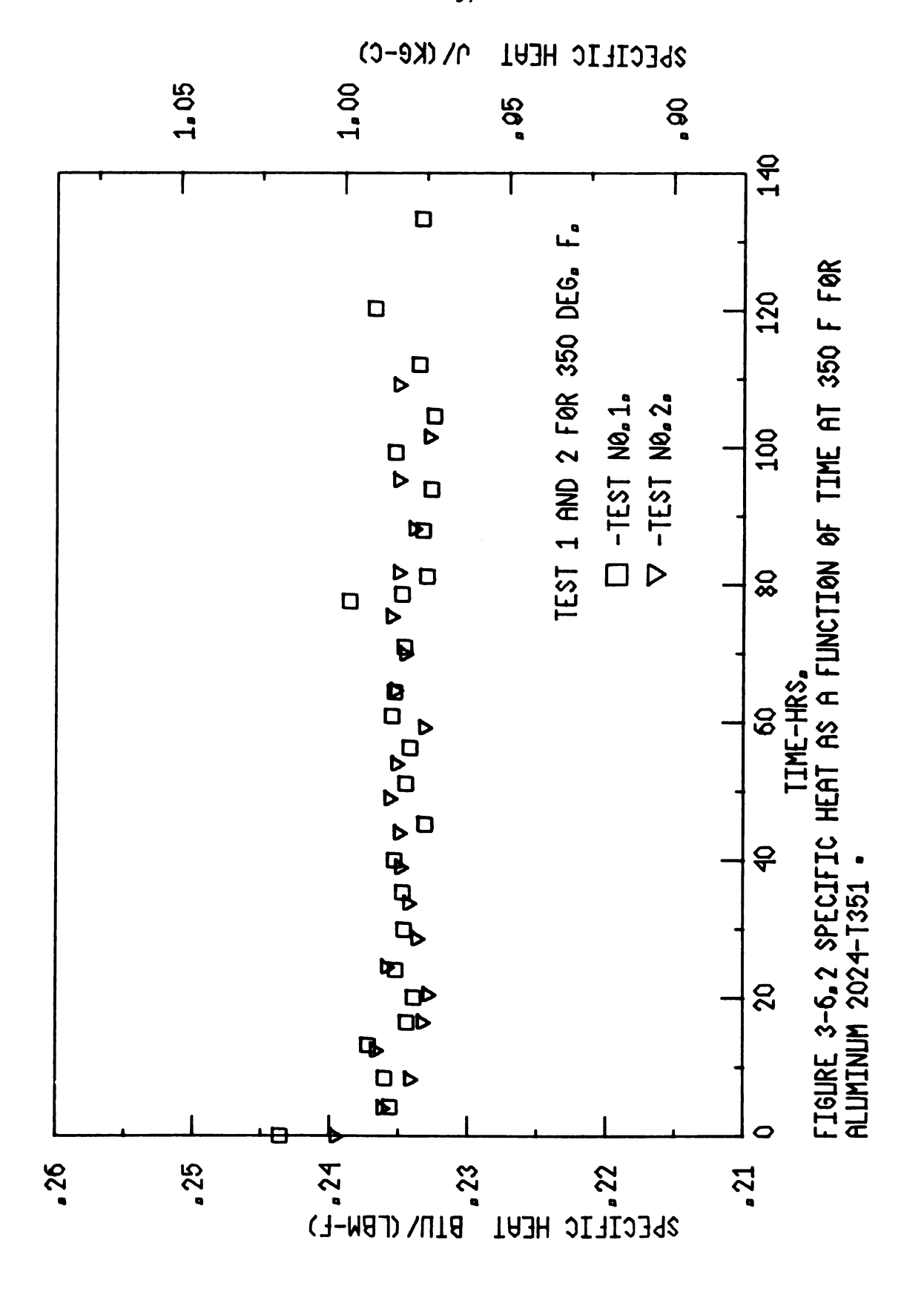
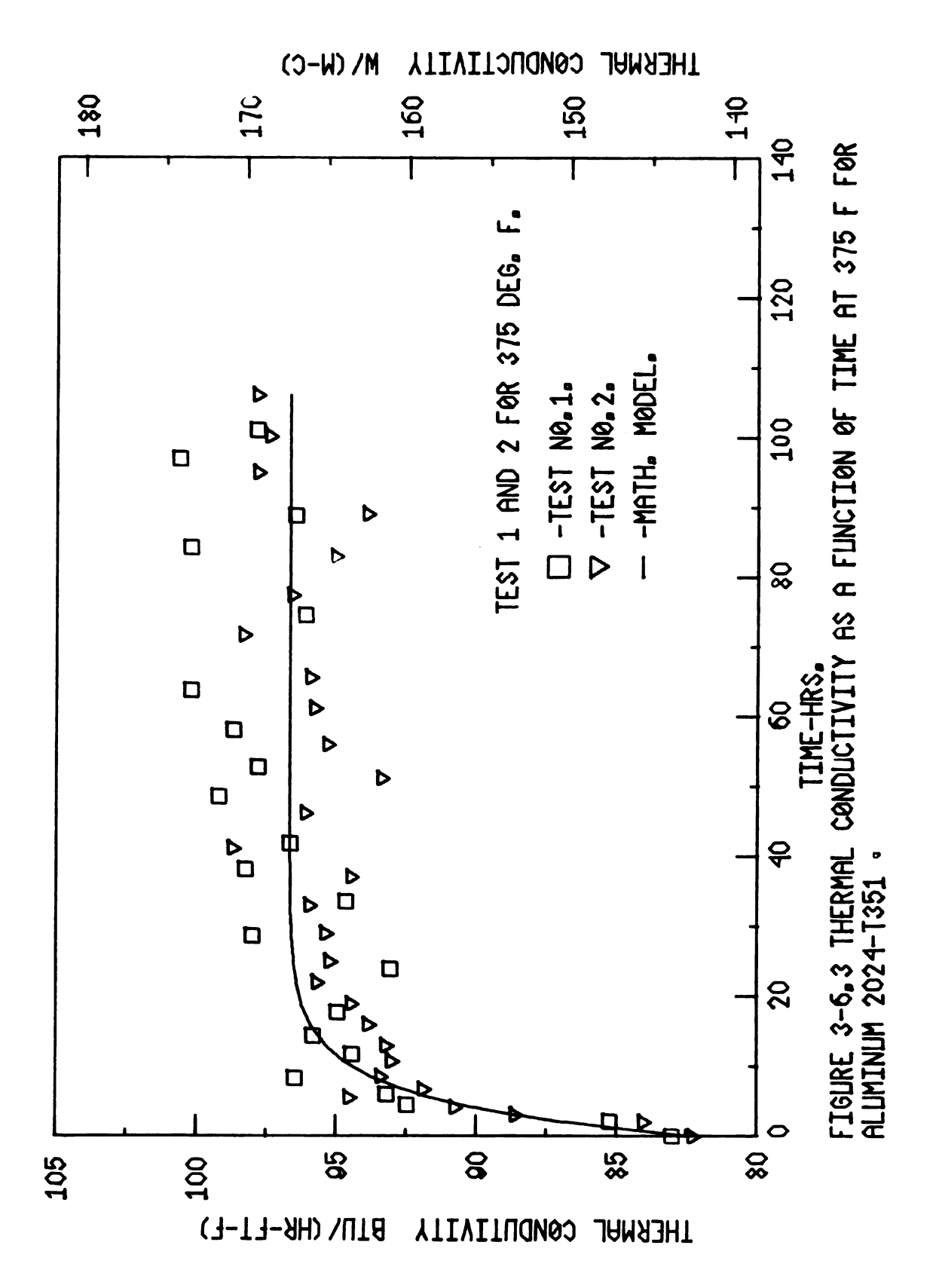


TABLE 3-6.3 ISOTHERMAL AGEING TEST AT 375 DEG. F. TEST NO. 1 FOR AL-2024-T351. VALUES OF \bar{K} AND $\bar{\bar{C}}_P$ AND THEIR RESPECTIVE STANDARD DEVIATIONS.

RUN	TIME	K	s _K	ιÇρ	\$ _{CP}
NO.		ВТ	П	ВТ	
	HR\$.	HR-F	T-F	LBM	I-F
1 1	_ 00	83,00	1.08	.2397	.00301
	2.05	85.23	1.64	₃ 2378	.00365
3	4.51	92, 48	1.22	.2374	.00214
	6.03	93.19	3.38	.2367	.00421
5	8.33	96.48	5.70	. 2362	.00525
4 5 6 7 8	11.66	94.43	3.4 0	. 2382	.00378
7	14.33	95.83	3.34	.2349	.00419
8	17.66	94.93	5.22	. 2360	.00246
9	23.93	93.08	2.31	.2366	•00446
10	28.62	98.01	3 . 43	.2357	.00481
11	33,50	94.64	4, 26	. 2356	.00345
12	38.05	98.24	4.07	.2357	.00281
13	41.76	96.66	2.06	.2370	.00472
14	48.53	99.19	0. 44	. 2351	.00545
15	52 . 70	97.79	6.63	. 2360	.00474
16	57 . 9 5	98.67	2.70	. 2345	.00471
17	63.70	100.19	3. 76	. 2354	.00522
18	74.53	95. 12	3. 76	.2362	.00463
19	84. 23	100.23	5.35	.2375	.00470
20	88. 76	96. 47	3. 41	.2340	.00564
21	96.93	100,62	4.54	. 2363	.00651
22	101.00	97.85	3.78	. 2369	.00618

TABLE 3-6.4 ISOTHERMAL AGEING TEST AT 375 DEG. F. TEST NO. 2 FOR AL-2024-T351. VALUES OF \bar{K} AND $\bar{\bar{C}}_P$ AND THEIR RESPECTIVE STANDARD DEVIATIONS.

RUN	TIME	K	\$ _K	ξ̄ _P	\$ _{CP}
NO.		ВТ	ח	BT	
	HR\$.	HR-F	T-F	LBM	
1	,00	82,28	2.91	. 2424	.00627
2 3	2.06	84.04	2.47	.2415	.00657
	3.10	88.63	2.13	_2394	.00423
4	4, 20	90.78	3.16	. 2399	.00302
5	5, 63	94.54	2.23	.2394	.00455
6 7 8	6, 76	91.90	2.13	2365	.00510
7	8.56	93. 43	3.38	.2373	.00341
8	10.75	93.04	2.10	.2376	.00394
9	12.96	93. 2 5	1.14	.2378	.00491
10	15.96	93.87	1.87	2 365	.00273
11	18.96	94. 48	3.79	. 2364	.00177
12	21.96	95. 71	2.71	.2387	.00504
13	24.96	95. 24	3.21	. 2357	.00262
14	28.96	95. 4 0	4.32	. 2358	.00461
15	32.96	95. 9 8	2.88	. 2357	.00277
16	37.10	94. 48	5.52	.2374	.00255
17	41.15	98.72	2.35	. 2367	.00502
18	46.15	96.14	3.22	.2347	.00085
19	51.15	93.4 0	3.00	.2354	.00441
20	55 , 9 5	95.34	5.98	.2334	.00458
21	61.23	95, 80	4.08	.2371	.00434
22	65.61	95. 9 5	2.68	. 2362	.00427
23	71.73	98.34	2.18	. 2350	.00376
24	77.38	96,60	4.72	.2373	.00518
25	83.00	95.06	5, 69	. 2363	.00447
26	89. 10	93.94	0. 85	.2347	.00369
27	94.95	97.84	3.80	. 2345	.00263
28	100.23	97.41	8. 55	. 2358	.00552
29	106,05	97.86	3.54	. 2358	.00175



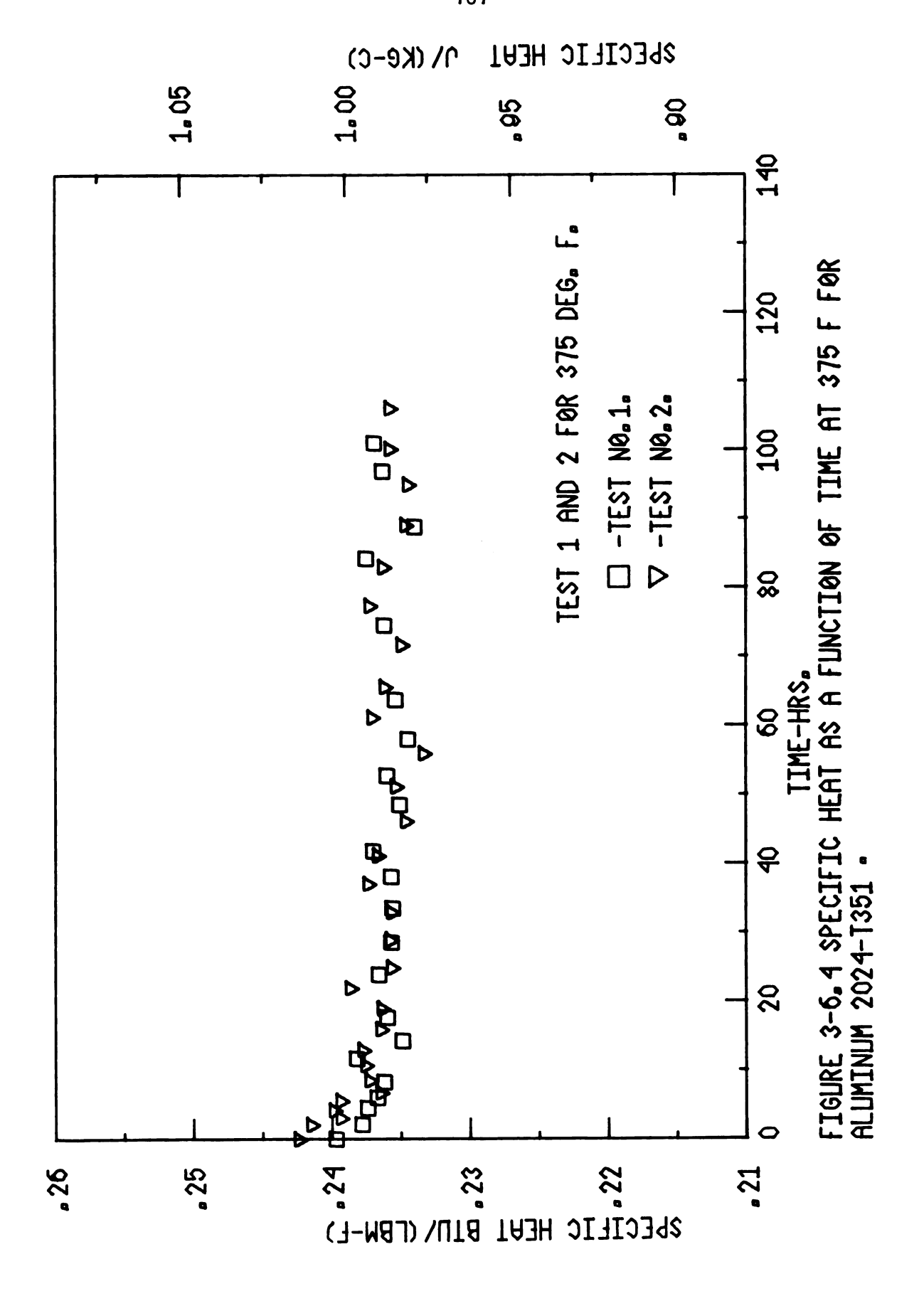
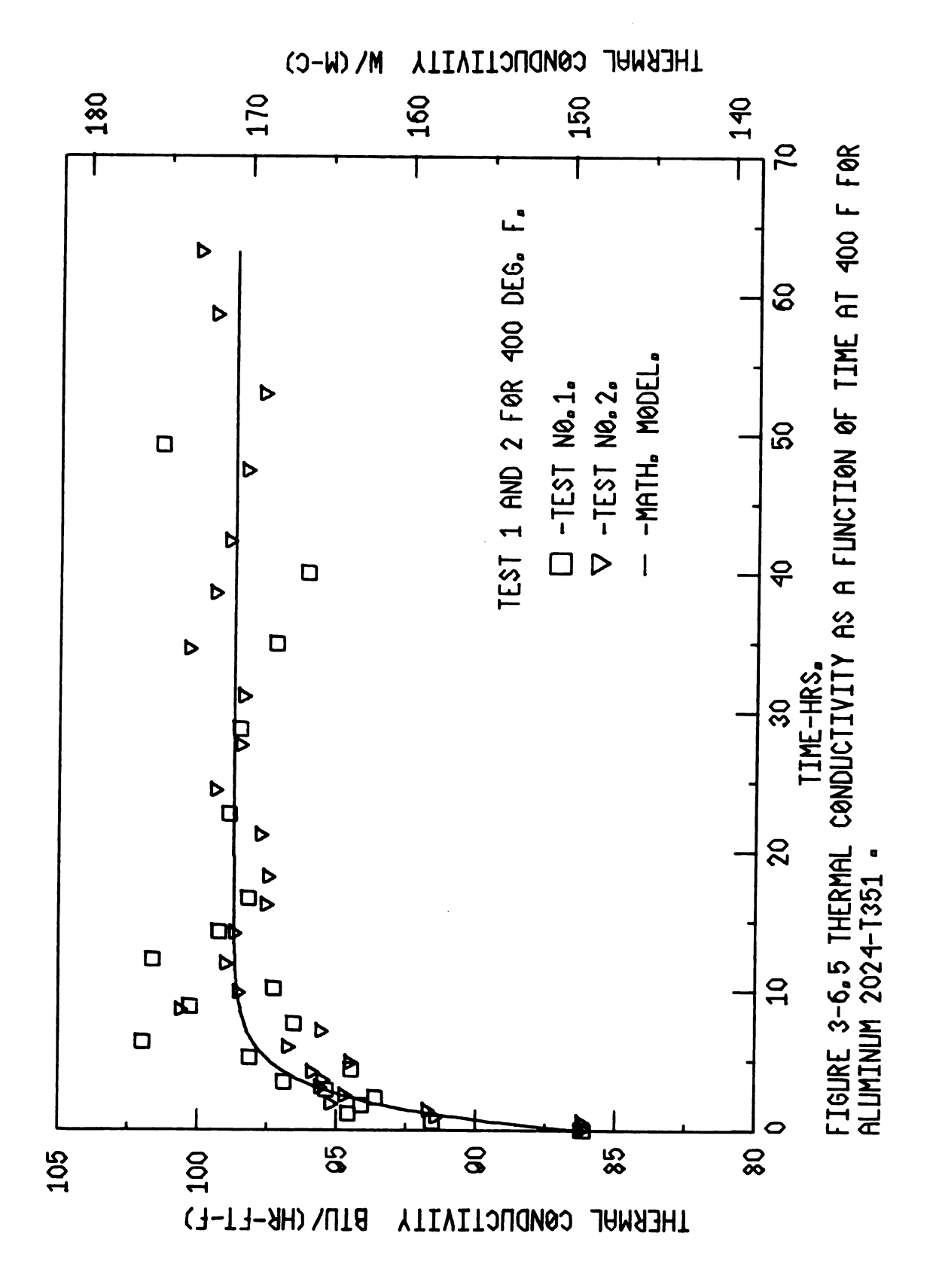


TABLE 3-6.5 ISOTHERMAL AGEING TEST AT 400 DEG. F. TEST NO. 1 FOR AL-2024-T351. VALUES OF \bar{K} AND $\bar{\bar{C}}_P$ AND THEIR RESPECTIVE STANDARD DEVIATIONS.

RUN	TIME	K	s _K	Ē₽	scp
NO.		BT	Ū	ВТ	
	HR\$.	HR-F	T-F	LBM	I-F
1	.00	86,11	2.28	. 2416	.00232
2	.58	91.56	2.97	. 2436	.00650
3	1.20	94.58	3.50	.2494	.00325
4	1.81	94.11	5 . 41	. 2480	.00387
5 6 7 8	2.35	93.60	1.58	. 2394	.00290
6	2.91	95.37	0. 41	. 2416	.00348
7	3.46	96.90	1.02	.2417	.00130
8	4.33	94.97	3.77	. 2411	.00604
0	5.21	98.13	6.02	.2404	.00124
10	6,30	101.98	5,00	. 2402	.00258
11	7.63	96.54	6.07	. 2385	.00382
12	8.86	100.28	2.79	.2381	.00199
13	10.15	97.28	2.64	.2391	.00107
14	12.18	101.61	4.16	.2377	.00356
15	14.18	99.24	9.79	.2372	.00821
16	16,60	98.21	2.11	. 2395	.00247
17	22.65	98.89	2.07	.2371	.00255
18	28.75	98.54	2.30	.2377	.00156
19	34.91	97.25	1.03	.2374	.00050
20	40.00	96.15	3 . 45	. 2385	.00154
21	49. 20	101.36	1.80	. 2331	.00103

TABLE 3-6.6 ISOTHERMAL AGEING TEST AT 400 DEG. F. TEST NO. 2 FOR AL-2024-T351. VALUES OF \bar{K} AND $\bar{\bar{C}}_{P}$ AND THEIR RESPECTIVE STANDARD DEVIATIONS.

RUN	TIME	Κ̄	\$ _K	ξ̄ _P	SCP
NO.		BT		BT	
	HR\$.	HR-F		LBM	
1	.00	86,30	2.57	2543	.00380
	.18	86.17	1.73	2511	.00440
2 3 4 5 6 7	.58	86.22	4.15	2480	.00288
4	. 98	91.48	1.81	.2477	.00268
5	1.46	91.76	2.08	2435	.00379
6	1.96	95, 25	2.83	2407	.00495
7	2.53	91.74	3.11	. 2435	.00214
8	3.08	95.64	1.07	. 2426	.00323
9	3.66	95.55	3.03	. 2420	.00421
10	4, 20	95.93	3.01	2420	.00370
11	4.90	94.56	0.38	. 2381	.00262
12	5.98	96.80	7.47	2389	.00397
13	7.14	95,60	2.58	2410	.00401
14	8,63	100.66	2.75	2400	.00382
15	9.91	98.59	3.79	. 2391	.00272
16	11.06	99.04	2.44	. 2392	.00399
17	14.13	98.73	4.30	. 2396	.00321
18	16, 21	97.60	2.24	2385	.00454
19	18.21	97.54	2.67	2396	.00131
20	21, 21	97.81	6,12	. 2368	.00499
21	24.38	99.44	4.00	.2396	.00427
22	27.65	98.54	2.58	2402	.00449
23	31.13	98.44	3.33	. 2386	.00330
24	34,55	100.41	2.16	-2371	.00365
25	38.53	99.48	3.73	2 376	.00310
26	42.31	98.99	4, 21	. 2396	.00426
27	47.38	98.37	2.00	.2357	.00301
28	52.93	97.77	1.78	. 2360	.00365
29	58.63	99.53	4.08	.2387	200369
30	63,16	100,12	3.10	.2354	.00350



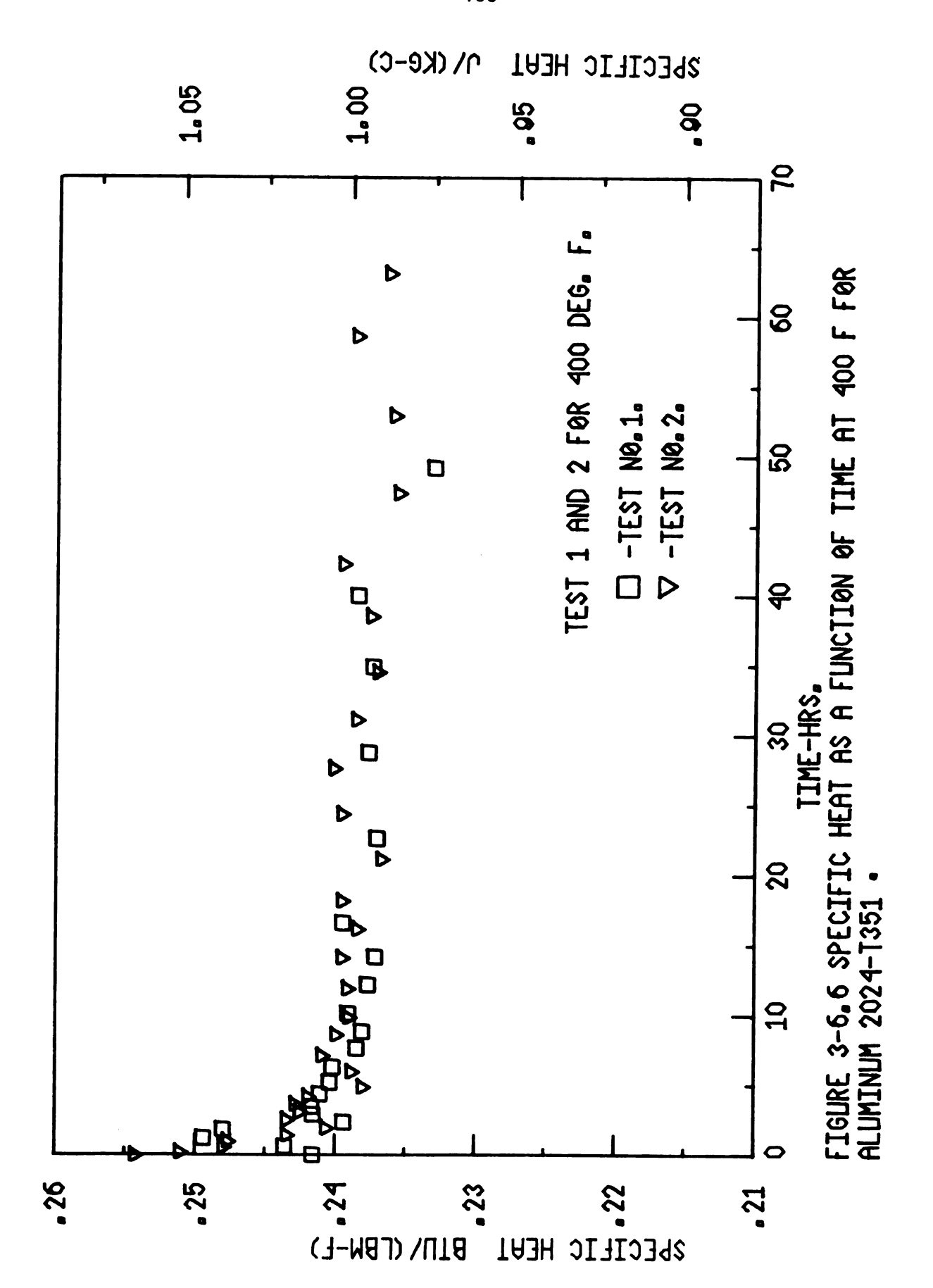
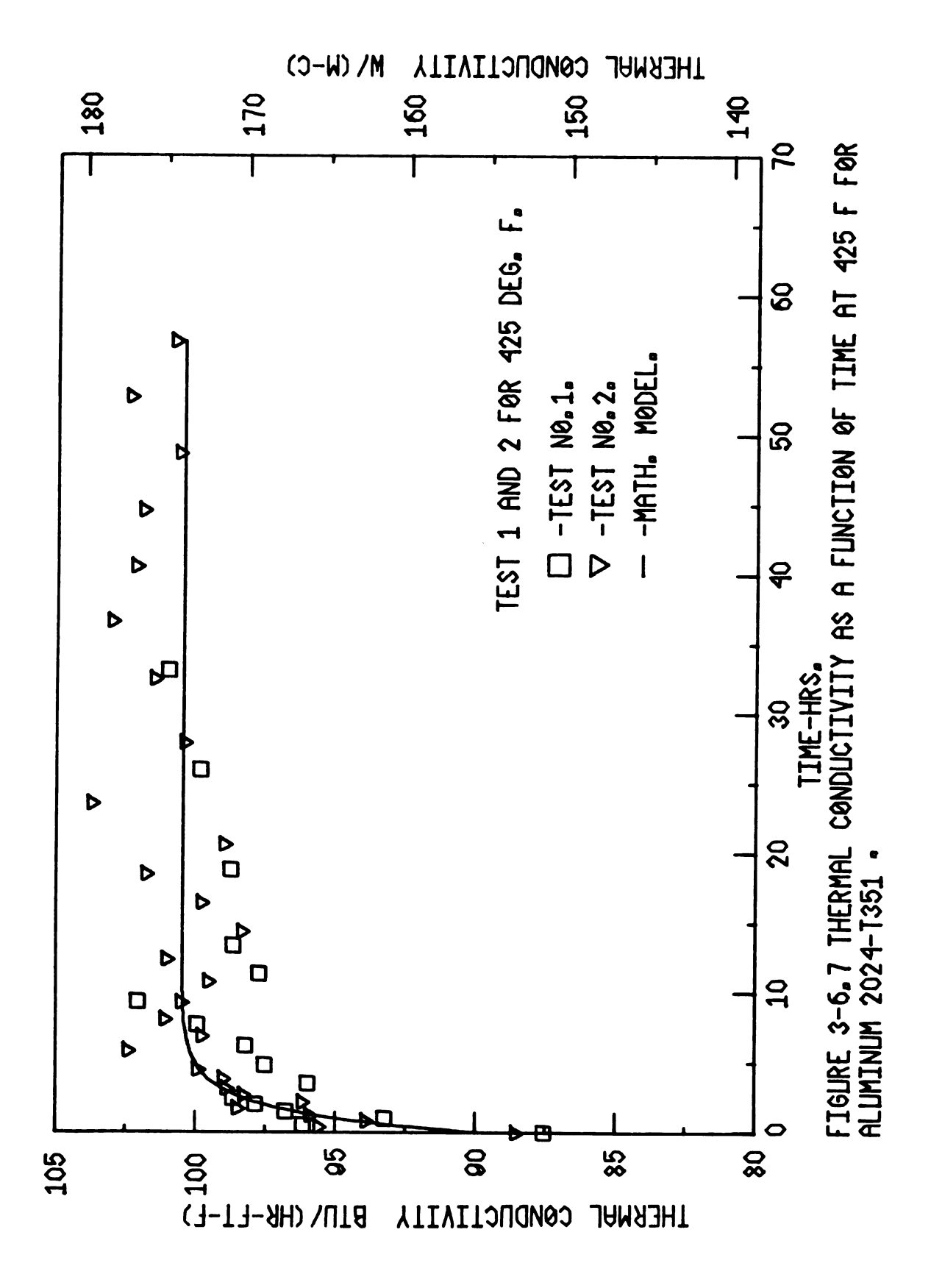


TABLE 3-6.7 ISOTHERMAL AGEING TEST AT 425 DEG. F. TEST NO. 1 FOR AL-2024-T351. VALUES OF \bar{K} AND $\bar{\bar{C}}_P$ AND THEIR RESPECTIVE STANDARD DEVIATIONS.

RUN	TIME	K	s _K	ξ̄ _P	SCP
NO.		ВТ	П	ВТ	
	HRS.	HR-F	T-F	LBM	<u> </u>
1	.00	87.54	3.64	.2421	.00226
2	.56	96.15	3.86	.2449	.00214
3	1.01	93.24	2.04	.2473	.00449
4 5 6	1.51	96. 78	3.81	. 2461	.00326
5	1.98	97.84	3.86	. 2463	.00607
	2.43	98.65	3.58	. 2454	.00569
7	3.48	95.99	2.81	. 2437	.00510
8	4.78	97.53	3.54	_2393	.00329
9	6, 20	98.22	3.85	. 2403	.00429
10	7.70	99.94	5.39	<u>.</u> 2412	.00213
11	9.36	102.07	7.88	.2420	. 00460
12	11.36	97.75	2.18	. 2390	.00197
13	13.36	98.67	2.77	. 2363	.00253
14	18.80	98.78	4. 42	.2389	.00348
15	25.93	99.88	6.80	. 2351	.00406
16	33.10	101.04	4.05	. 2400	.00412

TABLE 3-6.8 ISOTHERMAL AGEING TEST AT 425 DEG. F. TEST NO. 2 FOR AL-2024-T351. VALUES OF \bar{K} AND $\bar{\bar{C}}_P$ AND THEIR RESPECTIVE STANDARD DEVIATIONS.

RUN	TIME	Κ̈	s _K	Ĉ₽	\$ _{CP}
NO.		ВТ	П	ВТ	
	HRS.	HR-F	T-F	LBM	 -F
1	.00	88.58	4.00	. 2520	.00394
	. 43	95.61	2.30	. 2452	.00510
3	. 83	93.93	2.72	.2424	.00413
2 3 4 5 6 7 8	1.26	95.94	3.03	. 2450	.00288
5	1.73	98.52	5, 44	.2450	.00374
6	2.20	96, 21	3.80	24 52	.00301
7	2.68	98.31	2.17	.2432	.00233
8	3,15	98.93	1.56	.2416	.00202
9	3.83	99.04	2.13	.2400	.00830
10	4,50	99.94	5, 83	.2417	.00403
11	5.83	102.43	4.70	.2387	.00470
12	6.91	99.81	4.00	2386	.00349
13	8.11	101.13	2.78	.2394	.00424
14	9.30	100.55	7.48	. 2405	.00275
15	10.81	99.59	4,06	. 2399	.00228
16	12.38	101.07	2.49	.2408	.00232
17	14.38	98.39	2.43	. 2405	.00170
18	16. 43	99.83	2.23	. 2380	.00391
10	18.50	101.80	1.77	. 2396	.00145
20	20.63	99.02	3.15	. 2396	.00200
21	23.56	103.76	2.99	. 2405	.00331
22	27.90	100.46	3.00	.2374	.00260
23	32, 48	101.53	1.61	<i>.</i> 2380	.00328
24	36.63	103.07	5.50	. 2392	.00448
25	40,60	102.23	4.20	. 2380	.00435
26	44, 60	101.06	2.30	. 2382	.00275
27	48.68	100.69	2.80	. 2383	.00300
28	52.76	102.44	2.68	. 2399	.00277
20	56.76	100. \$5	4, 70	.2407	.00315



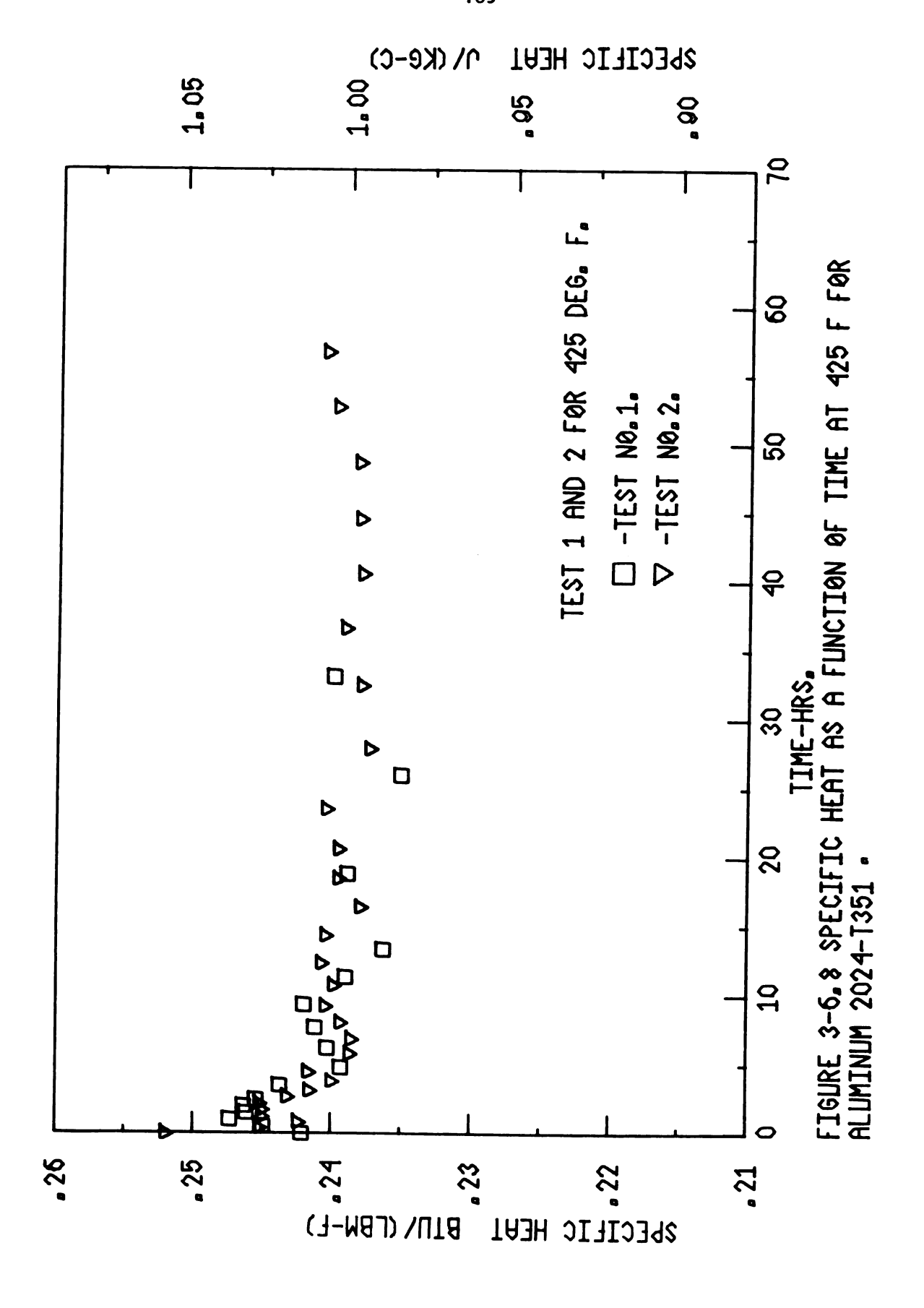


figure of thermal conductivity versus time is a plot of the mathematical model Equation (3-6.1).

The values of thermal conductivity and specific heat for all isothermal ageing tests at about room temperature are shown in Table 3-6.9. The last row of Table 3-6.9 contains the average temperature, average value of thermal conductivity, average value of specific heat, and estimated standard deviations of conductivity and specific heat. The values of standard deviation for 16 values of thermal conductivity and specific heat given in Table 3-6.9 were determined by:

$$S_{k} = \left[\frac{1}{15} \sum_{i=1}^{16} (\bar{k}_{i} - \bar{k})^{2} \right]^{1/2}$$
 (3-6.2)

$$S_{c_p} = \left[\frac{1}{15} \int_{i=1}^{16} (\bar{c}_{p_i} - \bar{c}_{p})^2\right]^{1/2}$$
 (3-6.3)

where \bar{k} and $\bar{\bar{c}}_p$ are the average of 16 values of thermal conductivity and specific heat, respectively, given in Table 3-6.9.

Table 3-6.10 shows the values of the thermal conductivity and specific heat after completion of precipitation for every isothermal ageing temperature, measured at about room temperature. The last row of Table 3-6.10 shows the average temperature, average specific heat, and estimated standard deviation of specific heat calculated by using Equation (3-6.3).

TABLE 3-6.0 VALUES OF \bar{K} AND $\bar{\bar{C}}_P$ AND THEIR RESPECTIVE STANDARD DEVIATIONS FOR AS RECEIVED AL-2024-T351 AT LOW INDICATED TEMPERATURES, THE SPECIMENS ARE THEN USED FOR ISOTHERMAL AGEING TESTS.

TEST	AGEING	SAMPLE	Κ̈	s _K	ξ̄ _P	Scp
NØ.	TEMP.	TEMP.	В	עד	ВТ	
	DEG.F.	DEG.F.	HR-F	T-F	LBM	 - F
1	350.	85.9	71.96	2.39	. 2226	.00239
-		86.6	72.74	2.75	2200	.00543
2		86.7	73.02	1.22	.2210	.00290
-		93.6	73.00	1.48	. 2215	.00471
1	375.	86.5	72.67	2.78	.2210	.00479
-		93.4	71.79	4.41	2195	.00447
2		35. 2	71.61	1.28	2211	.00255
-		93.4	72.81	2.23	2235	.00474
1	400.	101.5	72.76	0.43	-2248	.00283
-		105.5	72.94	2.98	.2247	.00060
2		86.7	71.42	1.87	2208	.00086
-		87.1	70.83	2.73	-2214	.00128
1	425.	85.0	71.66	2.52	2206	.00268
-		93.9	72.60	1.25	.2227	.00263
2		\$5.5	73.00	1.55	-2213	.00305
-		92.5	73.61	2.16	-2190	.00519
AVE	RAGE	90.6	72.41	* 76	_2216	* 00170

* SEE EQUATIONS (3-6.2) AND (3-6.3).

TABLE 3-6.10 VALUES OF \bar{K} AND $\bar{\bar{C}}_P$ AND THEIR RESPECTIVE STANDARD DEVIATIONS FOR AGED AL-2024-T351. THE SPECIMENS ARE AGED AT HIGH TEMP. AND THEN COOLED AT ABOUT ROOM TEMP. AND VALUES ARE OBTAINED.

TEST	AGEING	SAMPLE	Ř	\$ _K	ξ̄ _P	SCP
NO.	TEMP.	TEMP.	В	TU	ВТ	
	DEG.F.	DEG.F.	HR-F	T-F	LBM	I-F
1	350.	85.8	92.02	3.61	. 2220	.00173
-		92.8	92.10	1.46	-2231	.00242
2		86.2	93.40	1.63	-2208	.00307
-		93.2	92.59	3.14	.2232	.00210
1	375.	86.3	94.60	3.37	.2180	.00354
_		93.2	92.86	3.53	2204	.00367
2		86.6	93.16	2.44	-2228	.00147
-		93.7	92.89	2.97	.2219	.00245
1	400.	93.5	93.66	2.56	.2219	.00235
-		98.6	95.40	5.35	.2233	.00515
2		86.4	95.43	1.84	-2209	.00288
-		93.6	95.32	1.40	.2209	.00381
1	425.	86.1	95.97	2.79	.2205	.00257
-		86.2	97.46	3.12	.2208	.00300
2		86.1	97.55	2.66	2200	.00175
-		93.4	95. 77	5 . 47	.2206	.00024
AVE	RAGE	90.7			.2213	* 00130

* SEE EQUATION (3-6.3).

Table 3-6.11 gives the values of thermal conductivity and specific heat of as received A1-2024-T351 as a function of temperature. The experiment was carried out with a pair of fresh specimens and it is assumed that due to the relatively low temperatures and fast measurements that the amount of precipitation is negligible. The values of thermal conductivity and specific heat for the initial ageing time of isothermal ageing tests are also given in Table 3-6.11.

Several pairs of specimens were heated to the annealing temperature range (see Figure 3-1.1) and were held at that temperature for 24 hours, then cooled slowly to room temperature, and thermal conductivity and specific heat were determined as a function of temperature. Tables 3-6.12 and 3-6.13 show the thermal conductivity and specific heat of annealed A1-2024-T351 as a function of temperature. Data in Table 3-6.12 corresponds to the specimens which were heated to 575°F and cooled slowly in 24 hours, while data in Table 3-6.13 was obtained from a pair of specimen heated to 925°F and cooled slowly in several days.

3-7 Error Analysis

The procedure to estimate the errors is analogous to Section 2-4 of Chapter 2, with the following exceptions:

- 1. All experiments for A1-2024-T351 were performed with the low heat input.
- 2. The heater element was of the silicone rubber type.
- 3. The specimen thickness was 1.5 inches.

TABLE 3-6.11 VALUES OF \bar{K} AND $\bar{\bar{C}}_P$ AND THEIR RESPECTIVE STANDARD DEVIATIONS AS A FUNCTION OF TEMPERATURE FOR AS RECEIVED AL-2024-T351.

			UNCOR	RECTED		CORRE	CTED
RUN	SAMPLE	Ķ	s _K	ξ̄ _P	SCP	ĸ	Ēρ
NO.	TEMP.	В	עד	B.	ַ עז	עדפ	ВТИ
	DEG.F.	HR-	FT-F	LBI	1 -F	HR-FT-F	LBM-F
.1	86.3	73.01	2.06	. 2209	.00233	71.75	.2168
2	93.8	73.39	1.52	2237	.00068	72.18	.2192
3	151.4	73.64	2.02	-2209	.00212	72.56	2160
4	159.0	73.37	1.97	2215	.00205	72.29	.2166
5	199.7	76.81	1.59	2242	.00078	75.80	.2187
6	207.0	75.77	2.63	. 2223	.00106	74.78	.2169
7	247.5	76.31	1.04	2250	.00135	75.42	.2190
8	254.5	77.97	3.48	. 2264	.00149	77.07	.2204
9	308.7	80.59	1.45	. 2362	.00292	79.77	.2294
DATA	FROM I	NITIAL A	SEING	TIME OF	ISOTHERM	AL AGEIN	6 TESTS.
10	350.0	\$1.92	6, 46	2436	.00617	81.18	. 2361
11	350.0	82.06	3.38	2396	.00471	81.32	.2322
12	375.0	83.00	1.08	.2397	.00301	82.30	. 2321
13	375.0	\$2.28	2.91	-2424	.00627	81.50	.2347
14	400.0	86.11	2.28	.2416	.00232	85.43	.2337
15	400.0	86,30	2.57	2543	.00138	\$5.62	2460
16	425.0	87.54	3.64	. 2421	.00226	86.80	.2339
17	425.0	88.58	4.09	. 2520	.00394	87.92	.2435

TABLE 3-6.12 VALUES OF \bar{K} AND $\bar{\bar{C}}_P$ AND THEIR RESPECTIVE STANDARD DEVIATIONS AS A FUNCTION OF TEMPERATURE FOR AL-2024-T351. ANNEALED FROM 575 DEG. F.

			UNCOR	RECTED		CORRE	CTED
RUN	SAMPLE	K	\$ _K	ξ̄ _P	\$ _{CP}	ĸ	Ē₽
NO.	TEMP.	В	TU	B.	TU	ВТИ	ВТИ
	DEG.F.	HR-	FT-F	LBI	1-F	HR-FT-F	LBM-F
1	85.2	102.25	1.02	- 2225	.00191	100.49	-2184
2	86.1	103.60	1.14	2198	.00163	101.82	2158
3 4	86.2	104.05	1.12	2183	.00116	102.26	2143
4	87.9	100.97	2.85	2225	.00130	99. 23	2184
5	92.2	103.77	2.47	2209	.00428	102.06	2166
5 6 7	93.4	101.55	1.09	2211	.00291	99.87	2168
7	149.6	103.30	2.11	2205	.00190	101.78	-2156
8	150.9	102.33	2.90	2197	.00110	100.82	2149
9	156.4	100.13	3.63	2195	.00216	98.66	-2147
10	158.0	104.67	0.97	-2189	.00440	103.13	2141
11	198.7	103.60	4.20	-2190	.00216	102.24	.2137
12	203.8	101.15	1.50	2212	.00177	99.82	.2158
13	205.7	101.04	3.88	2193	.00106	99.71	2139
14	210.5	100.93	2.32	2210	.00249	99.61	2156
15	250.4	105.68	2.69	. 2223	.00209	104.26	.2164
16	255.0	104.18	2.28	2227	.00118	102.78	.2168
17	257.4	103.88	3.44	2227	.00298	102.49	2168
18	261.8	105.86	3.60	2233	.00346	104.44	2173
10	299.3	104.92	4.80	2303	.00396	103.85	2236
20	300.3	107.40	6.36	.2334	.00505	106.30	-2267
21	305.3	105.32	5.35	2333	.00376	104.25	2266
22	306.6	109.37	4.27	. 2322	.00621	108.25	2255
23	348.7	110.09	6.07	2320	.00469	109.10	-2248
24	340.5	103.84	5.20	. 2326	.00344	102.91	2254
25	355.5	105.07	4.40	2343	.00493	104.12	-2271
26	355.7	106.30	1.28	-2347	.00444	105.43	-2274
27	397.7	108.73	6.72	2363	.00466	107.87	.2285
28	308.3	106.55	4.03	2365	.00522	105.77	2287
20	404.3	106.61	3.88	2367	.00422	105.76	-2280
30	404.7	109.05	4. 85	. 2385	.00224	108.19	.2307

TABLE 3-6.13 VALUES OF \bar{K} AND \bar{C}_P AND THEIR RESPECTIVE STANDARD DEVIATIONS AS A FUNCTION OF TEMPERATURE FOR AL-2024-T351. ANNEALED FROM 925 DEG. F.

			UNCOR	RECTED		CORRE	CTED
RUN	SAMPLE	K	s _K	Ēρ	SCP	ĸ	Ēρ
NO.	TEMP.	В	עד	B1	עז	ЦТВ	ЦТВ
	DE6.F.	HR-	FT-F	LBN	1-F	HR-FT-F	LBM-F
1	86.3	101.45	2.35	. 2221	.00361	99.71	.2180
2	93.1	102.17	5,82	. 2244	.00286	100.48	. 2200
3	93.9	105.84	8.58	. 2231	.00395	104.09	-2188
4	99.5	103,60	3.34	- 2228	。00452	101.89	2185
5	150.7	102.00	4.62	.2212	.00122	101.48	2163
6	157.9	103.13	5.36	2208	.00192	101.61	2159
7	108.1	102.70	4.79	2206	.00183	101.35	2152
8	205.1	102.28	2.32	. 2238	.00294	100.94	-2183
0	211.3	100.29	2.75	2202	.00375	98.97	-2148
10	218.1	103.62	7.77	. 2266	.00440	102.26	2211
11	253.3	100.76	4.35	. 2266	.00278	99.59	2205
12	250.8	102.59	4.67	2265	.00214	101.25	. 2205
13	300.7	106.45	1.71	2324	.00245	105.36	. 2257
14	306.8	106.81	1.61	2351	.00539	105.72	.2283
15	307.3	103.39	3.65	2365	.00347	102.34	.2297
16	312.6	106.89	4.86	2353	.00665	105.80	. 2285
17	348.8	108.36	2.92	. 2381	.00107	107.38	.2307
18	355.1	106.76	4.60	2350	.00670	105.80	. 2286
19	400.5	104.07	2.93	. 2415	.00128	103.25	. 2336
20	405.7	105.85	4.18	2396	.00202	105.90	.2317
21	406,5	109.33	5.87	.2446	.00149	108.35	. 2366

After making the necessary calculations, the results are shown in Tables 3-7.1 and 3-7.2. Using Table 3-7.2, the measured values of \bar{k} and $\bar{\bar{c}}_p$ can be corrected for any given specimen temperature.

3-8 Comparison and Discussion

Analogous to Section 2-5 of Chapter 2, the least-squares technique was used for the corrected values of thermal conductivity and specific heat given in Tables 3-6.11, 3-6.12, and 3-6.13. The statistical F-test criteria (Section 2-4.3) was also used to determine the usefulness of the additional term. The following relationships for \hat{k} and \hat{c}_p of Al-2024-T351 versus temperature, using the

TABLE 3-7.1 CORRECTION DATA FOR A PAIR OF AL-2024-T351 SPECIMENS.

GUARD TEMP.	SAMPLE TEMP.	HEAT INPLIT	HEAT INPUT	Q _A (2-4,14)	H (2-4 . 13)	DL/L _Q
DEG.F.	DEG.F.	WATTS	ИТА	ита	ита	
80. 100. 150. 200. 250. 300. 350. 375. 400. 425.	84.2 104.2 154.1 204.0 253.9 303.8 353.7 378.6 403.6 428.5	272.85 272.52 271.70 270.88 270.08 269.25 268.43 268.02 267.62 267.21	3.8800 3.8750 3.8630 3.8520 3.8400 3.8280 3.8170 3.8110 3.8050 3.7990	.055 .054 .053 .052 .051 .050 .040 .049 .048	.076 .020 .030 .042 .052 .060 .070 .074 .078	.00009 .00037 .00107 .00176 .00246 .00316 .00386 .00421 .00456

TABLE 3-7.2 CORRECTIONAL MULTIPLIERS FOR A PAIR OF AL-2024-T351 SPECIMENS.

					 	,
GLIARD	SAMPLE	c _{KA}	CKTC	c _{KE}	cKH	cK
TEMP.	TEMP.				ĺ	(2-4, 15)
DEG.F.	DEG.F.					
80.	84.2	.9856	. 9933	.9998	1.004	.9828
100.	104.2	.9857	.9933	.9992	1.005	.9835
150.	154.1	.9860	.9933	.9979	1.008	. 9853
200.	204.0	. 9863	.0033	.9965	1.011	.0860
250.	253.0	.9866	.9933	.9951	1.014	.9884
300.	303.8	.0860	.9933	.9937	1.016	.0808
350.	353.7	.9 872	.9933	.9923	1.018	.9910
375.	378.6	.9874	.9933	.9916	1.019	.9916
400.	403.6	.9875	.9933	.9906	1.021	.9921
425.	428.5	.9 877	.0033	.0826	1.022	.992 6
GLIARD	SAMPLE	CCPA	CCPTC	C _{CPE}	CCPH	C _{CP}
TEMP.	TEMP.	VIII	0110	VI L	VIII	(2-4, 16)
DEG.F.	DEG.F.					
80.	84.2	.9856	1.	1.	.9959	.9816
100.	104.2	.0857	1.	1.	. 9948	-9806
150.	154.1	.0860	1.	1.	.9919	.9780
200.	204.0	.0863	1.	1.	.0801	.9756
250.	253.0	.0866	1.	1.	. 9865	.0733
300.	303.8	.0860	1.	1.	.0830	.9711
350.	353.7	.9872	1.	1.	.9816	.9591
375.	378.6	.0874	1.	1.	. 9805	.9 582
400.	403.6	.9875	1.	1.	.9794	.9672
425.	428.5	.9877	1.	1.	.0784	.9663

data in Tables 3-6.11, 3-6.12, and 3-6.13, are obtained. For the as received case:

$$\hat{k}_a = 124.05 - 3.74 \times 10^{-3} \text{ T} + 5.7 \times 10^{-4} \text{ T}^2$$
 (3-8.1)

$$\hat{c}_{p_a} = 0.8704 + 5.81 \times 10^{-4} T$$
 (3-8.2)

For the annealed case (annealed from 575°F):

$$\hat{k}_{an} = 171.17 + 6.49 \times 10^{-2} T$$
 (3-8.3)

$$\hat{c}_{p_{an}} = 0.8827 + 3.38 \times 10^{-4} T$$
 (3-8.4)

For the annealed case (annealed from 925°F):

$$\hat{k}_{an} = 171.82 + 5.45 \times 10^{-2} T$$
 (3-8.5)

$$\hat{c}_{p_{an}} = 0.8856 + 4.12 \times 10^{-4} T$$
 (3-8.6)

The units for \hat{k} and \hat{c}_p are w/(m-C) and J/(Kg-C), respectively. The temperature T is in the range of 30-225°C.

The values obtained for \hat{k} and \hat{c}_p for three temperatures are listed in Tables 3-8.1, 3-8.2, and 3-8.3. Table 3-8.3 is for thermal conductivity of as received A1-2024-T351, and also shows the results of [21, 24] and the percentage differences between the values given by [21, 24] and present \hat{k}_a . The values of thermal conductivity of annealed A1-2024-T351 obtained by the present investigation and that of TPRC are given in Table 3-8.2, which also shows the percentage differences between the values of TPRC and the

Comparison of present k_a and ref. [24]* and [21]** for as received A1-2024-T351 and their respective percentage differences. k_a , in w/(m-C), calculated by Equation (3-8.1). TABLE 3-8.1

Temp.	TPRC Ref. [24]	Ref. [21]	Present ka	% Difference Between Ref. [24] and ƙ _a	% Difference Between Ref. [21] and ƙ _a
143.6	149.7	138.90	136.27	9.83	1.92
91.7	134.0	128.54	128.50	4.25	.03
55.4	127.3	122.24	125.59	1.33	-2.38

*Y. S. Touloukian, ed., Thermophysical Properties of High Temperature Solid Materials, Vol. 1 (1966), pp. 583-585 for Armco iron, and Vol. 2 (1966), pp. 735-737 for aluminum alloys.

**D. R. Williams and H. A. Blum, "The Thermal Conductivity of Several Metals," Thermal Conductivity--Proceedings of the Seventh Conference, Gaithersburg, Maryland, 1968, pp. 349-354.

Comparison of values of \hat{k}_{an} of present study and ref. [24] * for annealed A1-2024-T351. kan, in w/(m-C), calculated by Equations (3-8.3) and (3-8.5) and their respective percentage differences. **TABLE 3-8.2**

, and	Anne	Annealed from 575°F		Annealed from 925°F	rom 925°F
٠. ٥. ا	TPRC Ref. [24]	Present Kan	% Diff.	Present Kan	% Diff.
143.6	188.4	180.45	4.40	179.65	4.87
91.7	186.3	177.12	5.18	176.82	5.36
55.4	182.1	174.77	4.20	174.84	4.16

*Y. S. Touloukian, ed., Thermophysical Properties of High Temperature Solid Materials, Vol. 1 (1966), pp. 583-585 for Armco iron, and Vol. 2 (1966), pp. 735-737 for aluminum alloys.

Comparison of values of \hat{c}_p of present study and ref. [24]* for Al-2024-T351. \hat{c}_p , in J/kg-°C, calculated by Equations (3-8.2), (3-8.4), and (3-8.6), and their respective percentage differences. TABLE 3-8.3

Temp.	TPRC	As Rec	As Received	Annealed	Annealed from 575°F	Annealed	Annealed from 925°F
ပ္	Ref. [24]	Present Ĉpa	% Diff.	Present Ĉpan	% Diff.	Present Ĉpan	% Diff.
143.6	.928	.954	-2.72	. 931	32	.945	-1.79
91.7	.912	.924	-1.29	.913	10	.923	-1.19
55.4	.878	.903	-2.76	106.	-2.55	806.	-3.30

*Y. S. Touloukian, ed., Thermophysical Properties of High Temperature Solid Materials, Vol. 1 (1966), pp. 583-585 for Armco iron, and Vol. 2 (1966), pp. 735-737 for aluminum alloys.

present \hat{k}_{an} . Table 3-8.3 shows the values c_{pa} and c_{pan} of this study and values given by TPRC and their percentage differences.

By comparing the present values of \hat{k} and \hat{c}_p and those given by [21, 24], the following conclusions can be drawn:

- 1. In the as received condition (Table 3-8.1), the \hat{k}_a values of this study generally agree within 2.4 percent of those given in [21]. At low temperatures the \hat{k}_a of the present study is within 1 percent of the TPRC values. However, as the temperature increases, the TPRC k values become somewhat higher than \hat{k}_a . This may be due to the higher precipitation rate at the higher temperatures.
- 2. In the annealed condition (Table 3-8.2), the annealing temperature range of the aluminum alloys, as indicated in Figure 3-2.1, is between 500 to 800°F. Heating the alloys to this temperature range and with sufficiently slow cooling (annealing), a stable microstructure will be formed. The properties of two annealed aluminum specimens at two different annealing temperatures, with equal cooling processes, should be equal within the measurement errors. Data for aluminum specimens at two different annealing temperatures which are in agreement within less than 0.5 percent are shown in Table 3-8.2. The values of $k_{\rm an}$ given by TPRC for the annealing temperature of 575°F is about 5 percent higher than $\hat{k}_{\rm an}$ of the present investigation.
- 3. From Tables 3-6.10 and 3-6.11, the specific heat of as received Al-2024-T351 at room temperature is $0.9272 \, \text{J/(kg-C)}$ and the average value of specific heat for four isothermal ageing

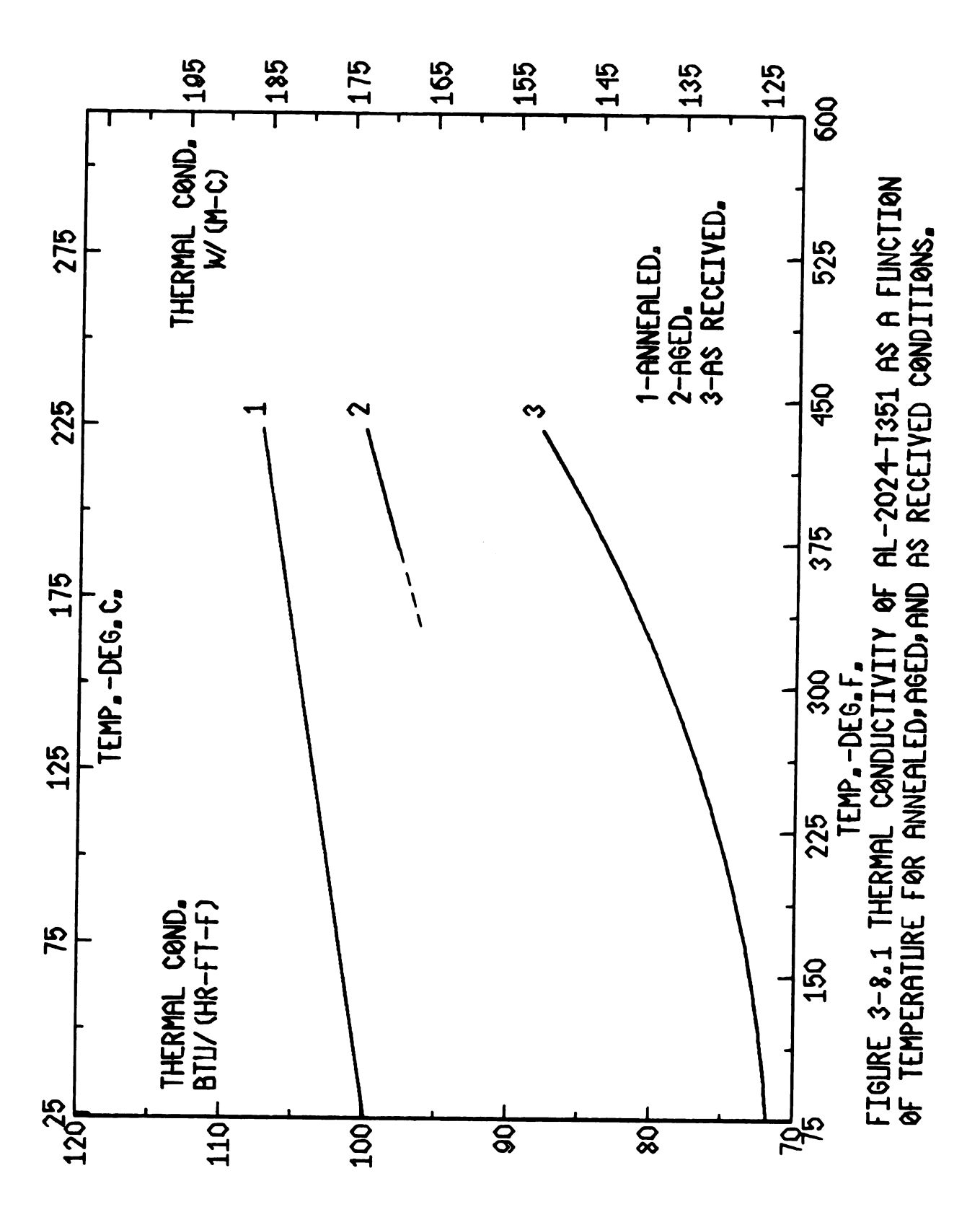
temperatures, after completion of precipitation, measured at room temperature is 0.9259 J/(Kg-C). It seems that the specific heat values are unaffected by the precipitation processes. The values of \hat{c}_p in the cases of as received, annealed from 575°F, and annealed from 925°F are shown in Table 3-8.3. By comparing these values at three different temperatures, support is given to the above mentioned discussion. The values of \hat{c}_p obtained in this investigation are within 3.3 percent of the TPRC values for all three cases.

A plot in the cases of as received, annealed from 575°F, and aged values of thermal conductivity, as a function of temperature, is shown in Figure 3-8.1. The aged values of thermal conductivity are obtained from thermal conductivity-time data when ageing time is maximum. Using the least-squares technique, a linear relation for aged values of thermal conductivity of A1-2024-T351 as a function of ageing temperature is found as:

$$\hat{k}_{aq} = 147.71 + 0.1137 T$$
 (3-8.7)

where \hat{k}_{ag} is the thermal conductivity of aged A1-2024-T351, in w/(m-C), in the ageing temperature range 175-220°C and T is the ageing temperature in °C.

Figure 3-8.1 shows the differences in thermal conductivity obtained for A1-2024-T351 in the cases of as received (zero precipitation), aged at a given temperature (partial precipitation), and annealed (complete precipitation). Holding the as received specimen at a given temperature for a sufficiently long time, the as received curve eventually meets the aged one. Then, increasing



the ageing temperature to the annealed temperature, the aged curve will reach the annealed one.

A procedure similar to that described in Section 2-5 has been devised to obtain coefficients of the estimated standard error equations for two and three parameter cases. The results are: For the as received case:

est. s.e.
$$(\hat{k}_a) = (2.98 - 9.99 \times 10^{-2} \text{ T} + 1.32 \times 10^{-3} \text{ T}^2$$

- 7.24 × 10⁻⁶ T³ + 1.41 × 10⁻⁸ T⁴)^{1/2} (3-8.8)

est. s.e.
$$(\hat{c}_{p_a}) = (1.23 \times 10^{-4} + 1.47 \times 10^{-6} \text{ T} + 5 \times 10^{-9} \text{ T}^2)^{1/2}$$
 (3-8.9)

For the annealed case (annealed from 575°F):

est. s.e.
$$(\hat{k}_{an}) = (1.64 - 2.23 \times 10^{-2} \text{ T} + 9.64)$$

 $\times 10^{-5} \text{ T}^2)^{1/2}$ (3-8.10)

est. s.e.
$$(\hat{c}_{p_{an}}) = (2.73 \times 10^{-5} - 3.73 \times 10^{-7} \text{ T} + 1 \times 10^{-9} \text{ T}^2)^{1/2}$$
 (3-8.11)

For the annealed case (annealed from 925°F):

est. s.e.
$$(\hat{k}_{an}) = (3.04 - 4.13 \times 10^{-2} \text{ T} + 1.73$$

 $\times 10^{-4} \text{ T}^2)^{1/2}$ (3-8.12)

est. s.e.
$$(\hat{c}_{p_{an}}) = (5 \times 10^{-5} - 6.79 \times 10^{-7} T + 2 \times 10^{-9} T^2)^{1/2}$$
 (3-8.13)

Using Equations (3-8.8) through (3-8.13) with corresponding error Equations (2-5.7) and (2-5.8), the percentage error, as defined in Equations (2-5.7) and (2-5.8), can be evaluated as a function of temperature in the range of 30-225°C. Typical values of percentage error are shown in Table 3-8.4.

No reference data with the exception of [1] was found to compare the thermal conductivity and specific heat of Al-2024-T351 as a function of time. The thermal conductivity of Al-2024-T351 obtained by [1] are generally higher than the k values of the present investigation, and in some cases certain inconsistencies exist which are discussed in Chapter 4.

In order to determine the accuracy of data, the experiment at every thermal ageing temperature was repeated at least once to ascertain the repeatability (as can be seen in Figures 3-6.1 through 3-6.8). The experimental results are generally repeatable. In each ageing test, the value of k increases to a maximum (aged) and then fluctuates about a mean value of k as ageing time increases.

TABLE 3-8.4 Typical values of percentage error, as defined in Equations (2-5.7) and (2-5.8), for \hat{k} and \hat{c}_p of A1-2024-T351.

Temp. °C	As Received		Annealed From 575°F		Annealed from 925°F	
	For \hat{k}_a	For \hat{c}_{p_a}	For \hat{k}_{an}	For $\hat{c}_{p_{an}}$	For \hat{k}_{an}	For $\hat{c}_{p_{\mathbf{a}n}}$
143.6	.43	.48	. 36	.28	.46	. 36
91.7	.43	.62	. 36	.28	.48	. 37
55.4	.50	.84	.48	.38	.65	.51

CHAPTER 4

MODEL ING

In this chapter the experimental data of Chapter 3 is utilized to develop a mathematical relationship for thermal conductivity which is time and temperature dependent. A correlation between dimensionless thermal conductivity and volume fraction of precipitation is found. The mathematical model for thermal conductivity is further extended to a more general case of transient thermal cycling. A differential equation is hypothesized to deal with thermal cycling. A practical example is given utilizing the mathematical model developed in this chapter.

4-1 Time and Temperature Dependence of Thermal Conductivity for Isothermal Ageing Condition

For each isothermal ageing temperature, a mathematical model was found using isothermal experimental data obtained from two ageing tests [see Equation (3-6.1)]. An analogous expression can be used to obtain a mathematical model covering any isothermal ageing temperature in the temperature range 175-225°C. Using 195 data points, given in Tables 3-6.1 through 3-6.8, the mathematical model for isothermal ageing condition is written as:

$$k_{ia}(T_{ag},t) = k_{ia}(T_{ag},0) + \Delta k_{ia}(T_{ag}) \{1 - \exp[-t/\tau(T_{ag})]^n\}$$
 (4-1.1)

where $\Delta k_{ia}(T_{ag}) = k_{ia}(T_{ag},t_{max}) - k_{ia}(T_{ag},0)$ and $k_{ia}(T_{ag},0)$ and $k_{ia}(T_{ag},t_{max})$ are the values of thermal conductivity obtained for initial (t = 0) and final (t = t_{max}) ageing times, respectively. T_{ag} is the ageing temperature, t is the corresponding ageing time, and $\tau(T_{ag})$ is the time constant. Note that values of $k_{ia}(T_{ag},0)$, $\Delta k(T_{ag})$, and $\tau(T_{ag})$ in Equation (4-1.1) depend on ageing temperature.

Equation (4-1.1) is chosen because (1) the experimental thermal conductivity-time plots given in Figures 3-6.1, 3-6.3, 3-6.5, and 3-6.7 show the exponential form, and (2) the dimensionless thermal conductivity $\{k_{ia}^{\dagger}(T_{ag},t) = [k_{ia}(T_{ag},t) - k_{ia}(t_{ag},0)]/[\Delta k_{ia}(T_{ag})]\}$ is in accordance with the form given for the kinetic law of precipitation [40, 41].

The values of $k_{ia}(T_{ag},0)$, $\Delta k_{ia}(T_{ag})$, and $\tau(T_{ag})$ in Equation (4-1.1) have been determined by the NLINA computer program using all 195 data points, obtained from 16 ageing tests, given in Tables 3-6.1 through 3-6.8.

The time exponent n in Equation (4-1.1) was calculated for every ageing temperature and the average value of 0.85 was obtained. The suggested value of n from other investigators varies from 1/2 to 5/2 depending upon the ageing temperature, the nature of the alloys, and the type of property. For rod-like precipitates a value of unity has been suggested [41]. For further discussion and experimental confirmation refer to [40, 41, 43, and 46].

In this investigation the time exponent n was chosen to be unity because the average value of 0.85 is near unity and the 195 data points do not contain sufficient information to accurately determine n (the estimation of n along with the other parameters requires extremely accurate measurements because n is correlated with the other parameters). Furthermore, with n = 1, a simple differential equation that leads to Equation (4-1.1) can be proposed.

By using the data of Tables 3-6.1 through 3-6.8, eight values of the time constant (τ) as a function of temperature were determined. Various forms of models were tried to obtain τ versus T relationships. The following three models each produced satisfactory results in the testing temperature range (175-220°C):

1.
$$\tau = \exp \left(-Q_0 + \frac{Q_1}{T + C} \right)$$
 (4-1.2)

2.
$$\tau = \exp \left(-Q_0 + \frac{Q_1}{T}\right)$$
 (4-1.3)

3.
$$\tau = \exp \left(-Q_0 + \frac{Q_1}{T + 273}\right)$$
 (4-1.4)

where T is in ${}^{\circ}$ C; Q_0 , Q_1 , and C are parameters estimated by the NLINA computer program. In this investigation the form of the model Equation (4-1.4) is preferred because of several reasons. First, the form itself is in accordance with the form of characteristic time (time constant) given by [40]. Second, the self-diffusion coefficient of precipitates (diffusion of copper into aluminum) and

characteristic time (τ) can be correlated [40, 47]. In this correlation the term Q_1 x R, where R is the gas constant [R = 1.987 cal./ (gram-mole-°K)], is called the overall activation energy or heat of diffusion. The overall activation energy for Al-Cu alloys was calculated using two methods [48]. The values obtained by these two methods are 31,400 and 34,900 cal. per gram-mole (see [48], p. 337). A value of 1.4 \pm 0.1 ev (1 ev = 23,047 cal. per gram-mole) has also been suggested by [43]. The value of Q_1 in Equation (4-1.4) calculated for Al-2024-T351 is 15,700°K, and therefore the overall activation energy can be determined as Q_1 x R = 15,700 x 1.987 \approx 31,200 cal. per gram-mole (1.35 ev). Third, the extrapolated values of τ at both ends of testing temperature range is consistent with the expectation of a precipitation phenomenon.

For each isothermal ageing test a value of $k_{ia}(T_{ag},0)$ and $\Delta k_{ia}(T_{ag})$ was obtained using the NLINA computer program. These values are also temperature dependent. Applying the least-squares technique, considering the F-test criteria (Section 2-4.3), and employing the third model for τ , the following relationships were found:

$$k_{ia}(T_{ag},t) = k_{ia}(T_{ag},0) + \Delta k_{ia}(T_{ag}) \left[1 - \exp\left[\frac{-t}{\tau(T_{ag})}\right]\right]$$
 (4-1.5a)

$$k_{ia}(T_{aq},0) = 73.24 + .3725 T_{aq}$$
 (4-1.5b)

$$\Delta k_{ia}(T_{ag}) = 74.94 - 0.2610 T_{ag}$$
 (4-1.5c)

$$\tau(T_{ag}) = \exp\left[-31.93 + 15.7 \frac{1,000}{T_{ag} + 273}\right]$$
 (4-1.5d)

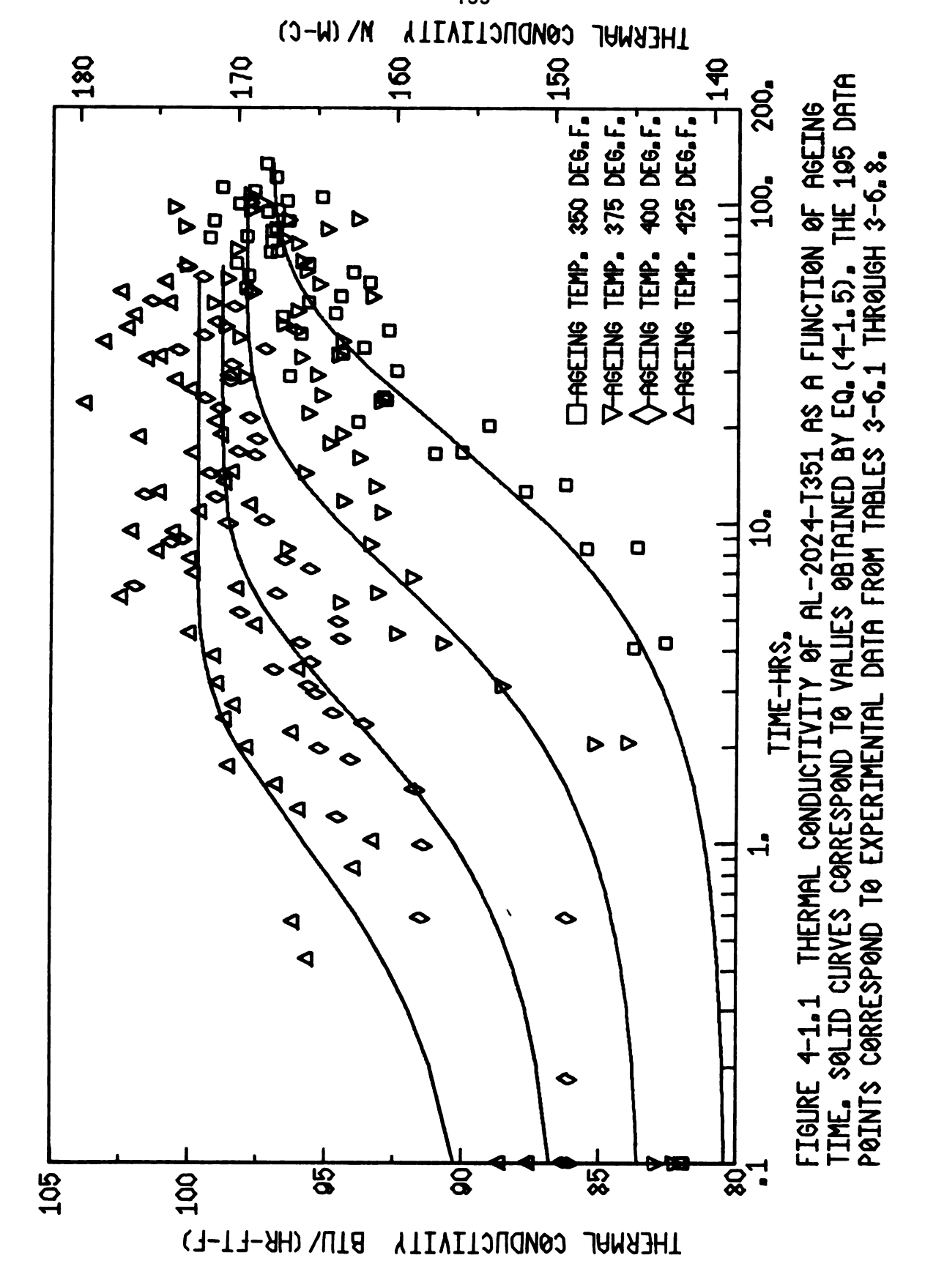
These relationships are valid for T_{ag} between 175-220°C. Units of $k_{ia}(T_{ag},t)$, $k_{ia}(T_{ag},0)$, and $\Delta k_{ia}(T_{ag})$ are w/(m-C).

A semi-log plot of $k_{ia}(T_{ag},t)$ versus ageing time is shown in Figure 4-1.1. Figure 4-1.2 is a plot of the time constant τ versus the inverse of absolute temperature. The value of overall activation energy can be calculated from the slope of the curve in Figure 4-1.2.

4-2 <u>Isothermal Experimental Data for Specific</u> <u>Heat of As Received Al-2024-T351</u>

The average value of specific heat (\bar{c}_p) of as received Al-2024-T351 (Table 3-6.9) measured at room temperature, and the average value of \bar{c}_p after completion of precipitation (Table 3-6.10) also measured at room temperature, indicates that the precipitation processes did not alter the value of \bar{c}_p significantly (0.13 percent). However, isothermal ageing data (Tables 3-6.1 through 3-6.8 and corresponding plots in Chapter 3) shows a slight increase in the value of \bar{c}_p in the initial stages of precipitation. In particular, this increase in the value of \bar{c}_p in the first five hours of ageing is moderate for low ageing temperatures. As ageing temperature increases, the increase in the values of \bar{c}_p is more noticeable. After this stage, there is a decrease in the value of \bar{c}_p to a range in the vicinity of the initial value. As the time of precipitation increases, the values of \bar{c}_p fluctuate within the range of initial values.

No attempt was made to find a mathematical model for isothermal experimental data of specific heat, for as received



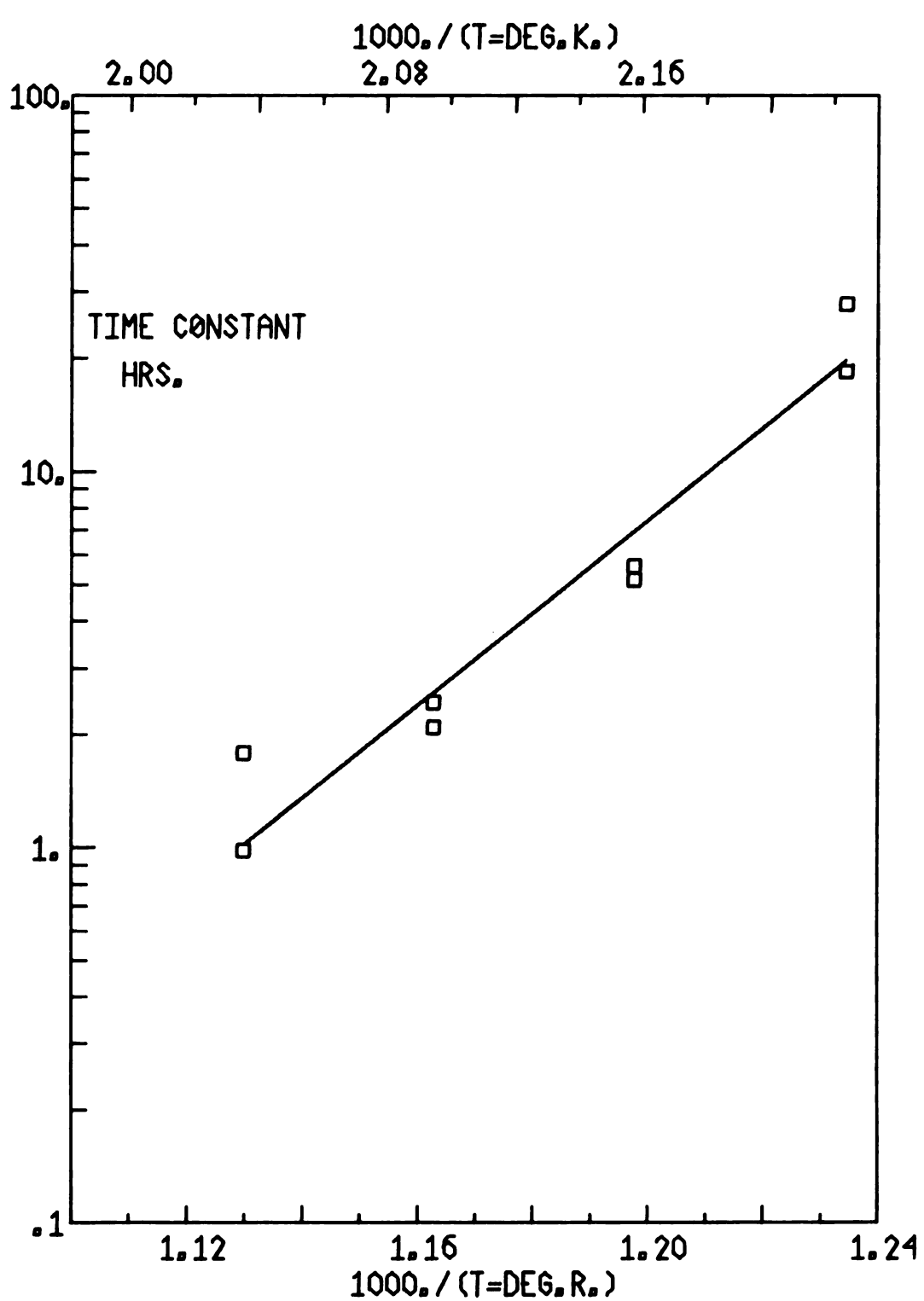


FIGURE 4-1.2 TIME CONSTANT VERSUS INVERSE ABSO-LUTE TEMP. THE SLOPE OF THE CURVE IS THE OVERALL ACTIVATION ENERGY. THE 8 EXP. DATA CORRESPOND TO VALUES OBTAINED FOR TIME CONSTANT BY EQ. (3-6.1).

Al-2024-T351, because irregular vairations in \bar{c}_p with ageing time are negligible and, at this time, are unexplainable. For each isothermal ageing temperature (Tables 3-6.1 through 3-6.8) an average value of specific heat is best at the present time.

4-3 Comparison Between Dimensionless Thermal Conductivity and Volume Fraction of Precipitation

The kinetic law of precipitation for the isothermal ageing condition (with time exponent n = 1) has the form [40, 41]):

$$X = 1 - e^{-t/\tau}$$
 (4-3.1)

We postulate the relation

$$X \equiv \frac{\eta(T_{ag},t)}{\eta_{m}(T_{ag})}$$
 (4-3.2)

where $\eta(T_{ag},t)$ is the volume fraction of precipitate at ageing temperature and time T_{ag} and t, respectively; $\eta_m(T_{ag})$ is the maximum volume fraction of precipitate at isothermal ageing temperature T_{ag} . The value of X in Equation (4-3.2) is the volume fraction of precipitation at isothermal ageing temperature T_{ag} when ageing time is t.

The dimensionless thermal conductivity (k_{ia}^{\dagger}) for isothermal conditions can be obtained from Equation (4-1.5) to be:

$$k_{ia}^{+}(T_{ag},t) = \frac{k_{ia}(T_{ag},t) - k_{ia}(T_{ag},0)}{\Delta k_{ia}(T_{ag})} = 1 - e^{-t/\tau(T_{ag})}$$
(4-3.3)

A comparison between Equations (4-3.1) and (4-3.3) yields:

$$k_{ia}^{\dagger}(T_{ag},t) = \frac{n(T_{ag},t)}{n_{m}(T_{ag})}$$
 (4-3.4)

which relates the thermal conductivity and volume fraction of precipitation.

In order to determine the denominator of Equation (4-3.4), let us first define the following:

- 1. Let $k_a(T)$ be the thermal conductivity of as received A1-2024-T351 as a function of temperature only. The value of $k_a(T)$ is determined for relatively low temperatures (below 300°F) where the amount of precipitation is negligible, or at high temperatures (300-500°F) when the ageing time is approximately zero; see Table 3-6.11 or recommended Equation (3-8.1).
- 2. Let $k_{an}(T)$ be the thermal conductivity of annealed A1-2024-T351. The annealing temperature range as shown in Figure 3-2.1 is given between 500-800°F. The value of thermal conductivity after annealing, at any temperature level, is also only temperature dependent; see Tables 3-6.12 and 3-6.13 and recommended Equations (3-8.3) and (3-8.5).
- 3. Let $k_{agr}(T_{ag})$ be the thermal conductivity of A1-2024-T351, aged at ageing temperature T_{ag} and determined at about room temperature. The value of $k_{agr}(T_{ag})$ is determined after holding

Al-2024-T351 specimens for a sufficient long time at the ageing temperature $T_{ag}(300\text{-}500^\circ\text{F})$ and then the value is obtained at about room temperature. It is shown (Table 3-6.10) that the values of $k_{agr}(T_{ag})$ increase as T_{ag} (the temperature at which the Al-2024-T351 specimens were aged) increases, indicating that the complete precipitation at any ageing temperature depends on the ageing temperature. It is postulated that a limiting ageing temperature, T_{m} , exists at which ageing and annealing temperatures coincide. At this limiting temperature, $\Delta k_{ia}(T_{ag})=0$. The value of limiting temperature can be determined from Equation (4-1.5) by equating $\Delta k_{ia}(T_{ag})$ to zero or $T_{m}=T_{ag}=74.94/0.2610=287.1^\circ\text{C}$. At this temperature the complete precipitation occurs instantaneously. (For more discussion see next section.)

Now, we propose the following equation for determining $\mathbf{n}_{m}(\mathbf{T}_{ag}),$

$$\eta_{\rm m}(T_{\rm ag}) = \frac{k_{\rm agr}(T_{\rm ag}) - k_{\rm a}}{k_{\rm an} - k_{\rm a}}$$
 (4-3.5)

where $\eta_m(T_{ag})$, as indicated in Equation (4-3.2), is the maximum volume fraction of precipitate at an ageing temperature T_{ag} and depends on T_{ag} . Note that, if as received A1-2024-T351 was aged at about room temperature, then $k_{agr}(T_{ag}) = k_a$ and $\eta_m(T_{ag})$ becomes zero. Note also, if $T_{ag} = T_m$ then $k_{agr}(T_{ag}) = k_{an}$ and $\eta_m(T_{ag})$ becomes 1.

The average room temperature at which the values of $k_{\rm agr}(T_{\rm ag})$ after ageing are determined is 32.6°C (90.7°F)

(see Table 3-6.10); using the least-squares technique, considering F-test criteria (see Section 2-4.3), a linear model is found as:

$$k_{agr}(T_{ag}) = 128.76 + 0.1751 T_{ag}$$
 (4-3.6)

where T_{ag} is the ageing temperature in °C and $k_{agr}(T_{ag})$ is the thermal conductivity value of aged A1-2024-T351 determined at 32.6°C in w/(m-C).

At the average temperature of 32.6°C, the values of k_a and k_{an} are determined using the recommended Equations (3-8.1) and (3-8.3), respectively. These values are 124.53 w/(m-C) for k_a and 173.29 w/(m-C) for k_{an} . Substituting these values into Equation (4-3.5), the $\eta_m(T_{ag})$ is determined as

$$\eta_{\rm m}(T_{\rm ag}) = 8.68 \times 10^{-2} + 3.59 \times 10^{-3} T_{\rm ag}$$
 (4-3.7)

Equation (4-3.7) is valid for ageing temperatures between 175-220°C and $\eta_{\rm m}$ varies between .715 for 175°C to .877 for 220°C.

4-4 Assumptions Regarding the Nature of Precipitation During Thermal Cycling

In practical applications, as received A1-2024-T351 may be subjected to ageing temperatures which vary arbitrarily with time. In such cases the isothermal ageing relationships developed thus far would not be applicable. To develop mathematical relationships for predicting values of volume fraction of precipitation for arbitrary temperature histories, certain assumptions are needed.

The change in volume fraction of precipitation during the thermal processes is related to the growth and redistribution of

solute atoms within solid-solution lattice structure. Generally, the enriched solutes or precipitates which are called GP zones (see Chapter 3) are assumed as an ideal physical model with a spherical shape having radius r. Gerold et al. [49] theorized that the precipitates, at a certain moment of time, have spherical zones with identical radii r and density z which is defined as the number of zones per unit volume. At any ageing temperature level (below limiting temperature T_m) z and r change with time continuously; r increases and z decreases in such a way as to move toward a new system having lower free energy. The system with minimum free energy is the one with stable precipitates. The kinetic theory of the precipitation processes [41] suggests the disappearance of the zones at the higher temperature levels. From this theory it is concluded that, at some limiting temperature T_m , all smaller zones will be absorbed into a single large zone. The size distribution of the spherical zones are therefore time and temperature dependent. In regard to the Gerold theory and the idealized physical model, the following is assumed in order to relate the change in physical model with the change in volume fraction of precipitation during the thermal processes:

- 1. At any ageing temperature, precipitation occurs when spherical zones' radii increase with time. This coincides with Equation (4-3.1). See also [43, p. 252] for plot of zone radius as a function of ageing time.
- 2. At any isothermal ageing temperature, the radius of spherical zones reaches a maximum and remains unchanged as ageing

time increases. This condition coincides with $\eta_m(T_{ag})$ defined in Equation (4-3.2).

- 3. A limiting temperature T_m exists, in which the zones become a single large zone with a maximum radius. The system at this temperature contains minimum free energy and precipitates become stable. In this condition, the maximum possible change in microstructure occurs and $\eta_m(T_{ag}) = 1$.
- 4. A sudden change in ageing temperature (below T_m) alters the size distribution of spherical zones only. At the up-cycling ageing temperature (step increase in ageing temperature), a certain number of zones dissolve to allow the remaining to grow. Conversely, if the ageing temperature is lowered, two possibilities exist. First, the zones' growth (volume fraction of precipitate) at the pre-aged temperature is less than the maximum possible growth of zones (4-3.7) at the down-cycling temperature (step drop in temperature); in this case, the up-cycling pattern of precipitation will be continued with a decrease in precipitation rate. Second, if zones' growth at the pre-aged temperature is equal to, or larger than, the maximum volume fraction of precipitate (4-3.7) at the down-cycling temperature, no change will occur in the zones' structure to contribute to a variation in precipitation. For more information, see [36, 40, 41, 42, 43, 50, 51, 52, 53, 54].

4-5 Proposed Differential Equations of Precipitation <u>During Arbitrary Thermal Cycling</u>

In order to predict the instantaneous values of volume fraction of precipitation of as received Al-2024-T351 at any temperature and time, the following two differential equations are proposed:

$$\partial \eta(T,t)/\partial t = \frac{1}{\tau(T)} [\eta_m(T) - \eta(T,t)] \text{ if } \eta_m(T) > \eta(T,t)$$
 (4-5.1a)

$$\partial \eta(T,t)/\partial t = 0$$
 if $\eta_m(T) \leq \eta(T,t)$ (4-5.1b)

where $\eta(T,t)$ is the volume fraction of precipitate at temperature T and time t; $\eta_m(T)$ is the maximum volume fraction of precipitate at temperature T, given in Equation (4-3.7); and $\tau(T)$ is the time constant, given in Equation (4-1.5d).

Equations (4-5.1a) and (4-5.1b) are differential equations describing the rate of volume fraction of precipitate during arbitrary thermal cycling. These equations to the best of our knowledge are original for the precipitation of A1-2024-T351. An equation with η_m being equal to 1 has been previously suggested, however, for the rate of transformation [40]. The values of $\eta(T,t)$, determined from Equations (4-5.1a) and (4-5.1b), are related to $k_{ia}(T,t)$ by Equation (4-3.4). There is no known model in the literature to relate the volume fraction of precipitate to the thermal conductivity of A1-2024-T351 material.

The differential Equation (4-5.1a) can also be used to obtain isothermal ageing volume fraction of precipitation. Solving Equation (4-5.1a) with the initial condition t=0, $\eta(T,0)=0$, the isothermal ageing volume fraction of precipitation, Equations (4-3.1) and (4-3.2), can be obtained. Subsequently, using the relation given in Equation (4-3.4), the isothermal ageing relationship for thermal conductivity of as received A1-2024-T351 can be determined.

4-5.1 Equation of Precipitation During Up-Cycling Thermal Process (Step Rise in Temperature)

From Equations (4-3.1) and (4-3.2), the equation of isothermal precipitation for ageing temperature T_1 is:

$$\eta(T_1,t) = \eta_m(T_1) \{1 - \exp[-t/\tau(T_1)]\}$$
 (4-5.2)

Note that T_1 equals T_{ag} because the ageing process starts at T_1 = T_{ag} . Prior to time zero, it is assumed that the as received A1-2024-T351 specimen was held at low temperatures (about room temperature).

At time t, there is a step increase (up-cycling) in temperature as shown in Figure 4-5.1. Since no time has passed during this abrupt change in temperature, the volume fraction of precipitate is constant during this change of temperature level or

$$\eta(T_1,t_1) = \eta(T_2,t_1)$$
 (4-5.3)

Integrating Equation (4-5.1a) for temperature T_2 results in:

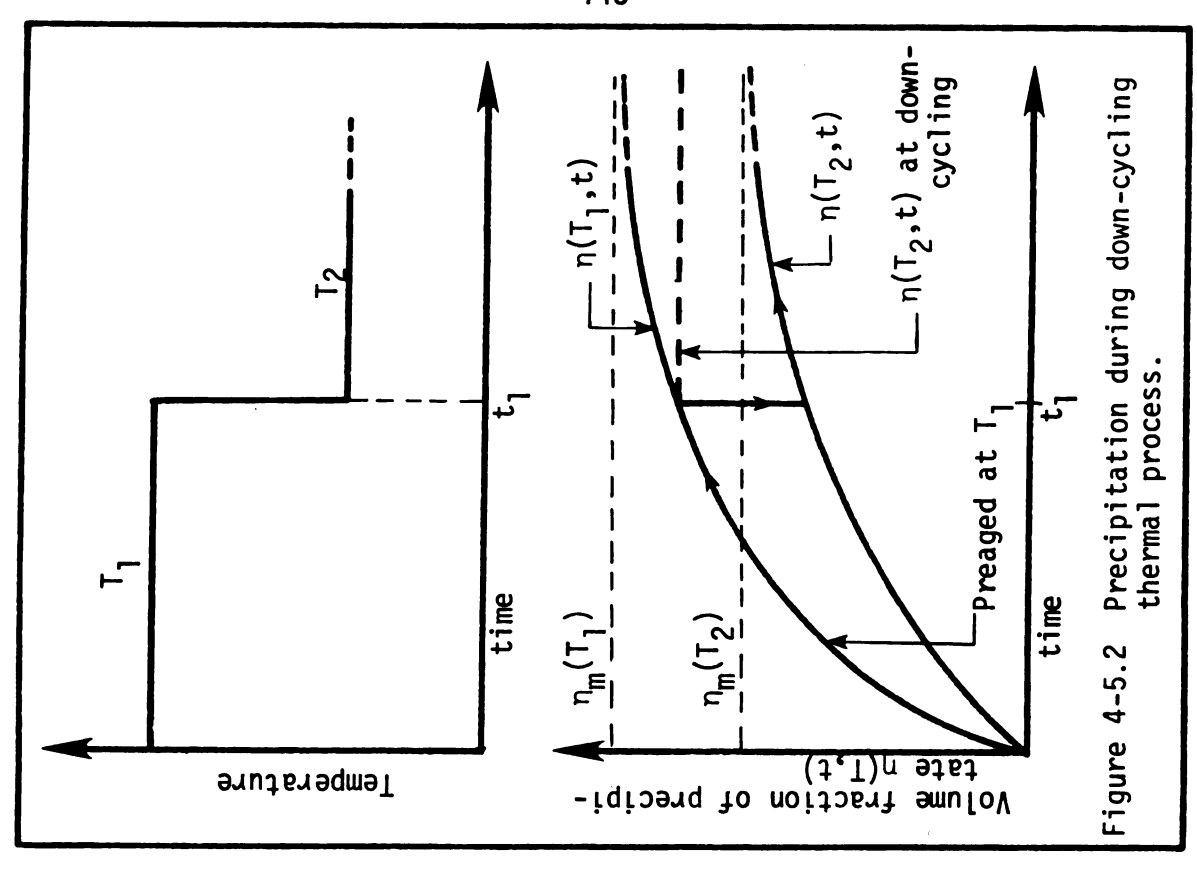
$$\eta(T_2,t) = \eta_m(T_2) + Ce$$
 (4-5.4)

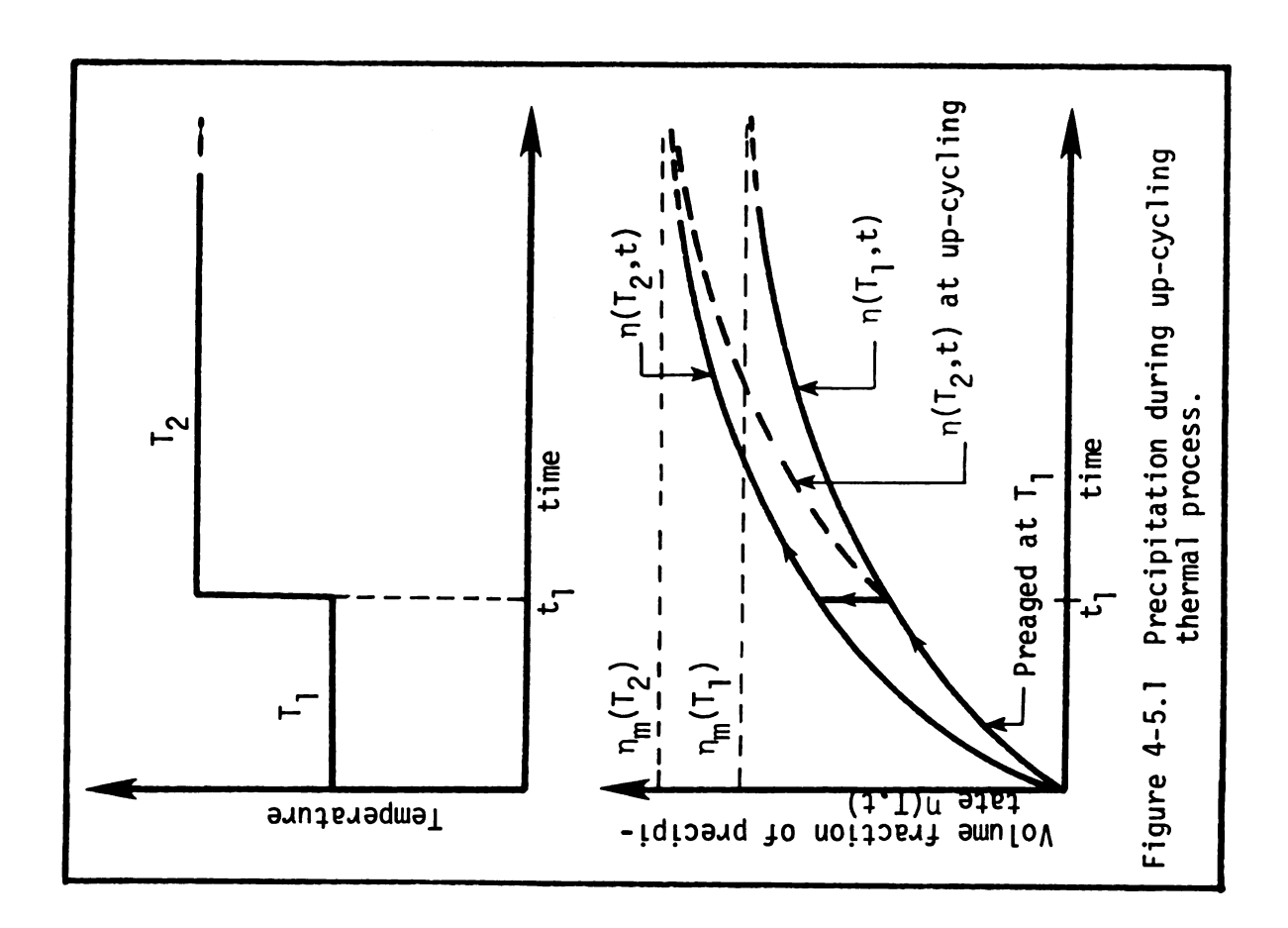
The constant of integration can be determined by the condition given in Equation (4-5.3). For $t > t_1$ one can obtain:

$$\eta(T_2,t) = \eta(T_1,t_1)e^{-(t-t_1)/\tau(T_2)}$$

$$+ \eta_{m}(T_{2}) [1 - e^{-(t-t_{1})/\tau(T_{2})}]$$
 for $t > t_{1}$ (4-5.5)

Thermal conductivity can be evaluated using Equations (4-3.4) and (4-5.5). For $t > t_1$ when $T = T_2$, the thermal conductivity is found using:





$$k_{ia}(T_2,t) = k_{ia}(T_2,0) + \Delta k_{ia}(T_2) \times \eta(T_2,t)/\eta_m(T_2)$$
 (4-5.6)

4-5.2 Equation of Precipitation During Down-Cycling Thermal Process (Step Drop in Temperature)

According to assumption 4 given in Section 4-4, two cases can be considered. In Case 1 if $\eta_m(T_2) > \eta(T_1,t_1)$, then precipitation during down-cycling and thermal conductivity can be calculated by the Equations (4-5.5) and (4-5.6) given for the up-cycling thermal processes.

In Case 2 if $\eta_m(T_2) \le \eta(T_1, t_1)$, then by Equation (4-5.1b) $\dot{\eta}(T,t) = 0$ or $\eta(T,t) = C$. For $t = t_1$ and $T = T_1$, and from Equations (4-3.1) and (4-3.2),

$$C = \eta(T_1, t_1) = \eta_m(T_1) [1 - e^{-t_1/\tau(T_1)}]$$
 (4-5.7)

For $t > t_1$ and $T = T_2$

$$\eta(T_2,t) = \eta_m(T_1) [1 - e^{-t_1/\tau(T_1)}]$$
 (4-5.8)

For $t > t_1$ the thermal conductivity can be evaluated using

$$k_{ia}(T_2,t) = k_{ia}(T_2,0) + \Delta k_{ia}(T_2) \times \eta(T_2,t)/\eta_m(T_2)$$
 (4-5.9)

The precipitation process in Case 2 is shown in Figure 4-5.2. Figure 4-5.3 shows the volume fraction of precipitate for four isothermal ageing temperatures as a function of ageing time. It also illustrates an up and down thermal cycling at t = 2 hours.

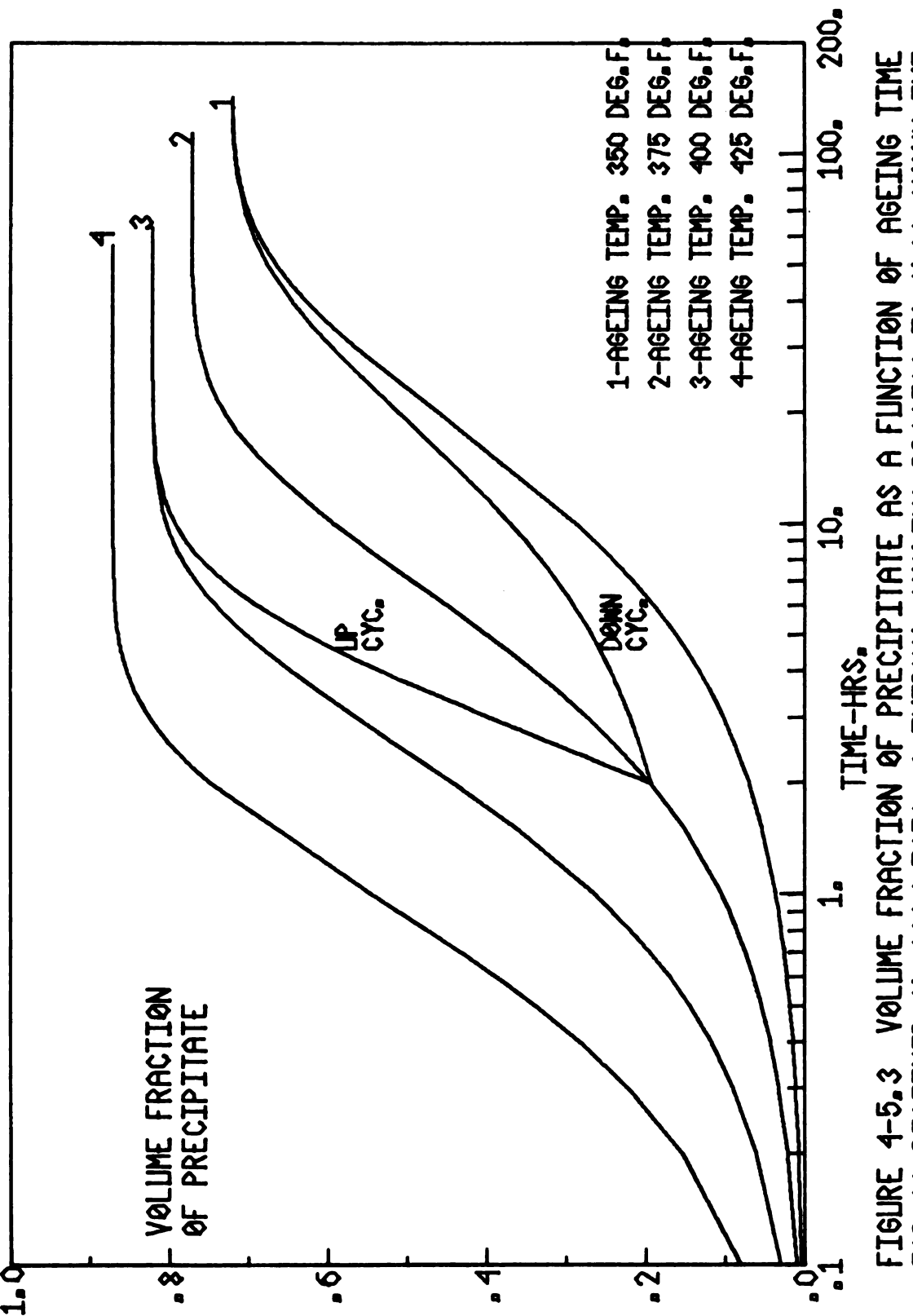


FIGURE 4-5.3 VOLUME FRACTION OF PRECIPITATE AS A FUNCTION OF AGEING TIME FOR AS RECEIVED AL-2024-1351. A THERMAL CYCLING PROCESS IS ALSO SHOWN. THE VALUES FOR UP AND DOWN-CYCLING PROCESS ARE CALCULATED BY EQ. (4-5.5).

In this illustration the pre-aged temperature is selected to be 375°F (190.6°C) and precipitation is completed at 400°F (204.4°C) or 350°F (176.7°C) for up- and down-cycling, respectively.

The thermal conductivity at $t = t_1$ and when $T_2 > T > T_1$ (Figure 4-5.1) can be found using:

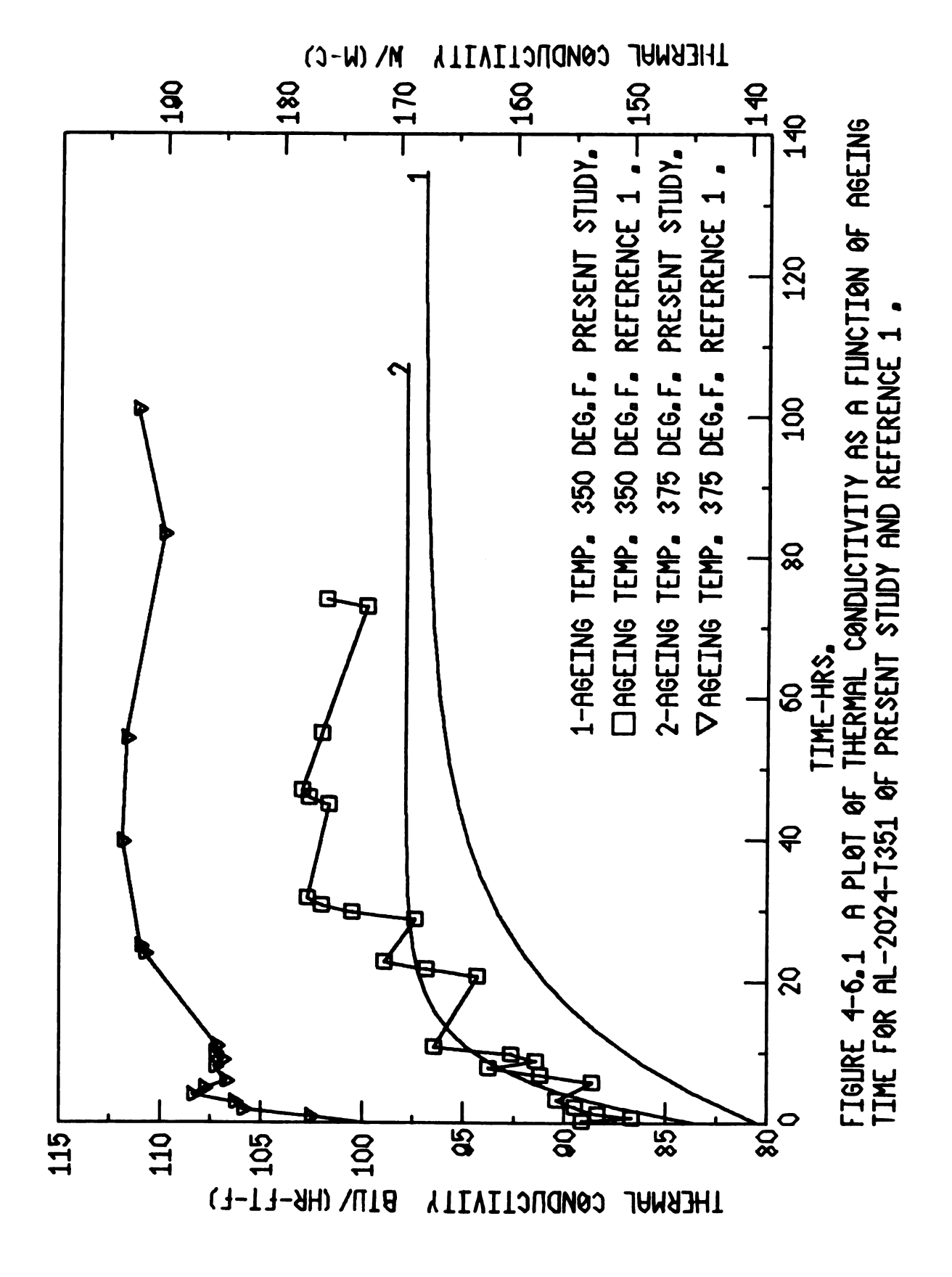
$$k_{ia}(T,t_1) = k_{ia}(T,0) + \Delta k_{ia}(T) \times \eta(T_1,t_1)/\eta_m(T)$$
 (4-5.10)

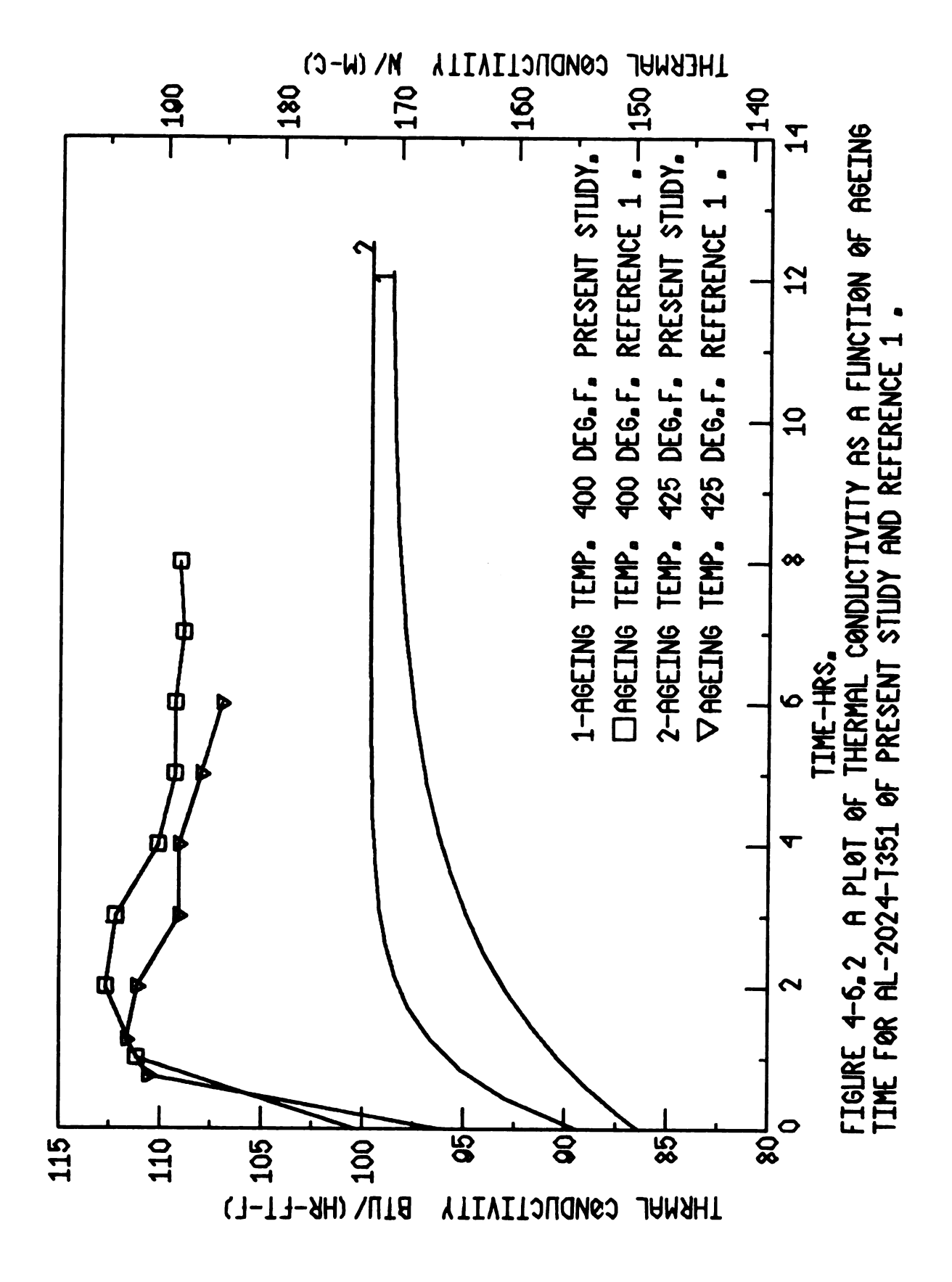
Since no time has elapsed in this abrupt change in temperature, the value of volume fraction of perecipitate remained unchanged. Since the temperature is changing, the value of thermal conductivity changes accordingly.

4-6 Comparison and Discussion

No reference data, with the exception of the data given by Al-Araji [1], was found to compare with the isothermal ageing data of the present investigation. The results of isothermal ageing tests of the present study and the ageing experimental data of Al-Araji [1] are shown in Figures 4-6.1 and 4-6.2. The following conclusions are drawn from these experimental results obtained from the same bar of Al-2024-T351 material at the same ageing conditions:

1. From Figures 4-6.1 and 4-6.2 at zero time, the value of thermal conductivity $k_{ia}(T_{ag},0)$ and the as received value of thermal conductivity $k_a(T)$ coincide (see Table 3-6.11). Corresponding values obtained by Al-Araji [1] for ageing temperatures 350, 375, 400, and 425°F are given as 88.5, 99.6, 100.2, and 96.0 Btu/ (hr-ft-°F), respectively. The values determined by the present





method for the same ageing temperatures, shown in Tables 3-6.1 through 3-6.8, are: 81.99, 82.64, 86.20, and 88.06 Btu/(hr-ft-°F), respectively. Note that the experimental ageing data given by Al-Araji [1] tends to take an abrupt increase from ageing temperature 350°F to 375°F.

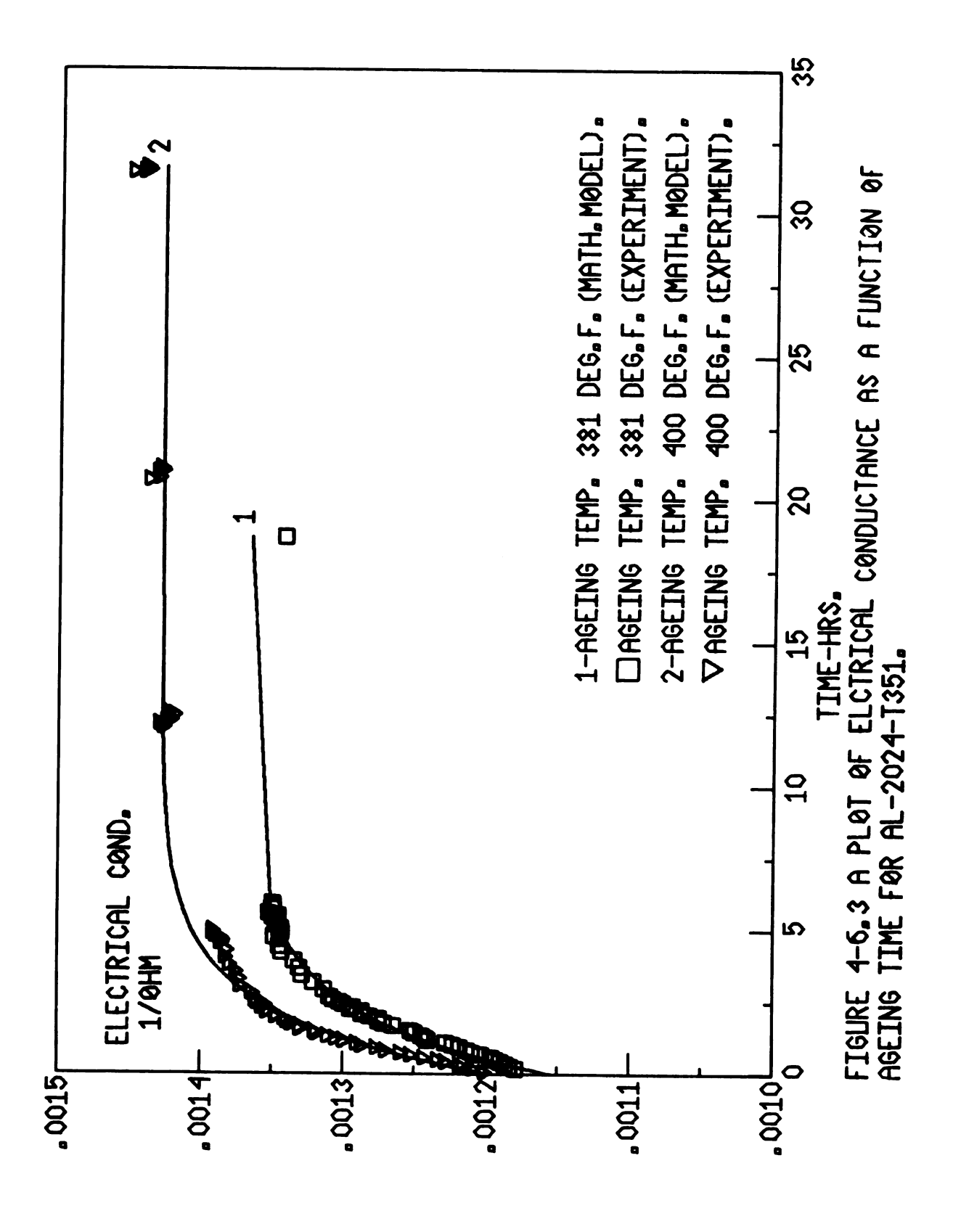
The present experimental results are considered to be more accurate because if we assume that the k values for Armco iron and A1-2024-T351 at about room temperature, given by TPRC [24], represent the best values found in the literature at the present time, then a comparison of the present results and those given by A1-Araji [1] with the results of TPRC supports the above argument. For Armco iron, the present value of k (see Chapter 2) is 1.23 percent lower than the k values given by TPRC while the value of k obtained by A1-Araji [1] is 2.5 percent higher than the result of TPRC. For as received A1-2024-T351, the value of k (see Chapter 3) obtained by the present method is 2.7 percent higher than the value of TPRC, and k value given by A1-Araji [1] is 11.11 percent higher than the value of k presented by TPRC. From these comparisons, it is concluded that the four values of k, given by A1-Araji [1], for zero time of the four ageing temperatures, may not be accurate.

2. Figure 4-6.2 shows thermal conductivity-time curve for ageing temperatures 400 and 425°F reported by Al-Araji [1] and the present investigation. The plots given by Al-Araji [1] are questionable because the values of k at the initial ageing time, and the maximum value of k for ageing temperature 425°F, are less than the corresponding values of k for ageing temperature 400°F. The

present experimental data (Tables 3-6.1 through 3-6.8) and corresponding mathematical model do not indicate a pattern following that of Al-Araji's [1] (as shown in Figure 4-6.2).

- 3. The values of specific heat obtained by Al-Araji [1] are more oscillatory and generally higher than the values determined by the present study; his values are also higher than the generally accepted literature values.
- 4. Al-Araji [1] concluded from his experimental data that at a given ageing temperature, the values of thermal conductivity increase to a maximum (aged) and subsequently decrease (overaged). This pattern can not be detected from the present experimental data (Figures 3-6.1, 3-6.3, 3-6.5, and 3-6.7) in which the ageing times are much longer than ageing times given by Al-Araji [1].

In order to confirm that the isothermal ageing data for thermal conductivity of as received A1-2024-T351 is exponential with time [the isothermal values of thermal conductivity of as received A1-2024-T351 increase with time to a maximum (aged) and remain unchanged as ageing time increases], two sets of unreported experimental ageing data of electrical conductance (inverse of electrical resistance) on the same bar of as received A1-2024-T351, as a function of ageing time, are shown in Figure 4-6.3. These data were not reported because refinement of experimental equipment and procedure is underway to modify the temperature-controlled specimen housing. It is interesting to note that these experimental data, shown in Figure 4-6.3, appear to be exponential with time and a mathematical model like that of Equation (4-1.5)



fits reasonably well. It is also interesting to note that the time constant found for electrical conductance for $T_{ag} = 400^{\circ}F$ is 2.095 hours. The corresponding time constant for k is 2.230 hours. Therefore, for the aging temperature $400^{\circ}F$, the shapes of curves obtained for thermal conductivity and electrical conductance versus time are almost identical. A theoretical relationship between thermal and electrical conductivity is the Weideman-Franz law, which states that the ratio of thermal conductivity to electrical conductivity at any temperature is proportional to that temperature [2, pp. 36-39]. Because thermal and electrical conductivity at each isothermal ageing temperature are theoretically proportional, and because the experimental ageing data obtained for thermal and electrical conductivity are both exponential, it is concluded that the thermal conductivity-time curve is an exponential form rather than any other characteristic curve given by Al-Araji [1].

Numerous reports [34, 40, 54) indicate that the hardness-time curve of solution-heat treated aluminum alloys reach a maximum and subsequently the values of hardness decrease to lower values as ageing time increases. The difference between solution heat-treated and as received A1-2024-T351 is in heat treatment prior to ageing tests. In all hardness ageing tests the specimens were heated to a temperature between 900-975°F (i.e., 48 hours in a salt bath at 965°F), followed by quenching in ice-water and immediately starting the ageing tests. Such heat treatment was not given to as received A1-2024-T351 neither in this investigation nor the investigation carried out by A1-Araji [1] using the same bar.

- 5. Al-Araji [1] reported the values of thermal conductivity, determined at room temperature, for aged specimens after completion of precipitation. These data indicate that holding the specimens at any ageing temperature for sufficiently long time periods allows complete precipitation to occur, or the value of $\eta_{\rm m}(T_{\rm ag})$ in Equation (4-3.5) is equal to unity. The present experimental data given in Table 3-6.10 appear to invalidate Al-Araji's experimental findings.
- Different procedures are applied to analyze the experimental ageing data. These include: First, the mathematical model given by Al-Araji [1] is proposed only until the time of the maximum $k_{ia}(T,t)$ values (t_{max}) . The model demonstrates a relationship between dimensionless k_{ia}^{\dagger} , T_{ag} , and dimensionless time t^{\dagger} (t^{\dagger} = The relationship is a form of a polynomial with linear parameters. The present model covers the entire ageing time and is exponential (4-1.5) with linear and nonlinear parameters. The time constant (4-1.4) obtained by the present method can be related to the overall coefficient of diffusion [47, 48]. Second, the present method of analysis relates the dimensionless thermal conductivity to volume fraction of precipitation. Third, for thermal cycling processes, a first-order differential equation is postulated to obtain the instantaneous volume fraction of precipitation and subsequently determine the value of thermal conductivity which is time and temperature dependent. In this respect, Al-Araji [1] introduced an algebraic procedure to

determine only values of thermal conductivity until $t^+ = 1$ (t^+ is a time when k_{ia}^+ is maximum for each ageing temperature).

4-7 Use of the Proposed Mathematical Models in an Engineering Problem

In the design of heat transfer equipment, sometimes it is desirable to predict temperature history of its components. The A1-2024-T351 material is one of the most versatile families of metal available to the metalworking industry for fabrication of various components of heat transfer equipment. This alloy, when solution heat-treated and subjected to elevated temperatures, undergoes considerable changes in mechanical, electrical, and thermal properties which influence the design performance. The objective of this section is to provide a method for determining temperature history of A1-2024-T351 material under temperature-and time-dependent thermal properties conditions. This is accomplished by proposing a numerical method of solution of the partial differential equation of conduction and pertaining equations for thermal conductivity simultaneously. The method is illustrated for the particular example of a step increase in surface temperature.

The problem is to solve the one-dimensional partial differential equation of conduction:

$$\frac{\partial}{\partial x} \left(k \frac{\partial T}{\partial x} \right) = \rho c_p \frac{\partial T}{\partial t}$$
 (4-7.1)

for the aluminim alloy 2024-T351 material with the boundary conditions of $T(0,t) = 450^{\circ}F$ and $\partial T(L,t)/\partial x = 0$ and the initial condition of $T(x,0) = 350^{\circ}F$.

Equation (4-7.1) is solved for the A1-2024-T351 material under the three cases of as received properties (no precipitation), as received with precipitation, and the annealed condition.

4-7.1 Thermal Properties

For all three cases, the values of c_p are considered to vary only with temperature. The c_p values are determined using one of the recommended equations given in Chapter 3. Values of ρ are found in [24]. Knowing the values of ρ and c_p at any temperature, a least-squares technique is applied to obtain:

$$\rho c_{p} = 35.8126 + 0.0116 T$$
 (4-7.2)

The values of thermal conductivity k for the cases of as received properties (no precipitation) and the annealed condition are also considered to vary only with temperature. The associated values of k are obtained using the recommended Equations (3-8.1) and (3-8.3).

The k values of as received A1-2024-T351 with precipitation depend on the amount of precipitation; consequently, the values are time- and temperature-dependent. To calculate the instantaneous values of thermal conductivity, the amount of precipitation must be calculated. The equation of volume fraction of recipitate is described by:

$$\frac{\partial \eta(T,t)}{\partial t} = \frac{1}{\tau(T)} \left[\eta_{m}(T) - \eta(T,t) \right] \text{ for } \eta_{m}(T) > \eta(T,t) \quad (4-7.3)$$

where T = T(x,t), τ (T) is given in Equation (4-1.5), and η_m (T) is determined using Equation (4-3.7).

In the case of as received with precipitation, prior to a step increase in temperature at location x=0, the as received A1-2024-T351 was preaged at 350°F for 25 hours. Before preageing it is assumed that the A1-2024-T351 was held at low temperatures (i.e., about room temperature) so that no recipitation had occurred.

Equation (4-7.3) was solved numerically to determine the value of volume fraction of precipitate $\eta(T,t)$. Then the instantaneous value of thermal conductivity for as received A1-2024-T351 with precipitation was calculated using:

$$k(T,t) = k_{ia}(T,0) + \Delta k_{ia}(T) \times \eta(T,t)/\eta_m(t)$$
 (4-7.4)

where $k_{ia}(T,0)$ and $\Delta k_{ia}(T)$ are defined in Equation (4-1.5).

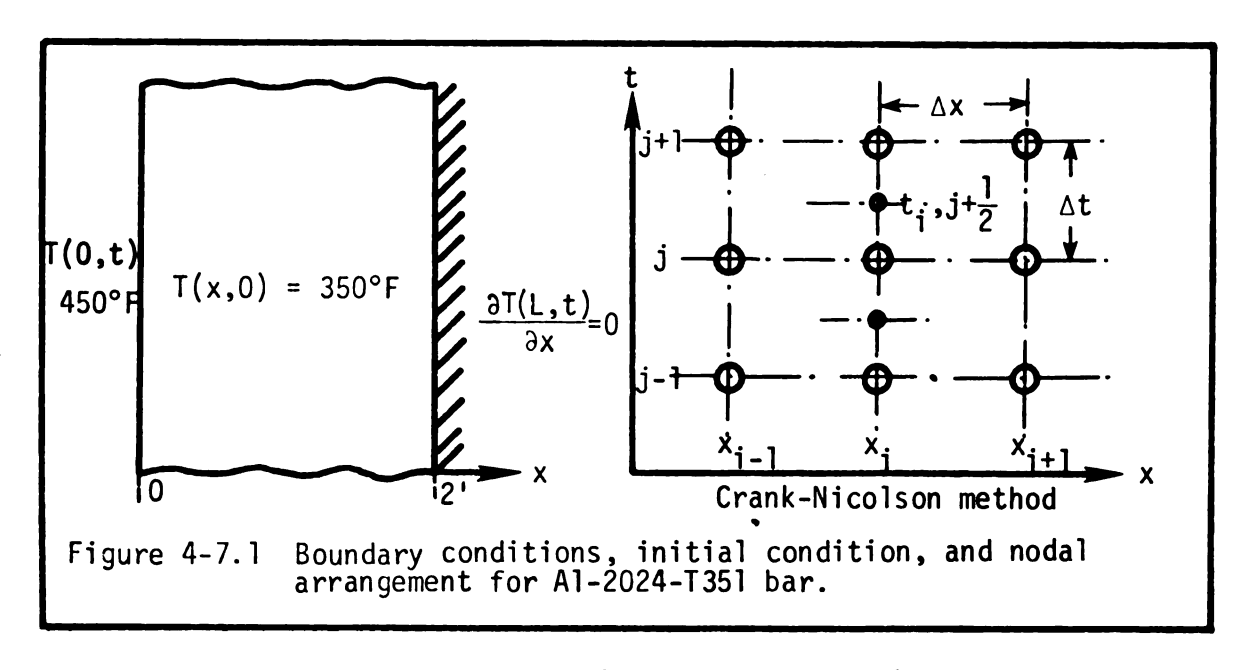
4-7.2 Method of Solution

The partial differential equation of conduction was solved using finite differences. An energy balance about node i (see Figure 4-7.1) can be written as:

$$q_{i-1,i} - q_{i,i+1} = \dot{E}_i$$
 (4-7.5)

where $q_{i-1,i}$ is heat flow rate from node i-1 to i; $q_{i,i+1}$ is heat flow rate from node i to i+1; and \dot{E}_i is stored energy at node i for a time interval j and j+1 (see Figure 4-7.1).

Equation (4-7.5) for node i and for time interval j and j+1 may be approximated by:



$$(1 - \beta) \left[Ak_{i-1/2}^{j} \frac{T_{i-1}^{j} - T_{i}^{j}}{\Delta x} - Ak_{i+1/2}^{j} \frac{T_{i}^{j} - T_{i+1}^{j}}{\Delta x} \right] +$$

$$\beta \left[Ak_{i-1/2}^{j} \frac{T_{i-1}^{j+1} - T_{i}^{j+1}}{\Delta x} - Ak_{i+1/2}^{j} \frac{T_{i}^{j+1} - T_{i+1}^{j+1}}{\Delta x} \right] =$$

$$(\rho c_{p})_{i}^{j} \Delta x A \frac{T_{i}^{j+1} - T_{i}^{j}}{\Delta t}$$

$$(4-7.6)$$

where $k_{i-1/2}^{j}$ is the thermal conductivity evaluated at temperature $(T_{i-1}^{j} + T_{i}^{j})/2$; similarly, $k_{i+1/2}^{j}$ is k value evaluated at $(T_{i}^{j} + T_{i+1}^{j})/2$.

Forward difference, backward difference, and Crank-Nicolson approximation can be specified by setting the value of β equal to 0.0, 1.0, and 0.5, respectively.

Equation (4-7.6) can be rearranged as:

$$\beta k_{i-1/2}^{j} T_{i-1}^{j+1} + \left[-\beta k_{i-1/2}^{j} - \beta k_{i+1/2}^{j} - \frac{(\rho c_p)_i^j (\Delta x)^2}{\Delta t} \right] T_i^{j+1} + \beta k_{i+1/2}^j T_{i+1}^{j+1} =$$

$$- (1-\beta) k_{i-1/2}^j T_{i-1}^j + \left[(1-\beta) k_{i-1/2}^j + (1-\beta) k_{i+1/2}^j - \frac{(\rho c_p)_i^j (\Delta x)^2}{\Delta t} \right] T_i^j$$

$$+ (1-\beta) k_{i+1/2}^j T_{i+1}^j$$

$$+ (4-7.7)$$

The values of $k_{i-1/2}^{j}$ and $k_{i+1/2}^{j}$ are determined using the relationship given in Equation (4-7.4). The value of $\eta_{i-1/2}^{j}$ (for simplicity the functional T and t notations are omitted; instead the subscript i and superscript j are used) for node i-1/2 and time j is determined using the fourth-order Runge-Kutta formulas [30]:

where
$$RK_0 = \Delta t (\eta_{m,i-1/2}^j - \eta_{i-1/2}^j)/\tau_{i-1/2}^j$$

 $RK_1 = \Delta t (\eta_{m,i-1/2}^{j+1/2} - \eta_{i-1/2}^j - RK_0/2)/\tau_{i-1/2}^{j+1/2}$ (4-7.8)

 $\eta_{i-1/2}^{j+1} = \eta_{i-1/2}^{j} + (RK_0 + 2RK_1 + 2RK_2 + RK_3)/6$

$$RK_2 = \Delta t (\eta_{m,i-1/2}^{j+1/2} - \eta_{i-1/2}^{j} - RK_1/2)/\tau_{i-1/2}^{j+1/2}$$

$$RK_3 = \Delta t(\eta_{m,i-1/2}^{j+1} - \eta_{i-1/2}^{j} - RK_2)/\tau_{i-1/2}^{j+1}$$

For $\eta_{i+1/2}^{j}$ a similar expression is written with subscript i+1/2. Note that the subscript i-1/2 or i+1/2 indicates that the components are calculated at a temperature $(T_{i-1} + T_{i})/2$ or $(T_{i} + T_{i+1})/2$, respectively.

Equation (4-7.8) was used to calculate the volume fraction of precipitates at time j, and subsequently the values of thermal conductivity are calculated by the relationship given in Equation (4-7.4). These values were then utilized in Equation (4-7.7) to obtain the temperature of the corresponding node at the time j+1. In this procedure the time step $\Delta t = 0.005$ hours and the effect of the past k(T,t), $\eta_m(T)$, and $\tau(T)$ used for one future temperature calculation is negligible.

For a total of m nodes, m linear equations like that of (4-7.7) were written. These equations were solved simultaneously to obtain the temperatures of all nodal points at each time step. Knowing all grid points' temperatures, the thermal properties were evaluated and this procedure was repeated for the next time step. These algebraic calculations were continued until the maximum specified time or specified temperature had been reached.

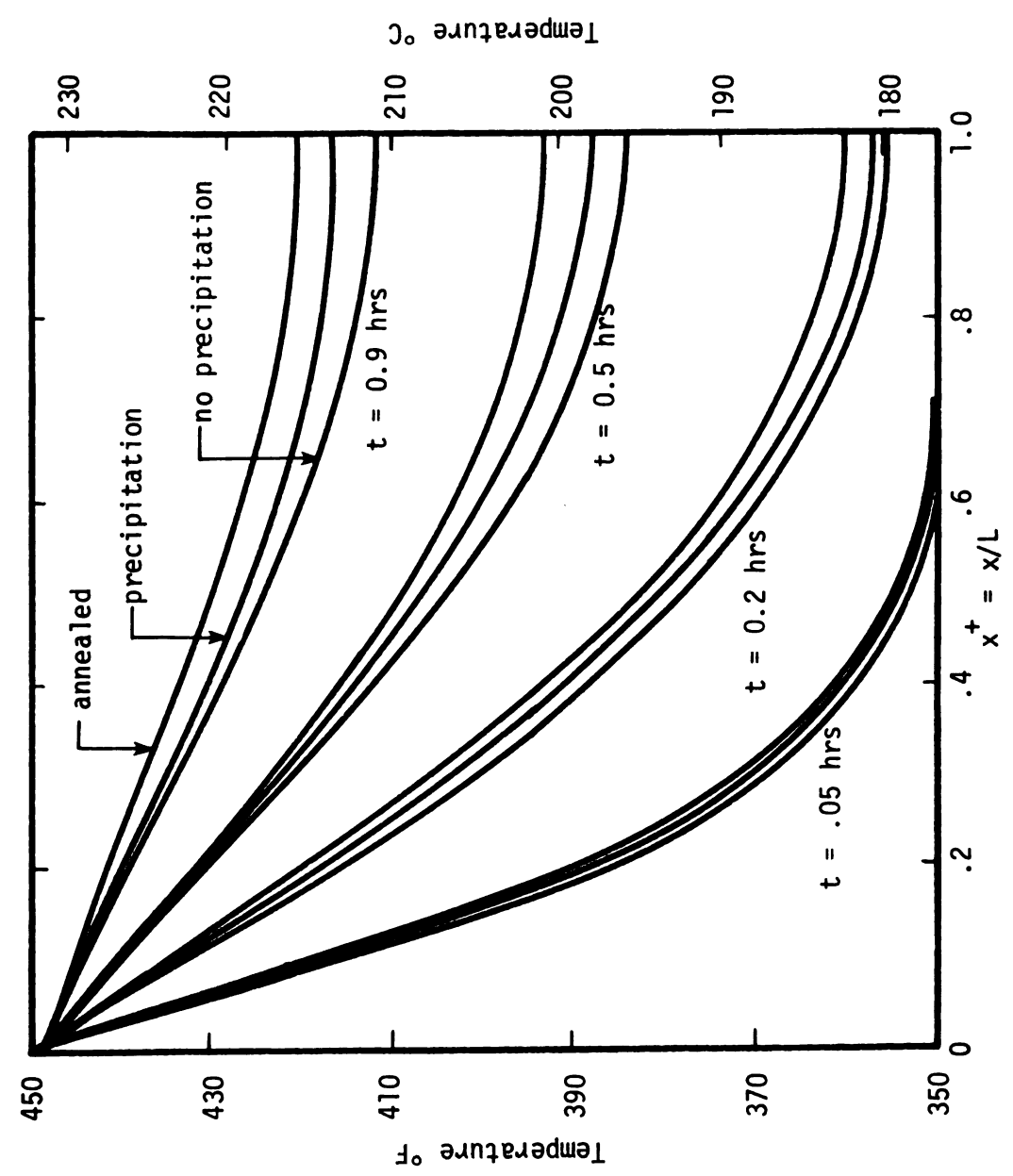
A FORTRAN computer program was developed to solve this problem; it contains the main program and three subroutines. In the main program inputs and outputs are specified. In one subroutine the temperature or temperature- and time-dependent thermal properties are calculated. In the case of as received with precipitation, the volume fraction of precipitate for all gridpoints is determined using the fourth-order Runge-Kutta formulas. The next subroutine uses the proper thermal properties to generate the coefficients of T_{i-1}^{j+1} , T_{i}^{j+1} , and T_{i+1}^{j+1} , given in the left-hand side of Equation (4-7.7) and the value of the right-hand side of this

equation. Finally, the last subroutine uses the matrix of coefficients and determines the nodal temperatures.

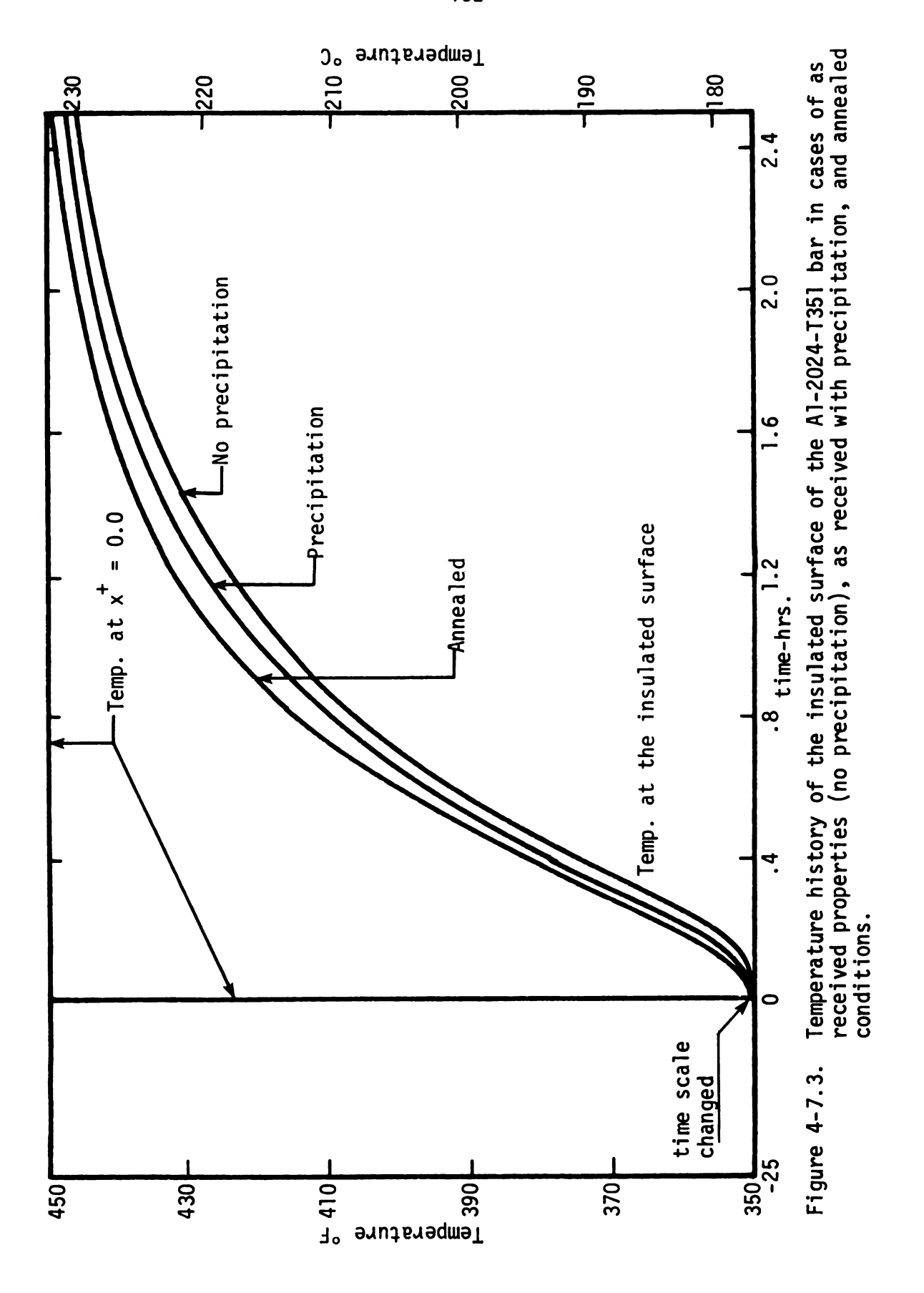
The results of Crank-Nicolson finite difference approximation for the as received with no precipitation, as received with precipitation, and annealed conditions are shown in Figures 4-7.2 through 4-7.6.

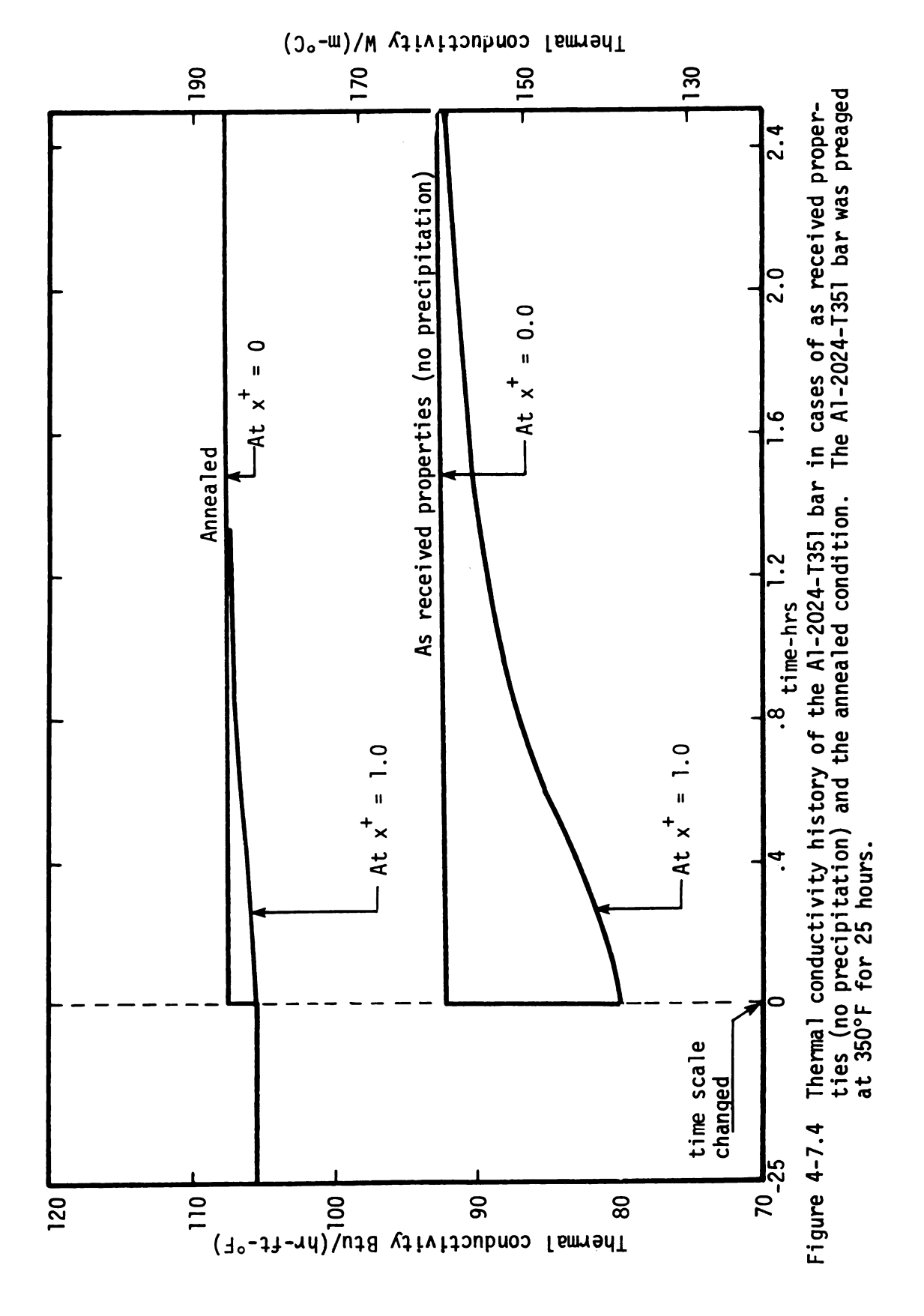
The numerical results using the Crank-Nicolson method are shown in Figures 4-7.2 and 4-7.3. Figure 4-7.2 shows temperature as a function of $x^+ = x/L$ for the three cases of as received properties (no precipitation), as received with precipitation, and annealed conditions for times 0.05, 0.2, 0.5, and 0.9 hours. The three aforementioned cases generate three distinct curves (temperature versus x^+) for any time t due to the differences in thermal conductivity k. The largest temperature differences for the three cases are obtained at $x^+ = 1$ (insulated surface) when the time is between 0.8 and 1.6 hours. The temperature history of the insulated surface for the three cases is shown in Figure 4-7.3.

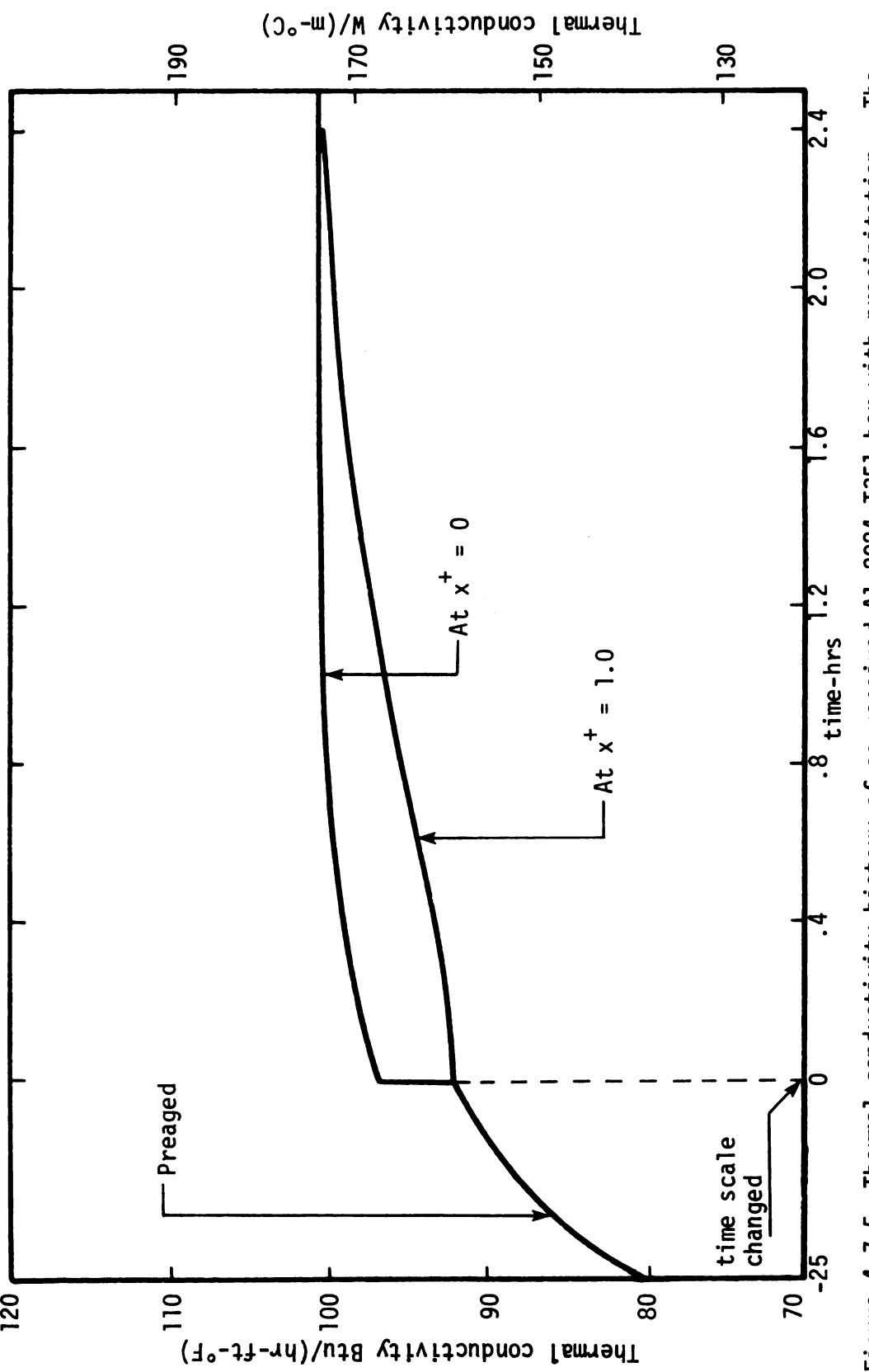
The thermal conductivity history of the A1-2024-T351 in the cases of as received with no precipitation and the annealed condition is shown in Figure 4-7.4. For time = 0, the value of k for the as received A1-2024-T351 bar is $80.3 \, \text{Btu/(hr-ft-°F)}$ while the corresponding value of k for the annealed condition is $105.5 \, \text{Btu/(hr-ft-°F)}$. Due to a sudden change in temperature at the heated surface, there is an abrupt change in the values of k for as received with no precipitation and the annealed condition, as



Crank-Nicolson finite difference solution of conduction equation for Al-2024-T351 bar in cases of as received properties (no precipitation), as received with precipitation, and annealed conditions. Figure 4-7.2







Thermal conductivity history of as received Al-2024-T351 bar with precipitation. The Al-2024-T351 bar was preaged at 350°F for 25 hours. Figure 4-7.5

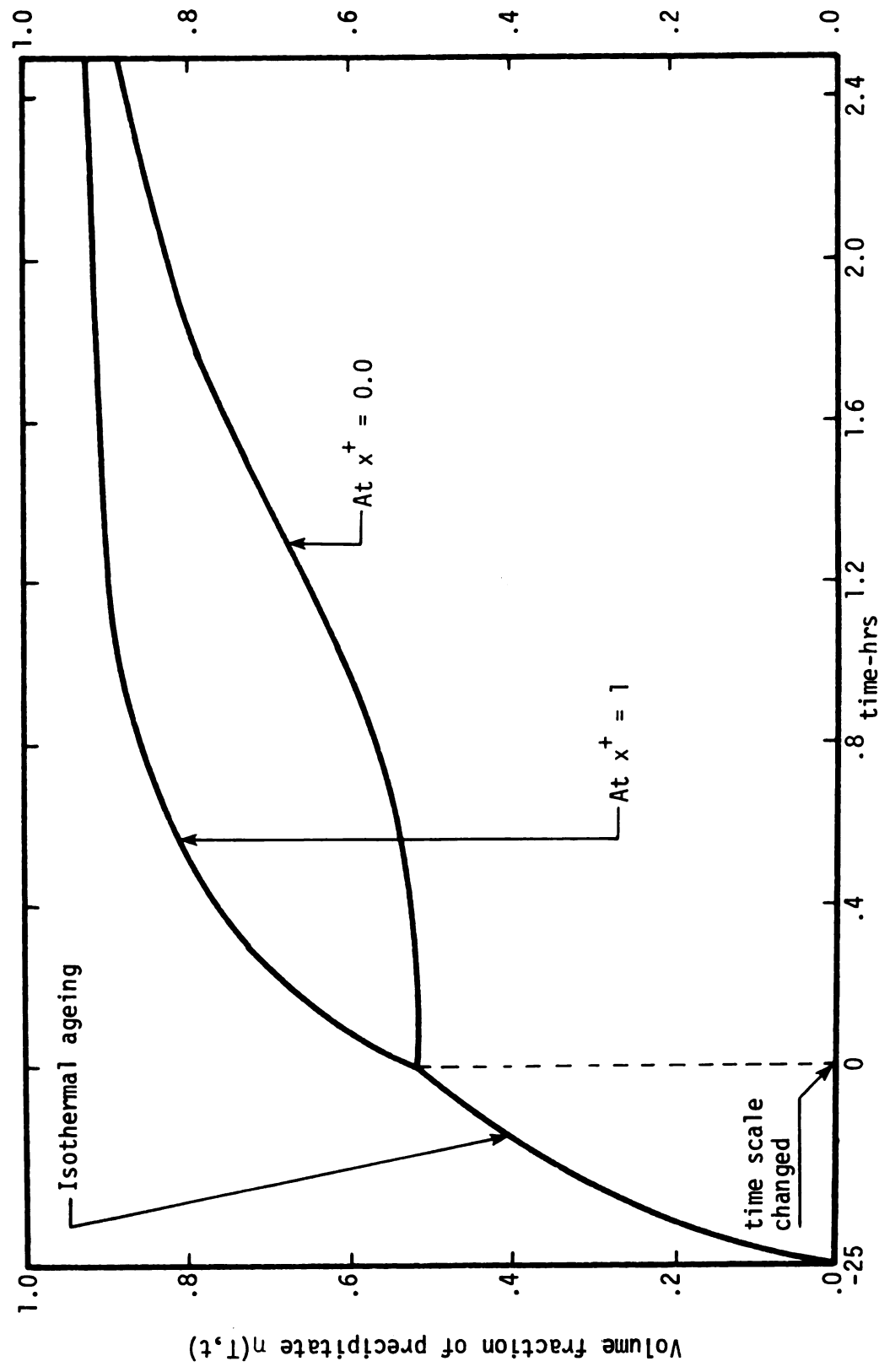


Figure 4-7.6 Volume fraction of precipitate of as received Al-2024-T351 bar. The Al-2024-T351 bar was isothermally preaged at 350°F for 25 hours.

shown in Figure 4-7.4. These values for as received with no precipitation and the annealed condition at 450°F are 92.3 and 107.6 Btu/(hr-ft-°F), respectively. The values of k at the insulated surface (for both cases) increase with time. The annealed A1-2024-T351 bar, due to a higher thermal conductivity, attains the final uniform temperature much faster than the as received A1-2024-T351 bar with no precipitation.

Figure 4-7.5 shows the thermal conductivity history of the Al-2024-T351 bar with precipitation. The volume fraction of precipitate of this bar is given in Figure 4-7.6. Prior to a step increase in temperature, the Al-2024-T351 bar was held at 350°F for 25 hours and before this time it is assumed that the bar was held at low temperatures (zero precipitation). For 25 hours of isothermal ageing at 350°F, the values of thermal conductivity (k) and the values of volume fraction of precipitate (n) increase with ageing time exponentially. After this period, due to an abrupt change in temperature at the heated surface, there is also an abrupt change in the values of k and a rapid increase in the values of η which are shown in Figures 4-7.5 and 4-7.6, respectively. After this abrupt change, the values of k at the heated surface, unlike the annealed and as received with no precipitation, change with time because of the influence of the precipitation. When precipitation at any location of the bar is completed, the corresponding k and η values remain unchanged thereafter as time increases. For 25 hours the k and η values given in Figures 4-7.5 and 4-7.6,

respectively, represent the thermal conductivity and volume fraction of precipitate of the entire A1-2024-T351 bar. After this period, the k and η values of two locations (heated and insulated surfaces) are shown in Figures 4-7.5 and 4-7.6. It is important to note that the precipitation at the heated surface, due to a higher temperature, is completed more rapidly than the precipitation at the insulated surface. Hence the k values calculated for the heated surface approach a constant value faster than the corresponding values of k obtained for the insulated surface.

CHAPTER 5

SUMMARY AND CONCLUSIONS

One of the most important objectives of the present study was to investigate the thermal property changes of aluminum alloy 2024-T351 (Al-2024-T351) under the influence of precipitation agehardening. In the course of acheiving this objective, a number of modifications in the previously available equipment were made and several new components were developed and added. The feasibility of using a thin thermofoil electric surface heater was studied.

A search was made to determine the best location for the placement of thermocouples on the flat surfaces of the specimens.

Numerous trial experiments were performed to evaluate the effects of various thermocouple arrangements, heating times, time intervals between data points, test durations, and power input levels.

A procedure was developed to calibrate the amplifiers and the associated system which transmits the thermocouples' output from the laboratory to the IBM 1800 computer. A FORTRAN computer program (Chapter 2) was developed to calculate the calibration coefficients to convert the millivolt output of thermocouples to temperature.

An analytical equation for estimating thermal properties [19] utilized the transient data generated by the calibrated equipment to determine values of thermal conductivity (k) and specific heat (c_D) . The newly developed transient facility was used to

determine k and c_p values of Armco iron (reference material) in the temperature range of 80-400°F (Chapter 2).

The measured k and c_p values of Armco iron were compared with values reported by the other investigators. These comparisons indicated that the present transient method can produce accurate thermal properties values. In addition, the present method is transient with short measurement time period (approximately 40 seconds in the present tests). Advantages of a transient method with short measurement times are that the heat losses have less influence on the values of thermal properties and that the method can be used for materials whose thermal properties are time, or temperature, and time/temperature-dependent. This transient method was also used to determine the thermal properties of A1-2024-T351 before precipitation occurred (fast measurement cycles) and the annealed material in the temperature range 80-425°F (Chapter 3).

Values of k and c_p of as received A1-2024-T351 with precipitation for isothermal ageing temperatures of 350, 375, 400, and 425°F were also measured using the developed method (Chapter 3). For each isothermal ageing temperature, the k values increase with ageing time to a maximum value. For higher ageing temperatures, the k values approach maximum more rapidly than the maximum k values for lower ageing temperatures. The increase in k values due to precipitation becomes zero at a limiting temperature of about 287°C (550°F).

The experimental ageing data obtained for k was mathematically modeled and the linear and nonlinear parameters were determined using the NLINA computer program (Chapter 2).

At each ageing temperature, the experimental values of c_p tended to increase slightly at the initial stage of ageing and subsequently decreased to the vicinity of the initial values. Because of the small and irregular variation in the values of c_p , no attempt was made to model the experimental ageing data of specific heat.

The isothermal mathematical model, obtained for k values versus ageing time, is related to the volume fraction of precipitation. The relation found for the volume fraction of precipitation and the associated time constant are in accordance with the general form given for the kinetic laws of precipitation and diffusion, respectively (Chapter 4). Relationships were also found by which the maximum values of k and the maximum value of volume fraction of precipitation, at any ageing temperature, can be determined.

In practical applications, the as received Al-2024-T351 alloy may be subjected to nonisothermal ageing temperatures. In this case, two differential equations are proposed which are believed to be original. The solution of these differential equations gives the volume function of precipitate (η) under any arbitrary ageing temperature and time and subsequently by a k - η relationship the values of k are determined.

The numerical solution of the one-dimensional partial differential equation of conduction for an Al-2024-T351 plate was given to demonstrate the influence of precipitation on temperature history

of the plate. Three cases were considered of the material being in its as received condition with no precipitation permitted, as received condition with precipitation permitted, and the annealed condition. The k and ρc_p values used in the partial differential equation of conduction for the cases of the as received with no precipitation and the annealed conditions are only temperaturedependent. The k values in the condition of as received with precipitation depend on the amount of precipitation and consequently are time/temperature-dependent. In this case the differential equation of precipitation is also solved numerically to determine the volume fraction of precipitate (n) as a function of time and temperature. The simultaneous solution of temperature and η is required because k is a function of η . The partial differential equation of conduction was approximated using the Crank-Nicolson method. The differential equation of precipitation was solved using the fourth-order Runge-Kutta formulas. The effect of precipitation on temperature history, the thermal conductivity history, and the volume fraction of precipitate versus ageing time of the A1-2024-T351 material are given graphically in Chapter 4.

5-1 Recommendations for Further Research

The following are some suggestions for further research:

l. From the isothermal volume fraction of precipitation two differential equations are postulated which are unique and quite useful not only for the isothermal ageing conditions but also for nonisothermal cases which happen frequently in practical

applications. The validity of the differential equations of precipitation for isothermal conditions was verified. To apply the differential equations to nonisothermal ageing cases, certain assumptions are made. Further research is needed to justify these assumptions and verify the differential equations for nonisothermal ageing cases; these cases include up- or down-cycling thermal processes or so-called double ageing.

- 2. Modifications of the present temperature-controlled specimens' housing are needed to more rapidly cool the specimens to the set isothermal ageing temperature after the end of each experiment. This will reduce the time interval between consecutive ageing experiments and consequently enable the performance of more ageing experiments in a short time period. The minimum time interval between consecutive ageing experiments for the present investigation was about 15 minutes. A shorter time interval is needed to obtain more information, particularly when ageing temperature is larger than 400°F or when experiments are being performed to study precipitation during up- or down-cycling the thermal processes.
- 3. A minicomputer is also needed in the laboratory to aid in reducing the time interval between consecutive ageing experiments.
- 4. The determination of the electrical resistivity of the as received A1-2024-T351 under influence of precipitation agehardening was initiated during this investigation. The results of two sets of ageing tests for electrical conductance (inverse of electrical resistance) are also given in Chapter 4. A mathematical model like that given for thermal conductivity fitted reasonably

well to the experimental ageing data of electrical conductance. Preliminary investigation indicates that the ageing experimental results of electrical conductivity can aid in providing quantitative information in an efficient manner in regard to the precipitation model proposed in this investigation. To determine the electrical conductivity of as received A1-2024-T351, a well-designed temperature-controlled specimens' housing is needed. The design should provide a method of fast heating of the specimens to a set isothermal ageing temperature and maintaining the specimen and its surroundings within about 1.5°F of the desired set isothermal ageing temperature. The developed equipment and measurement procedure should be tested and calibrated first using the Armco iron material which has fairly stable and known electrical conductivity. For accurate and detailed measurements, a digital data acquisition system should be used.

- 5. Other heat treatable alloys such as Al-Zn and Al-Mg alloys undergo similar property changes (like that of Al-Cu alloy) when solution heat-treated and subjected to a precipitation heat-treating temperature. Further study is needed to determine the behavior of the thermal property changes of such alloys under the influence of precipitation age-hardening.
- 6. This investigation uses a certain method to attach the thermocouples on the flat surfaces of the specimen. An attempt was also made to determine the disturbances created by these thermocouples using this method of thermocouple installation. A consistent conclusion could not be reached. It was assumed that the

disturbances created by the thermocouple itself in this investigation are insignificant. Further study is needed, however, to evaluate more precisely the disturbances created by the presence of the thermocouple. This is important not only for this investigation but also for other cases involving the transient temperature measurements with thermocouple installed in a similar manner.

REFERENCES

REFERENCES

- [1] Al-Araji, S. R. "Experimental Investigation of Transient Thermal Property Changes of Aluminum 2024-T351." Ph.D. dissertation, Michigan State University, 1973.
- [2] Tye, R. P. Thermal Conductivity. Vol. 1. New York: Academic Press, 1969.
- [3] Tye, R. P. Thermal Conductivity. Vol. 2. New York: Academic Press, 1969.
- [4] McElroy, D. L., and Moore, J. P. "Radial Heat Flow Methods for the Measurement of the Thermal Conductivity of Solids."

 In <u>Thermal Conductivity</u>, Vol. 1, p. 185. Edited by R. P. Tye. New York: Academic Press, 1969.
- [5] Watson, T. W., and Robinson, H. E. "Thermal Conductivity of Some Commercial Iron-Nickel Alloys." <u>Journal of Heat Transfer</u> 83 (1969):403.
- [6] Danielson, G. C., and Sidles, P. H. "Thermal Diffusivity and Other Non-Steady-State Methods." In <u>Thermal Conductivity</u>, Vol. 2, pp. 149-199. Edited by R. P. Tye. New York: Academic Press, 1969.
- [7] Sidles, P. H., and Danielson, G. C. "Thermal Diffusivity Measurements at High Temperatures." In <u>Thermoelectricity</u>, pp. 270-287. Edited by Paul H. Egli. New York: John Wiley and Sons, Inc., 1958.
- [8] Carslaw, H. S., and Jaeger, J. C. <u>Conduction of Heat in Solids</u>. 2nd ed. London: Oxford University Press, 1959, p. 261.
- [9] Taylor, J. R., and Underwood, W. M. "An Improved Line-Source Apparatus for Measuring Thermal Conductivity of Plastics."

 The Fifth Conference on Thermal Conductivity, Denver, Vol. 1, 1965, p. II-C-1.
- [10] Wechsler, A. E., and Kritz, M. A. "Development and Use of Thermal Conductivity Probes for Soils and Insulations."

 The Fifth Conference on Thermal Conductivity, Denver, Vol. 1, 1965, p. II-D-1.

- [11] Parker, W. J.; Jenkins, R. J.; Buttler, C. P.; and Abbott, G. L. "Flash Method of Determining Thermal Diffusivity, Heat Capacity, and Thermal Conductivity." <u>Journal of Applied Physics</u> 32 (1961):1679-1684.
- [12] Beck, J. V., and Dhanak, A. M. "Analytical Investigation of Optimum Heat-Pulse Experiment for Determining Thermal Properties." The Fifth Conference on Thermal Conductivity, Denver, Vol. 1, 1965, p. I-A-1.
- [13] Beck, J. V. "PROPERTY." Computer Center, Michigan State University, East Lansing, Michigan, 1975.
- [14] Kavianipour, A. "Analytical Estimation of Thermal Properties and Variation of Temperature in Asphaltic Pavements." Ph.D. thesis, Michigan State University, East Lansing, Michigan, 1971.
- [15] Beck, J. V. "Transient Determination of Thermal Properties." In <u>Nuclear Engineering and Design</u>, Vol. 3, pp. 373-381.

 Amsterdam: North-Holland Publishing Co., 1966.
- [16] Klein, A. H.; Shanks, H. R.; and Danielson, G. C. "Thermal Diffusivity of Armco Iron by Three Methods." The Fifth Conference on Thermal Conductivity, Denver, Vol. 1, 1965, p. II-G-1.
- [17] Carter, R. L.; Maycock, P. D.; Klein, A. H.; and Danielson, G. C. "Thermal Diffusivity Measurements with Radial Sample Geometry." <u>Journal of Applied Physics</u> 36 (1965) Part 2: 2333-2337.
- [18] Beck, J. V. "Determination of Thermal Conductivity and Specific Heat from Transient Temperature Measurement." AVCO Corporation, Wilmington, Mass., 1961.
- [19] Beck, J. V., and Al-Araji, S. "Investigation of a New Simple Transient Method of Thermal Property Measurement." <u>Journal of Heat Transfer, Trans.</u>, ASME 96 (1974) Series C:59-64.
- [20] Power Supplies Unlimited Manual, Fig. 2-2-8. NJE Corporation, Kenilworth, New Jersey.
- [21] Williams, D. R., and Blum, H. A. "The Thermal Conductivity of Several Methods." Thermal Conductivity--Proceedings of the Seventh Conference, Gaithersburg, Maryland, 1968, pp. 349-354.
- [22] Chang, H., and Blair, M. G. "A Longitudinal Symmetrical Heat Flow Apparatus for the Determination of the Thermal

- Conductivity of Metals and Their Alloys: on Armco Iron." Thermal Conductivity--Proceedings of Eighth Conference, West Lafayette, Indiana, 1969, pp. 689-698.
- [23] Larson, D. C.; Powell, R. W.; and DeWitt, D. P. "The Thermal Conductivity and Electrical Resistivity of a Round-Robin Armco Iron Sample, Initial Measurements From 50 to 300°C." Thermal Conductivity--Proceedings of the Eighth Conference, West Lafayette, Indiana, 1969, pp. 675-687.
- [24] Touloukian, Y. S., ed. <u>Thermophysical Properties of High</u>
 <u>Temperature Solid Materials</u>. Vol. 1, 1966, pp. 583-585 for
 Armco iron, and Vol. 2, 1966, pp. 735-737 for aluminum
 alloys. New York: The Macmillan Co., 1967.
- [25] "Manual on the Use of Thermocouple in Temperature Measurement." ASTM Special Technical Publication 470. Philadelphia, Pa.: ASTM, 1916 Race St., 1970.
- [26] Beck, J. V. "The Optimum Analytical Design of Transient Experiments for Simultaneous Determination of Thermal Conductivity and Specific Heat." Ph.D. thesis, Michigan State University, East Lansing, 1964.
- [27] Klamkin, M. S. Unpublished paper. AVCO RAD, Wilmington, Mass., 1957.
- [28] Beck, J. V., and Hurwicz, H. "Effect of Thermocouple Cavity on Heat Sink Temperature." Trans. of ASME, Sercies C, 1960, pp. 27-36.
- [29] Kreith, F. <u>Principles of Heat Transfer</u>. 3rd ed. New York: Intext Educational Publishers, 1973.
- [30] Carnahan, B.; Luther, H. A.; and Wilkes, J. O. Applied
 Numerical Methods. New York: John Wiley and Sons, Inc.,
 1969, p. 576.
- [31] Bevington, P. R. <u>Data Reduction and Error Analysis for the Physical Sciences</u>. New York: McGraw-Hill Book Co., 1969, p. 200.
- [32] Box, G. E. P., and Kanemasu, H. "Topics in Model Building, Part II, on Nonlinear Least Squres." Tech. Report No. 321. Dept. of Statistics, University of Wisconsin, Madison, 1972.
- [33] Beck, J. V., and Arnold, K. J. "Parameter Estimation in Engineering and Science." Bond notes at Michigan State University, East Lansing, 1975.
- [34] Van Horn, K. R. Aluminum, Vol. 1: Properties, Physical Metallurgy, and phase diagram. Metals Park, Ohio, 1967.

- [35] Fuss, V. Metallography of Aluminum and Its Alloys. Translated from the German by R. J. Anderson. Cleveland, Ohio: The Sherwood Press, 1936.
- [36] Panseri, C., and Federighi, T. "A Resistometric Study of Preprecipitation in an Aluminum-1.4% Mg₂Si Alloy." <u>Institute of Metals Journal</u> 94 (1966):99-105.
- [37] Guinier, A. Ann. Physique. 1939 [xi], 12, 161.
- [38] Preston, G. D. Proc. Roy. Soc. 1938 [A], 167, 526.
- [39] Hardy, H. K. "The Ageing Characteristics of Some Ternary Aluminum-Copper-Magnesium Alloys with Copper: Magnesium Weight Ratios of 7:1 and 2.2:1." <u>Institute of Metals</u> Journal 83 (1954-1955):17-34.
- [40] Hardy, H. K., and Heal, T. J. "Nucleation-and-Growth Processes in Metals and Alloys." The Mechanism of Phase Transformations in Metals, Symposium, Belgrave Square, London. Institute of Metals, Monograph and Report Series No. 18, 1956, pp. 1-46.
- [41] Turnbull, D. "Phase Changes." Solid State Physics 3 (1956): 225-306.
- [42] Guinier, A. "Heterogeneities in Solid Solutions." Solid State Physics 9 (1959):293-398.
- [43] Kelly, A., and Nicholson, R. B. "Precipitation Hardening." Progress in Materials Science 10 (1961-63):149-391.
- [44] Thomas, G., and Nutting, J. "The Precipitation of the θ' Phase in Aluminum-4% Copper Alloys." The Institute of Metals, Belgrave Square, London, Monograph and Report Series No. 18, 1956, pp. 57-75.
- [45] Cowley, J. M. "Crystal Structure Determination by Electron Diffraction." <u>Progress in Materials Science</u> 13 (1966-67): 267-321.
- [46] Fine, M. E., and Chiou, C. "An Acoustical Study of Low Temperature Aging in Al-4.2 Pct Cu." American Institute of Mining, Metallurgical, and Petroleum Engineers 212 (1958):553-557.
- [47] Seeger, A., and Schumacher, D. "Quenching Effects in the Noble Metals, and in Nickel and Ni-Co Alloys." In <u>Lattice Defects in Quenched Metals</u>, pp. 15-76. Edited by R. M. Cotterill, M. Doyama, J. J. Jackson, and M. Meshii. New York: Academic Press, 1965.

- [48] Brick, R. M., and Phillips, A. "Diffusion of Copper and Magnesium Into Aluminum." American Institute of Mining and Metallurgical Engineers, Trans. 124:331-337.
- [49] Gerold, V., and Schweizer, W. Z. Metallkunde 52 (1961):76-85.
- [50] Panseri, C., and Federighi, T. "A Resistometric Study of Preprecipitation in Al-10%Zn." <u>Acta Metallurgica</u> 8 (1960): 217-238.
- [51] Federighi, T. "Resistometric Researches on Point Defects in Quenched Al and Al-Rich Alloys." In <u>Lattice Defects in Quenched Metals</u>, pp. 217-268. Edited by R. M. Cotterill, M. Doyama, J. J. Jackson, and M. Meshii. New York: Academic Press, 1965.
- [52] Turnbull, D., and Treaftis, H. N. "Kinetics of Precipitation of Tin from Lead-Tin Solid Solutions." Acta Metallurgica 3 (1955):43-54.
- [53] Pashley, D. W.; Jacobs, M. H.; and Vietz, J. T. "The Basic Processes Affecting Two-Step Ageing in an Al-Mg-Si Alloy." Phi. Mag. 16 (1967):51-76.
- [54] Lorimer, G. W., and Nicholson, R. B. "The Nucleation of Precipitates in Aluminum Alloys." The Mechanism of Phase Transformations in Crystalline Solids, Monograph and Report Series No. 33, 1969, pp. 36-42.
- [55] Hardy, H. K. "Ageing Curves at 110°C on Binary and Ternary Aluminum-Copper Alloys." <u>Institute of Metals Journal</u> 82 (1953-54):236-238.